

**UCLA**

**UCLA Electronic Theses and Dissertations**

**Title**

Telementoring for Minimally Invasive Surgery

**Permalink**

<https://escholarship.org/uc/item/5h34p7p6>

**Author**

Nistor, Vasile

**Publication Date**

2017

Peer reviewed|Thesis/dissertation

UNIVERSITY OF CALIFORNIA

Los Angeles

Telementoring for Minimally Invasive Surgery

A dissertation submitted in partial satisfaction of the  
requirements for the degree Doctor of Philosophy  
in Mechanical and Aerospace Engineering

by

Vasile Nistor

2017

© Copyright by

Vasile Nistor

2017

# ABSTRACT OF THE DISERTATION

Telementoring for Minimally Invasive Surgery

by

Vasile Nistor

Doctor of Philosophy in Mechanical and Aerospace Engineering

University of California, Los Angeles, 2017

Professor Gregory P Carman, Chair

Laparoscopic, or minimally invasive surgery (MIS) has been shown to provide tremendous advantages for patients. Safe and efficient laparoscopic surgery requires advanced psychomotor skills; and novice laparoscopic surgeons face a steep and challenging learning curve to develop them. This problem is exacerbated by the lack of expert mentors who are concentrated in relatively few centers and often are not readily available to mentor novice surgeons, or to perform surgeries in person - thus creating a need for telesurgery. The goal of this dissertation is to address these challenges.

The overarching hypothesis of this dissertation is that telementoring systems in combination with machine learning algorithms and active haptic guidance can bridge the gap in learning the advanced surgical skills required for MIS.

To test this hypothesis we have developed two pieces of technology: the UCLA Laparoscopic Training Station (LTS) and the UCLA LapaRobot. Tracking the motion of surgical instruments via the UCLA–LTS, we have collected an intraoperative dataset from two separate experiments: (a) a combined phacoemulsification (PKE) and pars plana vitrectomy (PPV) procedure on a pig eyeball, and (b) a porcine laparoscopic cholecystectomy. From these datasets we have extracted a set of kinematically based performance metrics to evaluate the MIS surgical skills of novice trainees. We then conducted a construct validation test of the UCLA–LTS, where we evaluated the kinematic performance metrics from two populations of test participants, an expert group and novice. Our analysis shows that, when combined with machine learning algorithms, these performance metrics were successful in differentiating between the psychomotor skill of the expert mentors and those of novice.

We then built a prototype of the UCLA – LapaRobot and laid the foundation to demonstrate that active guidance from a haptic force feedback mechanism has the potential to facilitate the learning of MIS-specific surgical skills for remote trainees in a telementoring scenario. We conclude that we can further enhance the deployment of MIS to remote locations in a telesurgery scenario, with medic-trained personnel at the slave station, assisted by the kinesthetic force feedback of the UCLA–LapaRobot.

The dissertation of Vasile Nistor is approved.

Lynch, Christopher S

M'Closkey, Robert Thomas

Holmes, E Carmack

Dutson, Erik P.

Carman, Gregory P, Committee Chair

University of California, Los Angeles

2017

## Table of Contents

1	Introduction.....	1
1.1	Minimally Invasive Surgery .....	3
1.2	Benefits of MIS.....	3
1.3	Challenges of MIS .....	4
1.4	Benefits of telementoring to facilitate MIS .....	6
1.5	Technology overview for tracking systems .....	9
1.6	Commercially available tracking systems .....	15
1.7	Force generating haptic interface.....	16
1.8	Software .....	19
1.9	Military Significance .....	20
1.10	Hypothesis.....	20
1.11	Dissertation Structure.....	21
2	Methods.....	22
2.1	The haptic-guided telementoring system.....	22
2.2	Force Generating Haptic Interface.....	24
2.3	Verification of Haptic Perception .....	27
2.3.1	Hardness Perception.....	27
2.3.2	Motion perception.....	27

2.3.3	Performance Measures.....	28
2.3.4	Dry Lab Testing.....	28
2.4	Tracking System.....	28
2.4.1	System requirements.....	28
2.4.2	Proposed Tracking System.....	29
2.4.3	Proposed Software.....	31
2.4.4	Establishing Construct Validity for Training Simulator Function....	32
2.4.5	Feasibility Study for Telementoring System in Animal Model.....	34
3	Immersive Training and Mentoring for Laparoscopic Surgery.....	36
3.1	Abstract.....	36
3.2	Introduction.....	37
3.3	System Overview.....	40
3.3.1	Instrument Tracking.....	42
3.3.2	Sensor Integration.....	45
3.3.3	The Hardware-Software Interface.....	47
3.4	Test Description.....	49
3.5	Performance Metrics.....	51
3.5.1	Smoothness.....	53
3.6	Total Path Length.....	53



3.6.1	Time to completion.....	54
3.6.2	Volume described by the instrument tip.....	55
3.6.3	Specific Kinetic Energy .....	55
3.6.4	Scoring.....	55
3.7	Test Data.....	56
3.8	Conclusion.....	59
4	Quantification of Intraocular Surgery Motions with an Electromagnetic Tracking System .....	62
4.1	Abstract:.....	62
4.2	Introduction.....	62
4.3	Tools and Methods.....	63
4.4	Results.....	65
4.5	Conclusion and Discussion.....	66
5	Identification of Surgical Skills Specific to Laparoscopic Porcine Cholecystectomy .....	67
5.1	Introduction.....	67
5.2	Methods.....	69
5.3	Analysis.....	71
5.4	Discussion.....	75

5.5	Conclusion .....	78
6	Construct Validity for the UCLA-LTS .....	79
6.1	Abstract .....	79
6.2	Construct Validity Tests .....	81
6.3	Test Subjects Recruitment .....	84
6.3.1	Inclusion/Exclusion Criteria .....	85
6.3.2	Method and Subject Identification and Recruitment .....	85
6.3.3	Methods and Procedures Applied to Human Subjects.....	85
6.3.4	Data Collection, Storage and Confidentiality .....	86
6.3.5	Potential Risks and Discomforts .....	88
6.3.6	Potential Benefits .....	88
6.3.7	Personnel Inviting Participants .....	88
6.3.8	Process of Consent.....	88
6.3.9	Comprehension of Information Provided .....	89
6.3.10	Information withheld from subjects.....	89
6.3.11	Consent Access Forms.....	89
6.4	Data Analysis .....	89
6.4.1	Peg Transfer .....	89
6.4.2	Time to Completion .....	92

6.4.3	Path Length .....	94
6.4.4	Volume swept by instrument tips .....	96
6.4.5	Specific Mechanical Work.....	97
7	Motion Parameters of Surgical Instruments for the Assessment of Laparoscopic Psycho-Motor Skill .....	100
7.1	Abstract.....	100
7.2	Introduction.....	101
7.2.1	System Description .....	102
7.3	Methods.....	103
7.3.1	Test Subjects .....	103
7.3.2	Testing Method .....	104
7.3.3	Performance Metrics.....	104
7.3.4	Time to Completion .....	106
7.3.5	Path Length.....	108
7.3.6	Volume.....	110
7.3.7	Mechanical Work.....	112
7.3.8	Power .....	113
7.3.9	Learning Curve .....	115
7.3.10	Left hand vs. Right hand.....	119

7.3.11	Discussion.....	120
7.3.12	Conclusion .....	123
8	Support Vector Machines Improve the Accuracy of Performance Evaluation of Laparoscopic Training Tasks.....	125
8.1	Abstract.....	125
8.2	Introduction.....	126
8.3	Methods.....	127
8.3.1	Subjects.....	128
8.3.2	Evaluation Tasks.....	128
8.3.3	Motion Tracking System.....	129
8.3.4	Task Metrics.....	129
8.3.5	Combinations of Metrics.....	130
8.3.6	Summed Ratios .....	131
8.3.7	Score Normalization .....	132
8.3.8	Support Vector Machines (SVM).....	132
8.3.9	Evaluating Classification Performance.....	134
8.3.10	ROC Analysis .....	134
8.3.11	Validation Comparison.....	135
8.4	Results.....	136

8.4.1	Individualized Metrics .....	136
8.4.2	Combinations of Metrics.....	140
8.5	Discussion .....	143
9	Laparoscopic Telesurgery and Telementoring.....	146
9.1	Introduction.....	146
9.2	The UCLA LapaRobot.....	149
9.3	LapaRobot Kinematic Control.....	155
9.4	Two-handed LapaRobot.....	156
9.5	Reflective Force Feedback.....	157
9.6	Active Guidance in Training with the LapaRobot.....	158
9.7	Porcine Laparoscopic Cholecystectomy with UCLA-LapaRobot.....	162
9.8	Discussion .....	164
9.8.1	Milestones Achieved.....	164
9.8.2	Challenges.....	167
9.8.3	Future Work .....	168
10	Conclusion .....	169

## LIST OF FIGURES

<b>Figure 1:</b> Expert telementoring a novice surgeon through a procedure. Information exchange (b) takes place between the mentor station (c) and the novice surgeon (a).....	23
<b>Figure 2:</b> Expert surgeon's motions are recorded during the procedure (a) and then these data are used to develop a training simulation where novice surgeons practice by imitating the expert surgeon's gestures (b).....	24
<b>Figure 3:</b> Proposed tracking System Hardware Diagram.....	30
<b>Figure 4:</b> Operator's view of the UCLA-LTS. The laparoscopic instruments and trocars are inserted in the training box portholes visible in the fore plan. To the front of the box is the webcam providing video feedback on the computer monitor. The control box for the magnetic tracking system is placed on the top shelf. The active source electromagnet of the tracking system is placed in a fixed position behind the training box and not visible in this image.....	41
<b>Figure 5:</b> Ascension microBIRD sensor .....	43
<b>Figure 6:</b> Fixed and active DC source electromagnet.....	43
<b>Figure 7:</b> DC magnetic field of the source electromagnet .....	44
<b>Figure 8:</b> Tri-axial fluxgate sensor.....	45
<b>Figure 9:</b> (a) Ethicon grasper disassembled and (b) wiring from the sensors pulled through the metal shaft.....	46

**Figure 10:** (a) Ethicon grasper with the handle disassembled to show the sensor wiring and (b) the assembled grasper handle with the sensors wiring and their connectors to the Bird control unit..... 47

**Figure 11:** Coordinate systems for the fixed reference DC electromagnet and the sensors embedded in the instrument..... 48

**Figure 12:** Peg transfer training task: (a) start with both instrument tips in a central position, (b) pick the rubber piece located on the right side peg with the right hand needle driver and lift it off the peg, (c) bring it over the training board and pass the rubber piece to the left hand grasper. (d) Using the left hand grasper place the rubber piece over the peg located on the left side of the training board, (e) release the rubber piece and bring both instruments back to the starting point. .... 51

**Figure 13:** Trajectory for the right hand side instrument in the reference coordinates, with (x,y) the horizontal plane, x-axis pointing towards the operator and z the vertical axis. .... 52

**Figure 14:** Two examples of motion traces for the peg-transfer task showing clear differences in the character of motion tracked between an (a) expert surgeon, and (b) a novice trainee.... 56

**Figure 15:** Average acceleration at the tip of the instrument held in the right (R) and left (L) hand for both expert and novices..... 57

**Figure 16:** Smoothness for (a) expert surgeon, and (b) novice trainee ..... 58

**Figure 17:** Time to completion performance metric (a) over the 10 test repetitions and (b) aggregated..... 59

**Figure 18:** Baseline metrics and total score for the expert and novice user. The error bars indicate the standard deviation for each metric (for expert, n=2; for novices, n=3). ..... 59

**Figure 19:** Referential sensor mounted on the pig eye..... 64

**Figure 20:** Tool tip pathway for the (a) PVD procedure and (b) the 360 vitrectomy ..... 66

**Figure 21:** Instruments used in the porcine test have motion sensors clamped to their handle and are placed on the surgical table next to the reference electromagnet for the calibration procedure (a) Axes are plotted on the right pane to verify the transforms for orientation and sensor tip location (b)..... 69

**Figure 22:** Surgical team is in position and ready to start. Expert surgeon handles the instruments with sensors and the assistant surgeon handles the endoscopic camera. Surgical field is visible on the monitor sitting on top of the shelf carrying the other instrumentation..... 70

**Figure 23:** Instruments in position and ready to start the gall bladder procedure. Assistant surgeon operates the endoscopic camera (a); instrument axes are displayed in right pane (b) ..... 71

**Figure 24:** Pathways for the left (blue) and right (red) hands (a); and the instantaneous displacements between two consecutive readings (b) ..... 71

**Figure 25:** Pathway segmentation in one-minute long time increments: (a) 4th minute data, (b) 5th minute data..... 72

**Figure 26:** Task segmentation from the video recording: (a) clearing the tissue around the cystic duct, (b) inspection of the colon passing it from the right hand to the left hand grasper ..... 73



**Figure 27:** Pathway segmentation by tasks: (a) both hands push the liver around the cystic duct and (b) right hand dissects around the cystic duct while the left hand clears the tissue connecting it to the liver bed..... 74

**Figure 28:** Pass the rope with the right hand instrument at the 3 inch mark and the left hand instrument at the 2 inch mark..... 82

**Figure 29:** Pass the rope task: (a) start with each instrument grasping at the left side of the rope on the first two markings; (b) release the jaws of the right hand instrument and then grasp at the third marking on the rope: (c) now release the jaws of the left hand instrument and then grasp at the second mark on the rope..... 83

**Figure 30:** Cap the needle task..... 83

**Figure 31:** Cap the Needle; (a) start by placing the instruments in a central starting point; (b) grab the cap with the left hand instrument and the needle with the right hand instrument and lift them off the floor of the training box; (c) while in the air, align the cap and the needle and insert the needle in the cap; (d) release the needle and use the right hand instrument to push the needle completely inside the cap; (e) use the left hand to place the cap and needle in their rest position and release..... 84

**Figure 32:** Trajectories for expert (a) and novice (b) for the left hand (L) and right hand (R) instrument tips..... 90

**Figure 33:** Probability density and the box plot. The left pane plots the probability density for the path length of right hand (RH) for the first test run of the peg transfer task, for both the experts group and the novices group. .... 91

<b>Figure 34:</b> Time to complete the task, box plot representation for all test runs and for both expert and novice groups .....	94
<b>Figure 35:</b> Path Length for the Peg Transfer: (a) left hand (LH) and (b) right hand (RH) for both experts and novices.....	95
<b>Figure 36:</b> Volume used by the tip of the instruments in (a) left hand (LH) and (b) the right hand (RH).....	96
<b>Figure 37:</b> Mechanical work at the instrument tips for expert and novice groups for (a) left hand (LH) and the (b) right hand (RH).....	98
<b>Figure 38:</b> Time to completion for (a) Pass the rope and (b) Cap the needle.....	108
<b>Figure 39:</b> Path Length for the instrument in the right hand (RH) for (a) pass the Rope and (b) Cap the Needle.....	110
<b>Figure 40:</b> Volume swept by the tip of the instrument in the right hand (RH) for the (a) pass the rope and the (b) cap the needle tasks .....	111
<b>Figure 41:</b> Specific Mechanical Work for instruments in the right hand (RH) for (a) pass the rope and (b) cap the needle .....	113
<b>Figure 42:</b> (a) Mechanical Work and (b) Power Output for the right hand (RH) of Peg Transfer .....	114
<b>Figure 43:</b> Power output for the right hand instruments for (a) pass the rope and (b) cap the needle .....	114
<b>Figure 44:</b> Learning curve for (a) expert group and (b) novice group.....	116
<b>Figure 45:</b> Normalized Learning Curves for the peg transfer.....	118

<b>Figure 46:</b> Dominant vs. non-dominant hand .....	119
<b>Figure 47:</b> Histograms to compare the frequency distribution of observed metrics for the peg transfer task. The dotted vertical line indicates the optimal separating score. ....	138
<b>Figure 48:</b> Histograms to compare the frequency distribution of observed metrics for the pass the rope task. The dotted vertical line indicates the optimal separating score.....	139
<b>Figure 49:</b> Histograms to compare the frequency distribution of observed metrics for the cap-the-needle training task. The dotted vertical line indicates the optimal separating score..	139
<b>Figure 50:</b> Receiver-Operating-Characteristic curves for all three training tasks: peg transfer (top), pass the rope (middle) and cap the needle (bottom). The straight diagonal line represents a theoretical random classifier .....	142
<b>Figure 51:</b> Laparoscopic degrees of freedom.....	150
<b>Figure 52:</b> Delta mechanism for the three translational degrees of freedom.....	151
<b>Figure 53:</b> Delta mechanism actuating angles .....	152
<b>Figure 54:</b> Closing and opening of jaws .....	153
<b>Figure 55:</b> Axial orientation for the laparoscopic instrument.....	154
<b>Figure 56:</b> Dual axis gimbal at the top plate and sliding spherical axis fulcrum.....	155
<b>Figure 57:</b> LapaRobot kinematic control.....	156
<b>Figure 58:</b> Two-handed LapaRobot concept.....	157
<b>Figure 59:</b> UCLA LapaRobot concept “no fly zone” in yellow .....	158
<b>Figure 60:</b> LapaRobot master station, ready for the peg transfer.....	159

<b>Figure 61:</b> LapaRobot slave station with a synthetic human torso in position .....	160
<b>Figure 62:</b> Left Hand trace (red) of the master station is recorded .....	160
<b>Figure 63:</b> Slave station receives the transmitted pathway data from the master station and performs the identical peg transfer .....	161
<b>Figure 64:</b> Trocar locations for the porcine cholecystectomy.....	163
<b>Figure 65:</b> LapaRobot working space over the porcine model .....	164

LIST OF TABLES

**Table 1:** Haptic Devices Comparison..... 25

**Table 2:** Phacoemulsification range of motion and time..... 65

**Table 3:** Vitrectomy range of motion and time ..... 65

**Table 4:** Kinematic data collected from the four magnetic tracking sensors ..... 87

**Table 5:** Performance metrics example ..... 90

**Table 6:** Time to complete the task for the first test run in the series ..... 93

**Table 7:** Time to completion, t-test ..... 94

**Table 8:** Path Length for expert and novice groups, t-test ..... 96

**Table 9:** Volume used by instrument tip, t-test ..... 97

**Table 10:** Specific Mechanical Work imparted to each instrument, t-test ..... 98

**Table 11:** Time to Completion for the 1st test run in the series ..... 107

**Table 12:** Path Length for the instrument in the right hand ..... 109

**Table 13:** Volume swept at the tip of the right hand instrument for the first test run ..... 111

**Table 14:** Specific mechanical Work exercised on the instrument for the first run in the series 112

**Table 15:** Mean and standard deviation values for each of the individual metrics applied to each task and for each population sub-group ..... 137

**Table 16:** Comparison of area under the ROC curves (AUC) for each method of combining individual metrics..... 140

**Table 17:** Mean accuracy  $\mu(Acc)$  and standard deviation of the accuracy  $\sigma(Acc)$  for each task and method pair is calculated over 100 repetitions of classification on a randomly selected validation set. The mean cut-off score  $\mu(s_c)$  is the mean score used to divide predicted expert from..... 141

**Table 18:** Nissen fundoplication, hospitalization and convalescence time..... 148

## ACKNOWLEDGEMENTS

The following organizations provided material support for this work:

- U.S. Army Medical Research & Materiel Command's (USAMRMC) Telemedicine and Advanced Technology Research Center (TATRC).
- UCLA Center for Advanced Surgical and Interventional Technology (CASIT)
- UCLA Departments of Mechanical Engineering
- KARL STORZ Endoscopy-America, Inc.

As a portion of this manuscript is a version of the following articles, the author would like to thank the co-authors for their contributions.

Chapter 3 is a version of “Nistor V, Carman GP, Faloutsos P, Allen B, Dutson E. (2007). Haptic guidance for laparoscopic surgery immersive training and mentoring. *MMVR*, 2007 [1]” and of “Nistor V, Allen B, Dutson E, Faloutsos P, & Carman GP (2007). Immersive training and mentoring for laparoscopic surgery. *Proceedings of SPIE Nanosensors, Microsensors, and Biosensors and Systems 2007*, volume 6528, pp. 1-11, 2007, 6528, 65280Q-65280Q-65211. doi: 10.1117/12.717199 [2].”

Chapter 4 is a version of “Son J, Bourges JL, Culjat MO, Nistor V, Dutson EP, Carman GP, Hubschman JP. (2009). “Quantification of intraocular surgery motions with an electromagnetic tracking system,” *Studies in Health Technology and Informatics*, 142, 2009 [3].”

Chapter 6 is a version of “Nistor V, Allen B, Faloutsos P, Dutson E, Carman GP (2008). Construct validity for the UCLA laparoscopic training system, *ASME Conference Proceedings*, 2008(48337), 23-24 [4].”

Chapter 8 is a version of “Allen, B., Nistor, V., Dutson, E., Carman, G., Lewis, C., Faloutsos, P. (2010). Support vector machines improve the accuracy of evaluation for the performance of laparoscopic training tasks. *Surgical Endoscopy*, 24(1), 170-178. doi: 10.1007/s00464-009-0556-6 [5].”



## VITA

- 1993                                    B.S., Mechanical Engineering  
Polytechnic Institute Gheorghe Asachi  
Iasi, Romania
- 1997                                    M.S. Mechanical Engineering  
Mechanical Engineering  
SUNY Binghamton
- 1997-2004                            Product Development Engineer  
Kionix Inc. Ithaca, New York
- 2004 - 2009                           Graduate Student Research Assistant  
Department of Mechanical and Aerospace Engineering  
University of California, Los Angeles

### Refereed Publications

- Allen, B., Nistor, V., Dutson, E., Carman, G., Lewis, C., Faloutsos, P. (2010). Support vector machines improve the accuracy of evaluation for the performance of laparoscopic training tasks. *Surgical Endoscopy*, 24(1), 170-178. doi: 10.1007/s00464-009-0556-6
- Son J, Bourges JL, Culjat MO, Nistor V, Dutson EP, Carman GP, Hubschman JP. (2009). “Quantification of intraocular surgery motions with an electromagnetic tracking system,” *Studies in Health Technology and Informatics*, 142.
- Yeghiazarian, L, Arora, H, Nistor, V, Montemagno, C, & Wiesner, U. (2007). Teaching hydrogels how to move like an earthworm. *Soft Matter*, 3(8), 939-944.

### Patents

- Z-Axis Angular Rate Sensor, EP 1671135, 2011, Chojnacki E, Epstein JP, Nenadic N, Stirling N, Nistor, V.
- Z-Axis Angular Rate Sensor, US PTO 7,036,372 B2, 2006, Chojnacki E, Epstein JP, Nenadic N, Stirling N, Nistor, V.

### Conference Proceedings

- Nistor V, Allen B, Faloutsos P, Dutson E, Carman GP (2008). Construct validity for the UCLA laparoscopic training system, ASME Conference Proceedings, 2008(48337), 23-24.
- Nistor V, Allen B, Dutson E, Faloutsos P, & Carman GP (2007). Immersive training and mentoring for laparoscopic surgery. Proceedings of SPIE Nanosensors, Microsensors, and Biosensors and Systems 2007, volume 6528, pp. 1-11, 2007, 6528, 65280Q-65280Q-65211. doi: 10.1117/12.717199
- Nistor V, Liang L-J, Allen B, Faloutsos P, Dutson E, Carman GP. (2008). Construct validity for the UCLA laparoscopic training system. MMVR, 16.
- Nistor V, Carman GP, Faloutsos P, Allen B, Dutson E. (2007). Haptic guidance for laparoscopic surgery immersive training and mentoring. MMVR, 2007.

### Poster Presentations

- Bourges JL, Son J, Hubschman JP, Culjat M, Nistor V, Schwartz SD, “Surgical Motion Assessed by Electromagnetic Sensors during Ocular Surgery”, Poster presentation #6094, ARVO 05-07-2009
- Nistor V, Chien A, “Self-powered Pacing Device for Cardiovascular Implants”, 4<sup>th</sup> Annual Southern California Biomedical Engineering Student Symposium, Los Angeles, California, January 22, 2005.
- Nistor V, Sahay C, Kittinger K, White F, Mechanical analysis of a ride entertainment system. ADAMS, 1997
- Nistor V, Sahay C, (1997). “Analysis of Entertainment Simulator” ASME Mid-Atlantic, April 1997

### Invited Talks

- “Sensors & Actuators for Minimally Invasive Surgery” Dean’s Advisory Council, UCLA Los Angeles, CA, April 17, 2008

### Media Highlights

- “UCLA Researchers develop training tool” Daily Bruin, May 4<sup>th</sup> 2007,
- “Guided surgery tool brings expertise to remote locations. Collaborative tool offers new training method” UCLA Engineering, April 4<sup>th</sup> -2007

# 1 Introduction

Laparoscopic, or minimally invasive surgery (MIS) has been shown to provide tremendous advantages for patients. Safe and efficient laparoscopic surgery requires advanced psychomotor skills; and novice laparoscopic surgeons face a steep and challenging learning curve to develop them. This problem is exacerbated by the lack of expert mentors who are concentrated in relatively few centers and are often not readily available to mentor novice surgeons, or to perform surgeries in person - thus creating a need for telesurgery. The goal of this dissertation is to address these challenges.

We have developed two pieces of technology: the UCLA Laparoscopic Training Station (LTS) and the UCLA LapaRobot. The LTS is used for self-study, and the LapaRobot, a much more sophisticated system - for telementoring and telesurgery.

The LTS is a system of assessing the movements of surgical instruments. A training simulation is generated by recording an expert surgeon perform either a training drill specific to developing surgical skill or a real operation while using instruments equipped with motion tracking capabilities. Intraoperative data are stored and later accessed by trainees at one or multiple training stations. Trainees follow the expert's movements to learn techniques utilized in specific procedures.

A critical element of LTS is a system of objective performance metrics that we devised to quantify and facilitate the learning of specialized surgical skills. These metrics, coupled with

specialized machine learning algorithms, are used to evaluate the performance of the trainees and to compare it to that of the expert.

The UCLA LapaRobot is the logical progression from assessing trainee's surgical skill to actively guide their hands in the performance of surgery or training. It combines the functionality of real time intraoperative videoconferencing with haptic - kinesthetic force feedback guidance to enhance MIS training and telementoring. It is a cost-effective and portable system that is also poised to directly address the need for telesurgery.

The LapaRobot allows a novice operator perform MIS with the assistance of a remote expert. At his/her console the mentor defines the appropriate pathways for the novice surgeon's instruments and, at the remote station as the novice surgeon manipulates their own instruments, his/her hands are guided along the way by means of force feedback from the LapaRobot. Via this haptic guidance system a distant mentor can effectively lay his/her hands on the hands of the trainee and guide the movements as the novice surgeon executes the procedure.

We take advantage of this telementoring technology to develop an integrated training system. Similarly to the LTS, the experts instruments movements are recorded and later replayed at a LapaRobot console with haptic force feedback, that is designed to reproduce the operating surgeon's ergonomic experience in the recorded procedure. The system of performance metrics developed for LTS can be used with the LapaRobot to provide additional feedback to the trainee.

The LapaRobot can also be used directly for telesurgery, whereby the expert surgeon fully controls the instruments at the console in the operating room, from a remote location.

## 1.1 Minimally Invasive Surgery

Minimally invasive surgery (MIS) also known, as “key hole surgery” is a surgical concept that aims to reduce the tissue exposed to and affected by the surgical intervention. It stands in contrast to the traditional surgical approach the so-called “open access surgery” by employing instrumentation and surgical techniques specifically designed for this approach. In general the MIS replaces the traditional large incision with multiple small incisions of 8 ÷ 12 mm in length, placed strategically around the operative site. Specialized instruments called trocars are then inserted into these incisions and driven through the layers of skin, muscle and body fat until they reach the area of interest. Small amount of carbon dioxide gas is then pumped through one of the trocars to create a dome shaped space above the operative site, while a specialized visualization instrument called an endoscope is inserted through its center cannula. The endoscope consists of a small tube with a camera and a light at one end, and a handle with controls for the camera and the lights at the other end. The image acquired by the camera is then projected onto multiple monitor screens in the operating room for the surgeon and the rest of the team. Because of this visualization technique MIS is sometimes called endoscopy, and these two terms will be used interchangeably throughout this dissertation. Other specialized tissue graspers, scissors, staplers, cauterizers, *etc.* are inserted through the other two or three trocars to perform the actual surgery.

## 1.2 Benefits of MIS

Minimally invasive surgical techniques offer many benefits to the patient. A patient undergoing a laparoscopic procedure has less of a physiologic stress response and reduced

immune function depression than a patient undergoing the equivalent open procedure [6]. MIS patients experience fewer wound related complications, and the multiple small port scars are much more cosmetically pleasing than the scar associated with a single large incision [7, 8]. In addition, laparoscopy is associated with less adhesion formation than open procedures so late complications such as chronic abdominal pain and small bowel obstruction occur less frequently [9]. Most importantly, MIS patients experience less post-operative pain, and they resume their normal daily activities more rapidly [8-11].

### 1.3 Challenges of MIS

While MIS techniques have been shown to provide tremendous benefits for patients, novice laparoscopic surgeons face challenging learning curves when approaching MIS surgery. A considerable challenge facing novice surgeons learning these novel techniques is that expert mentors are concentrated in relatively few centers and are often not readily available for guidance and instruction.

Minimally invasive surgery is difficult to perform and perhaps even more difficult to teach. Endoscopy requires the surgeon to perform tasks in a three-dimensional (3D) field while watching a two-dimensional (2D) image acquired via an angled endoscope. These factors challenge the surgeons with problems such as depth perception and spatial orientation.

Trocar placement creates a fixed fulcrum that leads to multiple issues normally not encountered in open surgery. To begin with, the proper placement of the trocar is critical because a port in a suboptimal location will force the surgeon to perform the entire procedure with his/her instruments interacting with the surgical field in a suboptimal manner. The trocar,

once inserted, is fixed and the surgical instruments will have to move around this fixed point, resulting in the so-called “fulcrum effect” – *e.g.* where the surgeons hand moves to the right, the tip of the instrument moves in opposite direction, to the left.

Additionally, the surgeon’s hand motions are variably amplified depending on how deeply the instrument is inserted through the trocar. Most laparoscopic instruments provide only five spatial degrees of freedom, depriving the surgeon of intracorporeal wrist motions as s/he manipulates the tissues.

Lastly, surgeon’s hands are physically distant from the tissues. This leads to increased tremor at the instrument tips and, more significantly, a change in the nature of the tactile feedback.

Taken together these challenges lead to a perceived lack of dexterity until the surgeon develops a skill set specific to the MIS approach. This perceived lack of dexterity translates to a loss of confidence leading to a situation where the surgeon no longer feels that s/he is in complete control of the operation.

In this dissertation we study several technologies to address the difficulties in learning how to perform MIS, and the lack of expert surgeons. First, the UCLA Laparoscopic Training Station (LTS) has been designed to help students learn expert skills and assess their own through objective performance metrics based on kinematic analysis of instrument motion. Second, the UCLA LapaRobot has been developed to provide active haptic guidance via force feedback to remote trainees – telementoring, as well as assist in remote surgery - telesurgery.

## 1.4 Benefits of telementoring to facilitate MIS

As mentioned above, training in MIS techniques requires ready access to experts that can mentor novice surgeons. However, advanced minimally invasive surgeons are rare in the surgical community today. In a recent study focusing on general surgeons in Ontario, Canada, it was found that fewer than 50% performed even one advanced laparoscopic procedure in their practice [12]. This lack of experts on-site can be mitigated through telementoring.

MIS is amenable to telementoring because the surgeon's visual field is acquired via a camera and is therefore digital information. This information can be readily displayed on a local monitor, saved on digital storage media, or transmitted to another monitor down the hall or across the country.

Advances in telemedicine technology have allowed this promising tool to make its way to the operating room, giving birth to the integrated operating room (OR). The OR of the past was first and foremost a workspace and only secondarily a place where a mentor might teach one or at most two trainees about the procedure at hand. Through the power of telecommunication, an integrated OR retains its role as a place to work but has the potential to become a true classroom where every aspect of the procedure can be monitored and broadcast to trainees or colleagues in the room, across the city, or across the country. In 1997 Rosser and colleagues published their evaluation of the role of telementoring in training surgeons in advanced laparoscopic procedures [13, 14]. A real-time videoconferencing system with telestration capabilities facilitated communication between surgeon as the mentor and medical students as the mentees. Without being able to directly intervene and touch the tissues themselves, the remote mentors still found that they could safely guide trainees through complex MIS procedures. Around the same time,



Moore and colleagues at Johns Hopkins in Baltimore conducted a study focusing on telementoring surgical trainees through minimally invasive urologic procedures [15]. In this case, communication was achieved not only through real-time videoconferencing and telestration, but the camera was held by an AESOP (Automated Endoscopic System for Optimal Positioning) robot that could be controlled either locally or by the remote mentor. For the first time, a remote expert could directly impact visualization of the surgical field in real time. Their results also suggested that telementoring was a feasible modality for guiding surgical residents through complex endoscopic procedures.

In recent years, the Food and Drug Administration (FDA) has defined a new class of medical device that includes “telementoring devices”. In 2001, Socrates (Computer Motion, Goleta, CA) became the first telesurgical device. It is a combination between real-time videoconferencing, telestration and remote AESOP (Automated Endoscopic System for Optimal Positioning) control. Use of the Socrates system remote controller enables a remote surgeon to telecommunicate with any AESOP-HR (Hermes Ready) remote controller [16]. Socrates has been successfully used in a number of surgical disciplines ranging from general surgery to urology and neurosurgery [17-19]. With this system, all that is lacking is the ability to reach in and perform the task with the trainee and this is where a haptic telementoring system is posed to play a larger role.

M. Anvari, MD, Director of Centre for Minimal Access Surgery at St Joseph’s Healthcare Hamilton, Ontario, Canada conducted research into the feasibility of the clinical use of robotics and telesurgery for telementoring applications. Dr Anvari, an experienced laparoscopist, used the Zeus (Intuitive Surgical, Sunnyvale, CA) robotic telesurgical system to assist Dr Craig McKinley, a general surgeon with limited endoscopic experience, as Dr

McKinley performed advanced laparoscopic procedures on patients at North Bay General Hospital. These early experiences were so successful that the hospital has since started conducting regular telerobotic procedures [20].

The described telesurgical system, however, is not without its limitations however. First, it is very expensive (over \$1 million) to purchase the hardware for such a system. Second, the robotic effector device is physically large, has substantial energy requirements and is not portable. Finally, as the Zeus robotic platform has been discontinued it remains to be seen whether Intuitive Surgical's da Vinci system will work as well to allow a novice laparoscopic surgeon and robotic assistant to work on the same patient at the same time.

Intuitive Surgical is the recipient of a National Institute of Standards and Technology (NIST) grant to develop a "unique robot control architecture and system that allows a mentoring surgeon and a student to simultaneously control a surgical robot performing MIS procedures" [21]. The mentor could exercise varying degrees of "priority" control depending on the progress of the mentee learning the new technique and a key innovation would be the development of force feedback system in the controls that gives each surgeon tactile feedback of the motions of the other [21].

While this research effort strives to develop a haptic-guided system where one robotic surgeon mentors another, we propose to study a more cost effective system that allows an advanced laparoscopic surgeon to remotely mentor a novice using spatial tracking of the surgical instruments. We explore the potential to track both the mentor and the mentee in the process of performing training tasks as well as actual surgeries, by using sensors to monitor the spatial position and orientation of the surgical instruments. Data generated by these motion and

orientation sensors can then be analyzed using artificial intelligence algorithms and evaluate the progress of mentee training. Further, the electronic data can be communicated at great distances and have the potential to enable remote mentoring – telementoring, of MIS students across continents.

## 1.5 Technology overview for tracking systems

In this section we review the different motion and orientation sensing technologies that have been employed in several current or proposed MIS training systems.

Briefly, several surgical simulation tools were surveyed and evaluated by Kaufman [22], Howe [23], and Satava [24]. The LASSO (Laparoscopically Assisted Simple Suturing Obliteration) project [25] is an integrated effort to construct a laparoscopic simulation platform without any involvement in instrument tracking. The KISMET (Kinematic Simulation, Monitoring and off-line programming Environment for Telerobotics ) project [26] from Karlsruhe-Germany uses a joint angle measurement system to track the instrument motion. The AISIM project [27] from INRIA France places no interest in instrument tracking. The UC-Berkeley and UC-San Francisco collaborated on a Robotic Telesurgical Workstation for Laparoscopy [28, 29] with the tracking performed by a sensor enhanced glove device. Another effort at creating a surgical simulator is VEST (Virtual Endoscopic Surgical Training) [22], again with the instrument tracking being overlooked. Commercially available laparoscopy trainers are available from Surgical Science – LapSim [30, 31] and from Mentice – ProCedicus MIST [32], both using non force-reflecting interface from Immersion Medical [33, 34]. Funda has a comparative study of two early development robotic surgical systems [35] one from IBM Research and the other from the John Hopkins School of Medicine. Currently a number of

technologies are used in various applications for tracking objects in physical space. A survey of tracking technologies by Meyer et al [36] with potential use in telementoring does not mention the inertia based systems McInerney [37]. A more comprehensive review of motion tracking technologies is published by Foxlin of Intersense [38].

Mechanical motion indexing is one of the more mature tracking technologies. It employs mechanical digitizers and encoders at the joint of a robotic system to determine tool position and orientation. Major advantages include superior accuracy as well as support for the tools when not in motion. The major disadvantage is that it restricts the range of motion and has fairly stiff joints. Intuitive Surgical currently employs it in the Da Vinci robotic surgical systems [39]. Another system that uses mechanical indexing is the KISMET simulator [26]. Kosugi demonstrated an articulated neurosurgical navigation system [40] and Kwok worked with the Unimation Puma 200 robot [41] for similar applications.

Optical tracking such as infra-red (IR) technology is commonly used in remote controls for home electronics. Multiple instruments can be fitted with infrared emitting LEDs and easily tracked. While relatively inexpensive it has a major drawback because it requires uninterrupted direct line of sight. Some tracking systems employ a secondary inertial tracking system when the line of sight is obstructed. Brainlab is commercializing a passive marker system powered by IR cameras used in their VectorVision platform [42] with a demonstrated accuracy of  $1.3 \pm 0.9$  mm [43]. Another system often used for tracking the spatial position is Optotrack [44] manufactured by Northern Digital Inc. It uses active IR beacons that are flashing one at a time, while their position is sensed by three line-scan CCD cameras, with an absolute accuracy better than  $\pm 0.1$  mm. A tabletop simulator manufactured by Immersion Medical [32] delivers very good resolution as well,  $0.064^\circ$  angular and 0.05mm linear. Bucholz [45] has a detailed

comparison of these and ultrasound based systems. Theoretically, optical tracking is expected to be less sensitive than ultrasound tracking, in practice however both achieve satisfactory accuracies. Another variation of this technology uses a laser scanner is Laser BIRD [46] manufactured by Ascension Technologies.

Telecommunications based tracking systems have been most frequently used for outside of building position detection. Dempsey [47] of Radianse Inc has explored the indoor potential of this technology and outlined some of the basic requirements for instrument tracking. Bluetooth, IEEE 802.15 is a short-range communications protocol effective over distances typically less than 10 ft. Bluetooth enabled devices form mini-cells similar to the way the cellular telephony works. Theoretically it could be used as a positioning system by triangulating the signal between the surrounding cells, but so far it has not been proven to be accurate. Another technology, Wi-Fi IEEE 802.11b is a communication protocol for longer range and higher bandwidth ~ 11Mbps. It has the potential to give more precise location information because the software enabling it actually tries to approximate the location based on known radio wave propagation characteristics, while also providing a significant data channel. It is not expressly designed for positioning applications and therefore would require significant development work. Ultra Wide Band (UWB) is an experimental communication protocol specifically designed to achieve ultra wide bandwidth. The transmitted radio signals behave in a way similar to K-band radar and could therefore allow for accurate location of transmitters. The system has the potential for both small energy consumption in transmission mode as well as extremely large amounts of transmitted data. It is still in development so any deployed systems would require a temporary Federal Communication Commission (FCC) license. Also due to

their experimental nature the existing systems are fairly expensive but costs are expected to drop in the next decade in line with the IR systems of today.

Radio frequency tracking systems have been extensively reviewed by Reynolds [48] and Foxlin [38]. Depending on the measurement technique, there are basically two types: triangulation and multilateration.

Triangulation systems are very promising for indoor applications. It is a concept similar to the Global Positioning System (GPS) except it works inside the buildings. Instead of requiring radio signals to travel from transmitters to satellites, multiple antennas positioned inside the room act as transmitters, receivers or both. An item to be tracked has a tag affixed to it that radiates a signal. Multiple receiving antennas then pick up this signal. Each of the antennas is fixed to a known, well-defined location and the distances from the transmitted signal and the receiving antennae are calculated as radii of circles around each antenna. The position at which at which three or more of the calculated circles intersect is the location of the device. It uses complex signal processing techniques to distinguish the main line-of-sight from the superfluous multipath signals. The major disadvantage is the need to calibrate the systems every time the radio environment changes, *e.g.* when the system is moved to a new surgical room, or a metal table full of instruments is brought into the same room. The major concern would be with surgical instruments that emit strong electromagnetic noise signal that is random in time and space such as the electro-cautery instruments.

Multilateration systems are based on the principle that the farther a radio frequency (RF) signal travels, the weaker it becomes. If the received signal strength can be known accurately and the losses are well understood, the distance to the tag can be calculated. The major

advantage of this technology is that it eliminates the need for precise time synchronization of the receivers.

Radio frequency identification devices (RFID) are commonly used as office entry systems. The passive systems use a stationary antenna that transmits a radio signal to the RFID tag, which then disturbs the signal in a known and predictable way, and bounces it right back to the radiating antenna. The integrated circuit (IC) chip in these systems can carry small amounts of information, enough to uniquely identify each device. The active systems have their own batteries and can transmit continuously over a long range (6ft). A major advantage of this technology is that it can deliver both instrument location and unique identification at a very low cost.

Ascension Technology Inc. commercializes a product named Flock of Birds based on the direct current (DC) magnetic tracker. This magnetic tracking can provide both instrument location and orientation in real time. Tracking accuracy appears to be unaffected by the nearby presence of conductive metal objects such as surgical instruments, surgical tables, *etc* [49]. Polhemus Inc commercializes a similar product named FASTRAK [50]. Nixon et al [51] did a comparative study of the two systems and found both systems to be relatively accurate within less than 0.5 mm, but susceptible to errors induced by electromagnetic sources. The FASTRAK was found to be relatively insensitive to interference from the main power supplies, light sources and monitors but sensitive to eddy currents and ferromagnetic metals. The Flock of Birds displays the opposite behavior: it is relatively susceptible to the main power, lights and monitors but remarkably insensitive to non-ferromagnetic metals.

Ultrasound based systems work similarly to radio triangulation systems. Several piezoelectric transducers can be attached to the surgical instruments and at some known fixed locations around the surgical field. Ultrasonic systems determine the position of the instruments by measuring the distances between the transducers using time of flight algorithms. These systems can acquire the distances very fast and like the IR based systems do require direct line-of-sight [52, 53]. These systems are also known as sonic digitizers with commercial systems available from Science Accessories Corp, GP8-3D [54]. Sonometrics Inc system SonoWand [55, 56] has been used to for armless stereotactic neuronavigation, where position estimation is achieved by arranging the sensors on the vertices of a cube. A commercial product CustusX [57] designed specifically for surgical navigation has been developed by SINTEF Tech.

Inertial navigation systems use inertial sensors (accelerometers and gyrometers) to calculate position and orientation. The calculations are based on time integration of the acceleration and angular velocity values from a set of three linear accelerometers and three angular rate gyrometers. It is a relative tracking system in the sense that the current position and orientation is referenced to a known starting point. Time integration of acceleration or angular velocity leads to accumulation of error resulting in sensor drift, therefore the navigation and positioning system requires periodic zeroing of errors to an absolute reference frame. All the previously described positioning technologies create absolute tracking systems, *i.e.* at any given point the position information is independent of any knowledge about the starting point.

An inertial-based tracking system is able to provide additional important information not available on any of the other systems. For example instrument orientation is determined with regard to the gravitational field and it can provide other measures that can quantify the fluidity of motion such as instantaneous accelerations and angular velocities. By employing the novel



Micro Electro Mechanical Systems (MEMS) based sensors, a system with very small volume and low power consumption can be easily designed at low cost and with high accuracy. A plethora of systems are currently available for various applications Systron Donner [58], MEMSense,  $\mu$ IMU [59], Kionix, KXM52, KGF01 [60]. Nakamura [61] proved that a system based on optical fiber gyros and crystal resonating accelerometers of high accuracy can be used to navigate an augmented reality environment. Barshan [62] applied an inertial based navigation system and compared its performance to laser guided systems. Their results show that with careful modeling of error sources low cost inertial sensing systems can provide valuable orientation and positions information.

Combining two or more of the abovementioned technologies in order to take advantage of their strengths while minimizing their perceived weaknesses can create hybrid systems. Such a system [63] is currently manufactured by Intersense Inc that combines inertial sensing with optical tracking. Kindratenko has performed a comparative study [64] for a hybrid inertial-ultrasound system with an electromagnetic position tracking system and found that though immune to electromagnetic interference, the ultrasound hybrid still needs direct line-of-sight as well as a high density of receptors. Another hybrid system [65] uses inertial sensors from Watson Industries in combination with an optical tracking system, Optotrak from Northern Digital.

## 1.6 Commercially available tracking systems

As of today there is no easy to use tracking system designed specifically for laparoscopic surgical tools. The laparoscopic surgery robots that address the instrument tracking aspects do so by using the cumbersome mechanical joints and encoders. Instrument tracking is more

seriously addressed by the neurosurgeons for stereotactic navigation as seen in BrainLab [42] and Optotrack [44]. One notable effort at tracking laparoscopic instruments is the table-top simulator manufactured by Immersion Medical [32]. Most of the tracking technology in use today is employed in vehicle tracking on land, sea or air. These devices come in various grades according to their particular application: navigational, munitions, commercial, *etc.* All these systems are expensive and physically too large to use for tracking a laparoscopic instrument inside the operating room. This dissertation will investigate a design specifically suited for the laparoscopic instrument tracking during surgery and training.

## 1.7 Force generating haptic interface

Haptic interfaces connect the user to the virtual reality dimension. The ideal haptic interface operates transparently between two absolute states, the virtual constraint and the virtual free space. In order to recreate a high fidelity virtual sensory reality such a system would need to meet specific requirements [66]: (a) low inertia, high stiffness, low friction, no backlash mechanical systems, (b) force actuator should enable back-drivability, high dynamic range, high maximum force, high output resolution and force/torque precision, (c) good positioning and sensing resolution, (d) force sensors at the human/tool interface, (e) a high frequency local control loop and (f) a low frequency global control loop to graphic user interface (GUI).

However, satisfying one requirement is not without tradeoffs in the other areas. The low impedance approach nominally displays virtual free space. In this approach, high gains are necessary to present rigid surfaces but they tend to destabilize the system. For example, when we push against a wall, we expect the wall would not deform under pressure nor would it oscillate and vibrate. This problem is alleviated with the high impedance approach, which

eliminates any high frequency oscillations and reduces the gain required for display of virtual fixtures. However, it may prove antagonistic to the high fidelity display of virtual fixtures. Performance tradeoffs should therefore be carefully evaluated.

To change the impedance state of the device between virtual free space and virtual constraint in a haptic interface, actuators are utilized in conjunction with a feedback control loop. As the intrinsic impedance in the actuating mechanism and mechanical framework increases, the illusion of free space will be diminished. Therefore, position and force feedback mechanisms ought to be utilized in order to ensure that the minimum motion and force thresholds stay higher than human perception biases. The most important factors to high fidelity performances are speed of operation, safety, and mechanical transparency, size of the available workspace and degrees of freedom, magnitude of possible force output and stiffness range, compactness and achievable control bandwidth.

There are five general actuating mechanisms: (a) magnetic levitation, (b) non-holonomic displays, (c) cable driven linkages, (d) tense stringed system and (e) parallel mechanisms. Magnetic levitation devices have low mechanical impedance, high acceleration and high peak force value. Devices are limited however by the very small working space. Non-holonomic approach has a large workspace and high stability but the system's complexity grows exponentially with increasing degrees of freedom. Linkage devices are readily understood and they can achieve a large working space [67] but these designs are prone to backlash and limited bandwidth [68]. The tensed cable systems can achieve a large working space while maintaining low inertia; however, because of the tension involved, these mechanisms can exercise small forces only. The haptic interface based on parallel mechanisms, on the other hand, seemed most suitable for surgical applications. The parallel structures have better characteristics than standard

serial non-holonomic configurations. Namely, the main advantages are low inertia, high stiffness, high force and torque, large workspace and no backlash [69, 70].

The system proposed in this dissertation will enable us to study compound movements and positions of the human hands. Previous studies have mostly studied human perception by using small movements of the metacarpals and manipulations of the immediate objects. Recent study focusing on a human's ability to track delicate geometric features has yielded positive results [71]. Steele and Gillespie from the University of Michigan studied the accuracy of subject's abilities to duplicate large geometric features with only their isolated haptic sense [72]. They discovered that subjects were able to duplicate large curvatures but were less discriminatory of slight degrees of curvature. We, therefore speculate that human's haptic sense may be used to guide intricate surgical gestures in telementoring and likewise train our proprioceptive systems to duplicate the appropriate motions in the future. In this study we will test the effectiveness of this hypothesis [73].

Previous studies have shown that as haptic guidance helps reduce cognitive loads, is also improves user's motor performance [72, 74]. According to this multiple resource theory, reduced load leads to a cognitive resource surplus that subsequently aids the trainee's learning process [75]. During his investigation in haptic guided driving, Steele verified that haptic guidance did not significantly improve user's control performance under mundane conditions, but significantly improved the results when the user was interrupted by an overtaking maneuver [72]. The subjects were able to closely follow a reference path while requiring fewer visual cues. With haptic feedback, operator error was reduced by 50% [72]. By adding an intuitive modality of pedagogy, we hypothesize that haptic guidance improves the training of laparoscopic surgery.

The haptic exploration process comprises several distinct subsystems: cognitive, decision-making, control of hand motions and physiological sensations evoked by physical interactions. In other words, an explorer makes a decision to extract some qualities of an object such as shape, texture, *etc.* and this leads to a subconscious effort to explore optimal exploratory methods into various hand movements. It is therefore our goal to further characterize these movements.

Transforming these small movements with high fidelity over a long distance in real time poses a significant challenge. Fortunately, our haptic perception space is uniform throughout the workspace and individual biases, even though not insignificant, are small [72]. The study at University of Michigan found their subjects to duplicate better when the wait times are low. Our haptic guidance system will further explore the psychological variation due to these influences.

## 1.8 Software

The software technologies required for our haptic guidance system have largely been developed for other applications. The MS Visual C++ compiler [76] will be utilized to develop the software system. Libraries that are cross platform and robust are available to ensure that the resulting system is portable and will run on most operating systems. Open GL [77] is a technology with demonstrated real-time graphics. For the user interface, both FLTK [78] and GTK [79] have been demonstrated to be versatile, powerful technologies. These libraries are open source standards and are widely used in both the entertainment industry and academia.

## 1.9 Military Significance

This project falls under the auspices of the Telemedicine and Advanced Technology Program (Joint Telemedicine – Effective Employment of Medical Forces). Our haptic guidance system would be used for specialized skill transfer when expert surgeons are not available. Where rough terrain or scarce resources do not allow for specialized medical staffing, such as aboard a nuclear submarine or at research stations in Antarctica, our telementoring system can provide advanced skill transfer. Our intuitive means of guidance can direct the hands of medic trained personnel through MIS gestures executed with standard laparoscopic instrument or with robotic instruments by fusing this technology with the da Vinci robot system (Intuitive Surgical, Sunnyvale CA).

## 1.10 Hypothesis

The overarching hypothesis of this dissertation is that telementoring systems in combination with machine learning algorithms and active haptic guidance, can bridge the gap in learning the advanced surgical skills required for the performance of MIS. Specifically we test the hypothesis that (1) kinematic measures of the instrument spatial motion and orientation combined with machine learning algorithms can assess the state of training for novice surgeons, and lay the foundation for testing the hypothesis that (2) active haptic guidance via kinesthetic force feedback can provide assistance for telementoring and potentially telesurgery.

## 1.11 Dissertation Structure

This dissertation is structured as follows. We discuss the methods employed to execute the UCLA LTS and LapaRobot in Chapter 2. Chapter 3 details the implementation of the final version of the UCLA-LTS. In the following two chapters 4 & 5, we demonstrate the use of UCLA-LTS in a variety of surgical settings for the acquisition of intraoperative instrument motion data to identify procedure-specific surgical skills. In Chapter 6 we develop a system of kinematics-based performance metrics that are later used in Chapter 7 to test the first part of hypothesis #1, namely that kinematics-based performance metrics can be used to differentiate between experts and novices. We test the second part of hypothesis #1 in Chapter 8 when we study the ability of machine-based algorithms to refine the assessment of the state of training. We lay the foundation for testing hypothesis #2 in Chapter 9, where we detail the prototype of the UCLA-LapaRobot and discuss potential avenues for collecting live intraoperative data and providing active haptic guidance via force feedback. We conclude the dissertation with Chapter 10.

## 2 Methods

### 2.1 The haptic-guided telementoring system

In order to continuously monitor the positions of laparoscopic tool tips, MEMS gyrometers and accelerometers will comprise an inertial motion unit (IMU) that records angular velocities and linear accelerations. These velocity and acceleration data will be time-integrated to define the relative position and orientation of the conventional laparoscopic tools. The IMU system will be complemented by a magnetic sensor-based absolute positioning system to recalibrate sensor drift over time.

Software architecture will be developed to translate the two-way position inputs of mentor and mentee into appropriate resistances generated by a high fidelity haptic interface. In order for our users to communicate with each other effectively, an intuitive graphical user interface (GUI) will be constructed to display vital signs, endoscopic video information and video of mentor/trainee.

The user position and orientation input, video and audio of each surgery would be recorded and saved in a database for repeated training and behavior analysis. In order to quantitatively assess the benefits of this system, an evaluation study will be conducted to compare novice operative performance in an animal model when assisted by a mentor in the room versus when assisted by a mentor remotely via a haptic-guided telementoring system.

Our system combines the functionality of real time, intraoperative videoconferencing with haptic guidance that together allow a novice operator to perform an endoscopic procedure with the assistance of a remote expert.



The expert mentor can be any distance away from the operating room, with a monitor at his/her location displaying the novice operator's endoscopic image (**Figure 1**). When the mentor activates his/her control console, phantom instruments are superimposed on the shared endoscopic image. As s/he manipulates his/her instruments, the system tracks and records the starting and ending positions of their path, and orientations coupled with the kinematic and dynamic information such as velocities and accelerations for all six degrees of freedom (DOF). These data are translated into the motion of virtual instruments on a computer screen; a haptic-guidance system provides resistance if the trainee moves off the motion pathway defined by the mentor. The haptic experience for the novice surgeon would be comparable to moving the gearshift in a standard transmission car. Via this haptic guidance system a distant mentor can effectively lay his hands on the hands of the trainee and guide their motions as the novice surgeon executes the procedure.

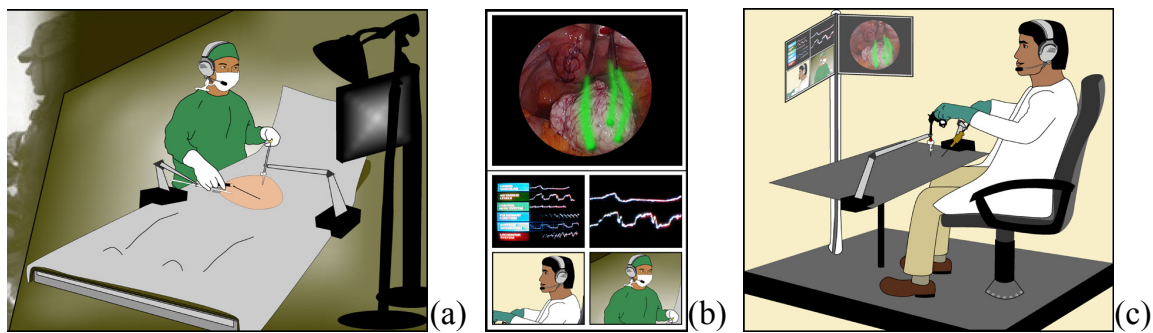


**Figure 1:** Expert telementoring a novice surgeon through a procedure. Information exchange (b) takes place between the mentor station (c) and the novice surgeon (a)

There are multiple potential applications for a system of this nature. In addition to the telementoring application already described, a training simulation could be generated by recording an expert surgeon perform a real operation while using instruments equipped with the

motion tracking sensors, see **Figure 2**. These data are store and later accessed at one or multiple training stations that are designed to reproduce the operating surgeon's ergonomic experience in the recorded procedure. The procedure appears on the screens and the trainees must do their best to make their phantom instruments mimic the motions of the recorded expert's instruments.

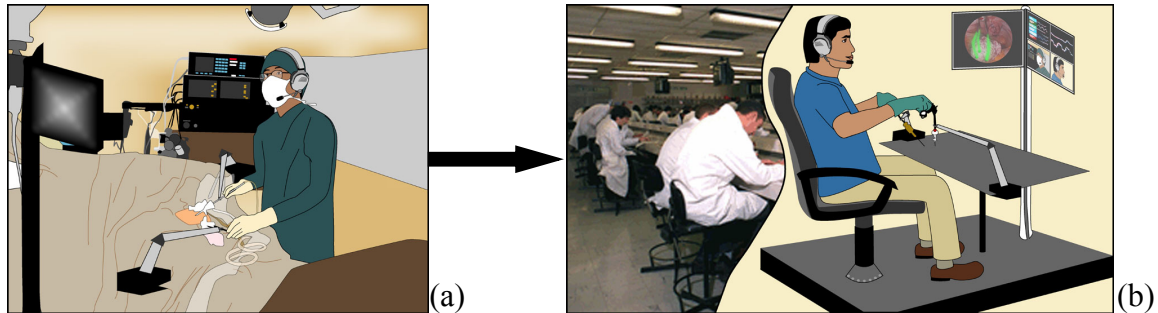


**Figure 2:** Expert surgeon's motions are recorded during the procedure (a) and then these data are used to develop a training simulation where novice surgeons practice by imitating the expert surgeon's gestures (b)

A validation protocol for the telementoring application has been developed which will be described hereafter. Briefly, we will incorporate MEMS inertial sensors into the MIS instruments, design a haptic feedback workstation and engineer a software solution to (1) enable haptic guidance system that allows a remote expert to take medic-level trained personnel through MIS cases and (2) train novice MIS surgeons by providing them with training simulations.

## 2.2 Force Generating Haptic Interface

With the development of video games virtual reality and more recently robotic surgery, the symbiosis of computers and humans has created a strong demand for a more efficacious information-exchange interface.

The focus of this study is an adaptive learning platform that provides an intuitive way of learning via proprioceptive information. In addition to receiving video and audio feedbacks the Haptic Guided Telementoring System will generate resistance upon deviation from the mentor’s desired motion, effectively creating a virtual surgical gearshift.

In consideration of application requirements we plan on adapting one of three different commercial haptic interfaces in our haptic system: Phantom from SensAble, Delta from Force Dimension and Impulse Engine from Immersion. These point interaction interfaces fit perfectly with the inherent point nature of laparoscopic surgeries. Anticipating the force level required in surgical gestures as listed in the literature and verified experimentally, we anticipate the highest resistance to be around 20 Newton (N) in order to maximize the palpable range for the operating surgeon. Such range shall provide significant resistance that discourages the novice trainee from deviating from the mentor-defined path.

**Table 1:** Haptic Devices Comparison

Manufacturer	SensAble	Force Dimension	Immersion
System	Phantom	Delta	Impulse Engine
DOF	6	6	6
Translation (mm)	260 x 460 x 120	360 x 360 x 300	152 x 152 x 152
Linear Resolution (mm)	0.03	0.03	0.02
Angular Resolution (mm)	0.002	0.04	0.02
Translation Force (N)	8.5	20	8.9
Operating System	Windows	Windows/Linux	Windows

As shown in **Table 1**, upon comparing three commercial systems we find Delta to be our best candidate. Phantom’s motor drive electronics are voltage driven, and for DC motors, torque is proportional to current, therefore high frequency stimuli may likely lead to instability.

Further, the limit on Phantom's indirect velocity measurement is 30mm/s. Exceeding this limit may induce instability at moderate velocity gains in the control loop [80].

Given the typical length of a laparoscopic tool the working space needs to be large in order to be practical. Coincidentally, Delta has the biggest workspace among all commercial haptic platforms. But due to its actuating mechanisms, we expect the kinematic models to be complex.

The Delta device is a six degrees-of-freedom mechatronic device driven by a desktop computer. Based on this platform we plan to develop an innovative adaptive training system that meets the high fidelity required for surgical applications with its high strength, high stiffness and high sensitivity.

Our proposed adaptive mentoring system will promote learning by introducing a virtual gearshift that guides surgical pathways. The haptic interface will keep a detailed record of the tool's position and orientation and generate smooth resistance when the trainee deviates from the mentor's pathway, thus creating a gross perception of the appropriate path. The haptic guidance will result in the proprioceptive feedback to the Golgi tendon organs (GTO) and muscle spindles, sensitive to force and position/velocity respectively. This proprioceptive feedback is an intuitive and superior modality to learn the laparoscopic gestures from a remote mentor. Further, our haptic feedback guiding system ensures that only the position and orientation data of the mentor's instruments is transmitted from a remote environment. The signal processing and generation of psychophysical resistance is created entirely on the trainee's haptic interface. The few fidelity requirements and local communication minimizes signal delay and system complexity and is therefore more suitable for telementoring.

Based on the mechanical sensitivity of our bodies [81], specific requirements to realize adequate haptic perception remain to be investigated. We address these in the following section.

## 2.3 Verification of Haptic Perception

### 2.3.1 Hardness Perception

High stiffness control is critical to accomplish perception of material hardness. Based on its published specifications, the Delta system is more suitable to convey the hardness sensation. At the same time, changing the ratio of initial rate of change ( $\partial F/V$ ) of force F and initial velocity V upon penetrating the surface is shown to be major factor that humans use to differentiate virtual surfaces. This will further be explored by adding damping in the virtual surface, effectively stabilizing the control system. This apparent perception paradox can be used to improve the performance in haptic interfaces. At the same time, such dynamic compensation does not require mechanical modifications in the hardware [82].

### 2.3.2 Motion perception

Taking advantage of the natural capacity of the nervous system to adapt to altered mechanical conditions we will design a resistance field to test the psychological perception of the field. Position, velocity and acceleration will be measured with our instrument tracking system. Significant variability between each user is expected as well as low threshold of differentiation. We also expect that the subjects will retain this new information if extensive practices were ordered. We speculate that subjects will be able to duplicate such gestures with lower count of mistakes afterwards.

### 2.3.3 Performance Measures

An assistant will administer the test instruction and this test will be administered with and without visual cues. The participants will get a brief training on the operating site and on generating the desired gestures. The software will record the number of obstacles collisions and the instrument's lateral deviations from the mentor's path. The other variable is haptic guidance: both variables will be turned on/off randomly.

### 2.3.4 Dry Lab Testing

Force transducers will be attached to the laparoscopic surgical instruments in order to compare the generated resistance to forces measured by the force transducer. Force field and frequency response of the modified haptic interface will also be assessed. We do not expect any change in resistance output from our modifications however. By means of software engine the reactive forces will be generated to guide the subject. We will also investigate the appropriate amplitude and period of forces in order to guide the user to the desired movements.

## 2.4 Tracking System

### 2.4.1 System requirements

Ideally the system requires a high accuracy navigation system to track the instruments. As part of the study we will investigate the levels of accuracy desired for this particular application. Another important requirement is that additional equipment does not interfere with other instruments within the operative space, and therefore the chosen communication system has to be immune to the various sources of interference, such as electromagnetic, optical, *etc.*

That being said, wireless operation is highly desirable in such an environment. Additionally the system has to operate continuously, while maintaining the ability to be turned OFF by the operator. Real-time capability is also very important, as position data have to be updated frequently enough that human operators are not aware of the time delays, or at least not seriously disturbed by them.

#### 2.4.2 Proposed Tracking System

It is assumed that identical tools are to be used by both the mentor and the student, which means that tracking the handle of the tool is equivalent to tracking the tip of the tool. Tool orientation is defined by both the handle orientation and the orientation of the rotary knob on the handle.

The tracking system will be using as many off-the-shelf components as possible. This study will help identify the commercially available materials and then assess their performance characteristics and further define those parameters and their values that are critical to a deployable final version.

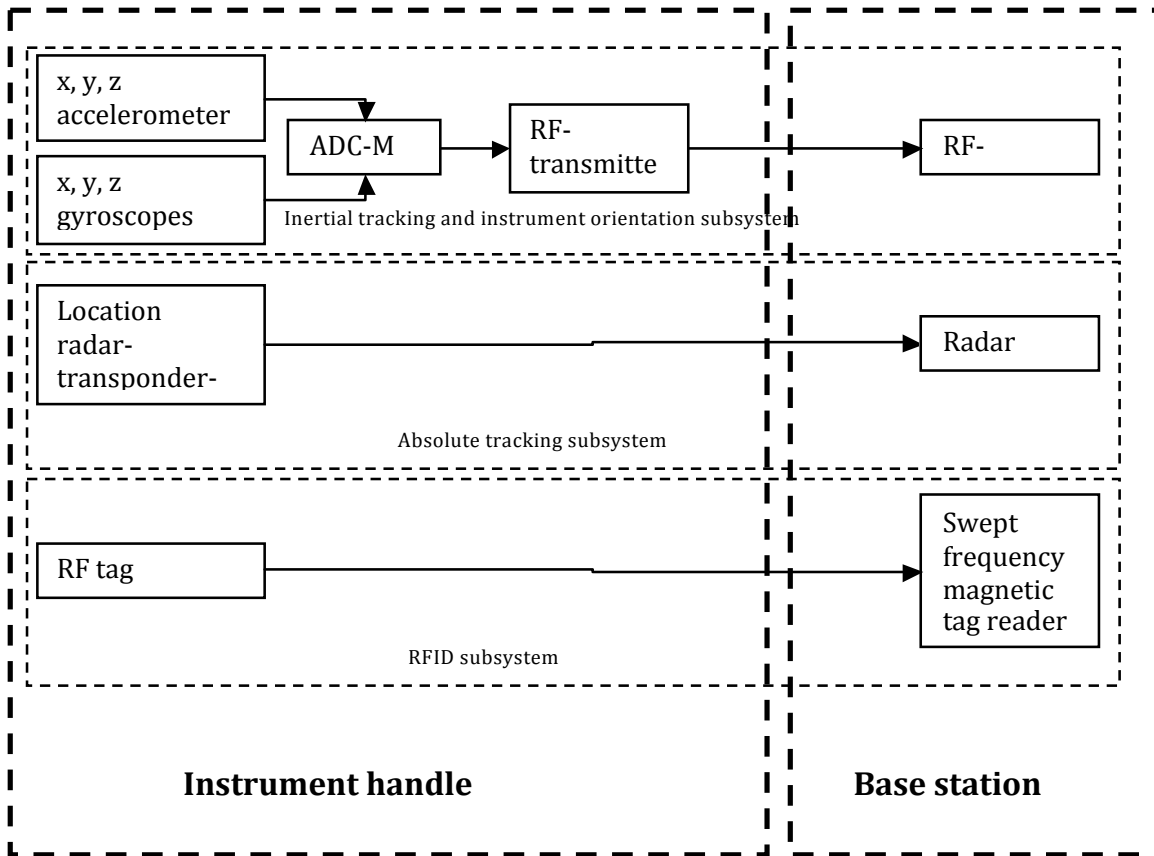


**Figure 3:** Proposed tracking System Hardware Diagram

We propose a hybrid tracking system composed of several subsystems as described in **Figure 3**. An absolute tracking system is based on the previously described tracking technologies. First part of this study is to identify the most suitable technology to the demands of the operative environment and then build a prototype based on the chosen technology. This is to be supplemented by a six degrees of freedom (DOF) inertial tracking unit (IMU) and an instrument orientation system based on three linear accelerometers and three angular rate gyrometers aligned to the axes of an orthogonal coordinates system. MEMS inertial sensors will be used for the IMU for their small size, low power consumption and sensitivity to the range of human accelerations and angular velocities. Each surgical instrument will be uniquely identified with a RFID tag. A radio frequency (RF) wireless communication system will be used for



connecting the laparoscopic instrument with the base station. The base station computer will provide the master control unit. It integrates the tracking subsystems components with the rest of the haptic guidance system. The control unit tracks each tool in the operative environment for identity, position and orientation. As a final step, for the hardware component we will develop a packaging solution for the instrument handle. The goal is to assemble all the mobile subsystems in the instrument handle in a design solution that would satisfy requirements for small size of 50 x 30 x 30 mm, reduced weight of around 100 grams and ease of sterilization.

### 2.4.3 Proposed Software

The proposed software system will be used in two different applications: (a) Telementoring, where an expert surgeon at a remote location will guide in real-time a less experienced surgeon to perform an MIS procedure. (b) Training, when it will use recorded sessions of expert surgeons performing MIS procedures to guide and evaluate the performance of surgeons in training.

The technical challenges behind the dual goals of the proposed software are mainly due to the hardware's complexity and the real-time operation requirement. The software system will support a range of sensors; process their information in real-time and display the computed information on both the student and telementor screen. The most interesting technical challenge here is the control of the haptic interfaces that provide force feedback to the student or the operating surgeon. To achieve this control, the software system will need to directly access device drivers and include low-level access to the hardware components.

Training and remote operation systems require careful design and effective user interfaces. Choosing the correct representations and forms of feedback will require input from

actual users. For example, it may turn out that users prefer to hear prompts about their errors rather than see flashing screens or vice-versa. Similarly, we need to evaluate our performance metrics and identify the correct ways to display them to the users during the training or telementoring session. To ensure the most effective software design, we plan to consult regularly with users during the development of the system and revise our design choices accordingly.

The initial programming for interfacing all the components will be done in C++ using object-oriented design. The motion representation will be based on standard B-spline interpolation [83]. The scripting language that will be part of the interface will be based on Python and the interface will be based on FLTK. Finally the real-time graphics subsystem will be based on OpenGL.

#### 2.4.4 Establishing Construct Validity for Training Simulator Function

To establish a training simulation, an expert MIS surgeon will be monitored and recorded via our haptic guidance system as s/he performs a laparoscopic cholecystectomy in a pig model. The recorded data will be analyzed and broken down into series of tasks including: initial exposure, initial dissection, cystic duct dissection, cystic artery dissection and gall bladder fossa dissection. The training simulation is then loaded into a haptic guidance system that is set up on a table such that the ergonomic experience of the mentor is recreated for the student. For each task, the trainee watches the video first and then as the video replays, s/he attempts to duplicate the recorded mentor's hand and instrument motions with his/her own virtual instruments. In order to establish construct validity we will assemble a total of 10 participants: 5 novice laparoscopic surgeons in their fellowship training and 5 expert laparoscopic surgeons.

After each training session is completed, the system will present the student with an overall assessment of his/her performance. Our initial approach includes the following metrics: (1) time required to complete the task, (2) efficiency, *i.e.* how long was the path-length of the instrument tip required to complete the task, (3) error, *e.g.* deviation from the assigned path above a permissible value could be displayed on the monitor as a red bar of increasing length for increasing error size. The system will show the student where the most serious errors were made, so that on a follow-up session the student can work on fixing those errors. To compute the overall error we will first align the motion of the student's instruments to the recorded motions using Dynamic Time Warping (DTW). Then will compute the root mean square (RMS) error of the aligned motion curves.

The above criteria are established outcome measures for surgical simulators as described by Cosman and colleagues [84]. In addition, by virtue of the accelerometers in our training station instruments, we can monitor the student's hand orientations *e.g.* to determine if his/her hands are in an ergonomically correct position during movement. Score deductions are based on the degree of deviation and duration of time the participant's hands are positioned differently than the recorded mentor's hands. This does assume that the videotaped mentor's hands were ergonomically correct to begin with. Ergonomic correctness is determined by assessing character of motion and tremor. Character of motion evaluates whether the motion was characterized by many rapid motions (accelerations and decelerations) consistent with "jerky" movements or was it smoother. Tremor looks at the amplitude of the user's natural tremor. Each participant completes the same training simulation twice. Each participant is then scored in term of the outcome variables described above. The mean scores of the novice participants are compared to the mean scores of the expert participants. In order for construct validity to be

satisfied, expert laparoscopists should consistently outperform the novices in each of the outcome criteria and in their overall scores.

#### 2.4.5 Feasibility Study for Telementoring System in Animal Model

We feel that the first generation device is most practically applied to more basic MIS procedures including cholecystectomy, appendectomy, and diagnostic laparoscopy. In these situations, a patient in a remote location would normally require expensive transport and /or a period of disability associated with an open procedure. Via our device, we hope to offer a safe, local laparoscopic procedure that minimizes both cost and patient disability.

The goal of the in-vivo experiments is to determine whether a novice surgeon may complete a laparoscopic procedure with a similar level of safety when (1) there is an expert mentor in the room or (2) the expert mentor guiding the procedure remotely via our haptic-guidance system.

For the purposes of this pilot study we will recruit twelve third and fourth year medical students. Power analysis (STATA, StataCorp LP, College Station, TX) revealed that six subjects per group should be sufficient to detect clinically significant difference between groups. These students are individuals who have an understanding of anatomy and had some patient contact, but have minimal personal experience with surgery or laparoscopy. We feel that they represent a group comparable to army medics. All participants will complete a survey that gathers demographic information and reviews criteria that have been associated with superior laparoscopic performance. Then all participants will watch a video that describes step-by-step how to perform a laparoscopic cholecystectomy in a pig model. The pig model was selected because it is a well-established, readily available model for laparoscopic procedures. An

approved ARC (Animal research Committee) protocol (#2002-190-02) at UCLA includes the procedures described hereafter.

The students are then randomized by coin-flip into one of two groups. Group A members will perform a laparoscopic cholecystectomy with the assistance of an expert mentor in the room performing assistant tasks. Group B members will perform the same procedure with two differences: the assistant tasks will be performed by someone who simply drives the endoscope and grasps per student's directions, while the expert mentor guides the procedure remotely via our haptic guidance system. Upon completion of the procedures the animals abdomens from both groups are thoroughly inspected by a staff member to rule out any previously unrecognized bleeding, injuries, *etc.* and the animals are then euthanized.

Outcome measures include: (1) a validated score sheet for laparoscopic cholecystectomy prepared by Eubanks et al [85], (2) operative time, (3) estimated blood loss, (4) participant survey (addresses how comfortable novice is performing the procedure), (5) expert mentor survey (addresses how comfortable the mentor is guiding the procedure).

# 3 Immersive Training and Mentoring for Laparoscopic Surgery

Chapter 3 is a version of the article published in SPIE-2007, Authors: V Nistor, B Allen, E Dutson, P Faloutsos, GP Carman [2]

## 3.1 Abstract

We describe in this paper a training system for minimally invasive surgery (MIS) that creates an immersive training simulation by recording the pathways of instrument from an expert surgeon while performing an actual training task. Instrument spatial pathway data are stored and later accessed at the training station in order to visualize the ergonomic experience of the expert surgeon and trainees.

Our system is based on tracking the spatial position and orientation of the instruments on the console for both the expert surgeon and the trainee. The technology is the result of recent developments in miniaturized position sensors that can be integrated seamlessly into the MIS instruments without compromising their functionality. In order to continuously monitor the position and orientation of laparoscopic tool tips, DC magnetic tracking sensors are used. A hardware-software interface transforms the coordinate data points into instrument pathways, while an intuitive graphic user interface displays the instruments spatial position and orientation for the mentor/trainee together with endoscopic video information. These data are recorded and saved in a database for subsequent immersive training and training performance analysis. We use two 6DOF, DC magnetic trackers with a sensor diameter of just 1.3 mm – small enough for

insertion into 4-French catheters, embedded in the shaft of an endoscopic grasper and needle driver. One sensor is located at the distal end of the shaft while the second sensor is located at the proximal end of the shaft. The placement of these sensors does not impede the functionality of the instrument. Since the sensors are located inside the shaft there are no sealing issues between the valve of the trocar and the instrument.

We devised a peg transfer training task in accordance to validated training procedure and tested our system on its ability to differentiate between the expert surgeon and the novice trainees, based on a set of performance metrics. These performance metrics: motion smoothness, total path length and time to completion are derived from the kinematics of the instrument. An affine combination of the above-mentioned metrics is provided to give a general score for the training performance.

Clear differentiation between the expert surgeons and the novice trainees is visible in the test results. Strictly kinematics based performance metrics can be used to evaluate the training process of MIS trainees in the context of the UCLA-LTS (Laparoscopic Training System).

## 3.2 Introduction

Minimally invasive surgical (MIS) techniques such as laparoscopic surgery are used for many common operations such as gallbladder removal, appendectomy and hernia repair [86]. MIS technique provides many advantages over the classical approaches such as: shorter hospital stays, faster recovery times and minimal scarring resulting in improved cosmetics [87]. While the MIS advantages are mostly affecting the patient outcomes the extended training time required to achieve proficiency are among its major disadvantages. Currently employed training

methodologies rely on dry box simulators followed by actual surgical operations. Given the extensive growth of simulation software during the last couple of decades, for example training airplane pilots on computer simulations, one would expect the medical profession to be at the forefront of these simulation systems. While there have been attempts at developing training platforms, a widely accepted system by the medical and surgical community for interventional training does not currently exist. Therefore, there is an immediate need to develop superior cost effective training systems that are to teach the next generation of laparoscopic surgeons.

The general consensus of the surgical community is that training should be structured and skill level assessed at various levels. Rosser and collaborators [88, 89] addressed this aspect when they evaluated the suturing skills of trainees in a dry box environment. Similarly, in a study aiming to compare the reliability of various scoring systems, Martin et al [90] tested overall surgical skills following live animal tissue training compared to dry box models and concluded that the acquired skill set was equivalent between the two methods. Traditional apprentice-model type training during actual surgical procedures is time consuming [91] and does not obviate the need for additional skills-acquisition training as found in a study by Chen [92]. Furthermore, training in the operating room (OR) exposes the patient to risk and the opportunities for OR training are further reduced by the recently mandated reduced working hours for surgical trainees [91]. Therefore a need exists for virtual reality (VR) based trainers to at least master the basic skills and thereby reduce the length of the learning curve involved in acquiring the MIS skills [91, 93]. Additionally the digital nature of these training systems allows automated and standardized scoring of performance, thus eliminating the confusion and bias of subjective performance interpretation.



There have been several attempts at creating VR based trainers for laparoscopic surgery [92-94]. Some of these projects have yielded commercially available products but so far none has gained wide acceptance in the surgical community. For example the Virtual Laparoscopic Interface (VLI) and the Laparoscopic Surgical Workstation (LSW) [32] from Immersion Corp. tracks two instruments for their spatial position and orientation (a total of five degrees of freedom) with near real-time representation of hands movement on screen with the addition of touch sensitivity to visual cues for the LSW. Both of these technologies have been licensed to other developers such as LapSim [95-97] (Surgical Science, Minneapolis, MN) and MIST-VR [94] and ProCedicus-MIST (Mentice AB, Göteborg, Sweden). Similar training systems have been investigated elsewhere: Xitact (Xitact SA, Lausanne, Switzerland) [98-100], Virtual Environments for Surgical Training and Augmentation (VESTA) [101], the Computer-enhanced laparoscopic training system (CELTS) [102]. The MIST-VR system appears to have been the most intensively validated [103, 104]. This system was also used to investigate various aspects of laparoscopic training such as the set of skills required to transfer from VR training to surgical endoscopy [105], VR sensitivity to user's experience [106], establishing target scores and benchmarks [107] defining performance baselines [108], measuring the skills of novice trainees [109] and their ability to differentiate between experts and novices [110].

This brief overview indicates that a variety of training systems with varying degrees of complexity or specialization have been proposed for teaching laparoscopic skills. Their wide spread adoption has been limited however by questions about how relevant these skills are to the actual endoscopic surgery [111, 112]. The primary concern is that these VR simulators are limited in their ability to transfer a general set of endoscopic surgical skills and primarily focus on simple psychomotor skills [113]. Furthermore, even when addressing psychomotor skills,

these simulators have not proven to be superior to basic training techniques such as videotape [113] or basic trainer boxes [30, 111]. Some of the shortcomings highlighted in these studies include the limited number of tasks available for training, inability to reflect anatomical variation in patients and variability in technical approach to a given situation. Therefore, there still exists a need for a virtual trainer that transfers surgically relevant psychomotor skills in the context of a realistic surgery scenario. This study details the development of a hybrid training system that will ultimately combine dry box trainers with virtual reality to specifically address these needs.

### 3.3 System Overview

The computer based UCLA-LTS (Laparoscopic Training System) is based around the idea that surgical procedures must be taught on actual surgical devices rather than simulated systems. To that end the UCLA-LTS uses actual laparoscopic instruments with seamlessly integrated position and orientation-tracking sensors. The sensing signals are visually produced on a screen in real time graphic form, as well as recorded for later feedback. The sensing data are fed into a software package to assess the performance metrics of the surgeon as well as provide individual scores on specific metrics and a final compound score. In general terms this system consists of a mechanical interface with instruments and tracking sensors, a software interface that acquires the data relating to the motion of each instrument, and a cognitive and psychomotor skills evaluation software, based on analysis of the instrument kinematics. This system combines the advantages of computer-based simulation with the features and simplicity of the traditional training boxes, which allows it to be easily customized in situ for a wide array of training tasks.

The general configuration of the UCLA-LTS is illustrated in **Figure 4**.

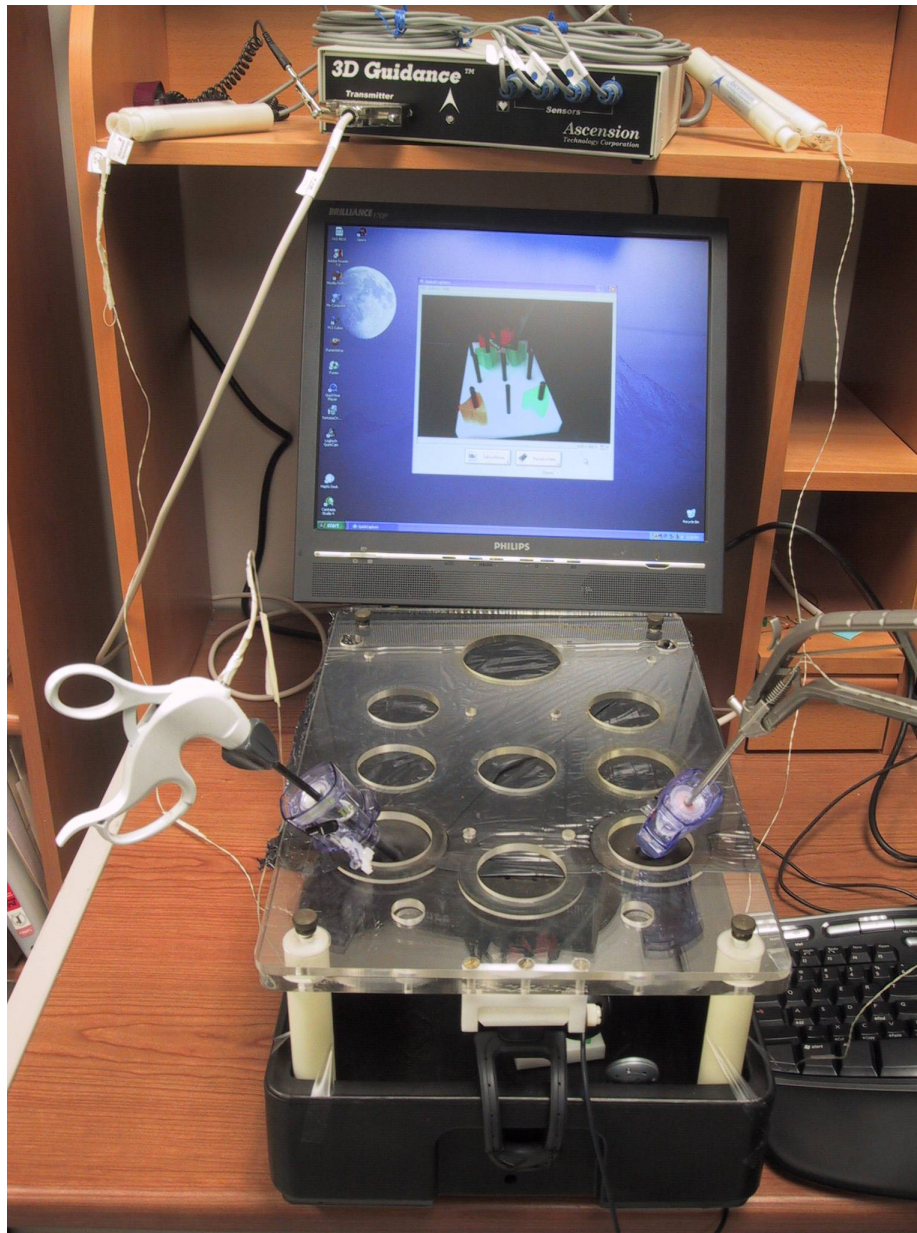


**Figure 4:** Operator's view of the UCLA-LTS. The laparoscopic instruments and trocars are inserted in the training box portholes visible in the fore plan. To the front of the box is the webcam providing video feedback on the computer monitor. The control box for the magnetic tracking system is placed on the top shelf. The active source electromagnet of the tracking system is placed in a fixed position behind the training box and not visible in this image.

The laparoscopic training box has the porthole plate covered with an opaque rubber material such that operators will see their instruments in action only on the computer monitor.

Each laparoscopic instrument is inserted into the porthole through a trocar, just like in an actual endoscopic surgery, which forms a friction joint with the rubber of the porthole simulating the friction normally encountered between the trocar and the abdominal tissue.

A pegboard from the training kit approved by Society of American Gastrointestinal and Endoscopic Surgeons (SAGES) is placed inside the training box and fixed in place with Velcro fasteners. A DC electromagnetic tracking system (Trackstar, Ascension Technologies, Shelburne VT) is used to continuously monitor the position and orientation of each laparoscopic instrument. The active source electromagnet is rigidly attached to the far side of the training box, not visible in **Figure 4** and provides a fixed reference of coordinates. The control box is placed on the top shelf behind the control box. Wiring from the electromagnetic tracking sensors is routed from each laparoscopic instrument to the control box, which in turn is linked to the desktop computer via a USB port. Visual feedback normally coming from an endoscopic camera is currently provided by a USB based webcam, rigidly attached to the front of the training box to allow for single user operation. An assistant is needed to operate the endoscopic camera in actual surgeries. The computer monitor displays the video feed from the webcam as well as a graphic user interface with performance monitoring graphics.

### 3.3.1 Instrument Tracking

For this study two most commonly laparoscopic instruments were modified: a tissue grasper (Ethicon Endosurgery, Cincinnati OH) and a needle driver (Karl Storz GmbH & Co. KG, Tuttlingen, Germany). Each of the two instruments was adapted to accommodate two seamlessly integrated DC electromagnetic sensors (microBIRD, Ascension Technology, Shelburne, VT) as shown in **Figure 5**. These are three-axis magnetic sensors that contain three

orthogonally oriented coils, encased in an epoxy-based coating that forms a basic three-axis ring core fluxgate magnetometer.



**Figure 5:** Ascension microBIRD sensor

The fluxgate magnetometer makes use of an active source DC electromagnet, **Figure 6**, employing three orthogonally oriented coils excited by a several millisecond long pulsed DC current applied sequentially to the three coils. The active electromagnet is rigidly attached to a fixed and known spatial position and orientation with respect to the training box.



**Figure 6:** Fixed and active DC source electromagnet

The active source electromagnet generates a known flux density vector  $\vec{B}$ . A sensing coil at radius  $r$  and angle  $\theta$  away from the center of the source electromagnet will produce a current  $I$ , proportional to the flux density  $B$ , which in turn is proportional to  $\cos(\theta)/r^3$ , **Figure 7**.

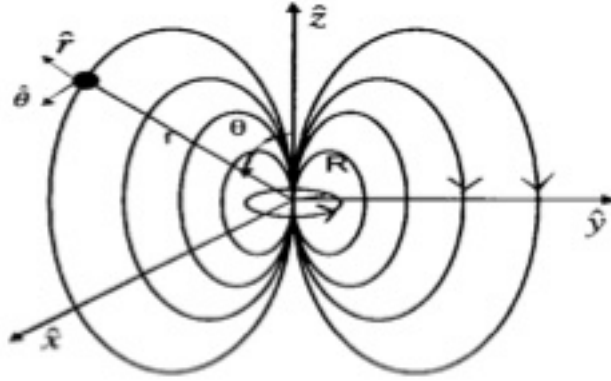


**Figure 7:** DC magnetic field of the source electromagnet

By employing a sensor with three orthogonally aligned coils as seen in **Figure 8**, all three  $B$  vector projections  $\vec{B}_x, \vec{B}_y, \vec{B}_z$  are captured together with their angular rotations  $(\alpha, \beta, \gamma)$ . According to the manufacturer, the working space for this arrangement is a sphere of 0.5m radii from the fixed electromagnetic unit. The training box restricts the working space to a much smaller radius of less than 0.3m, where the static resolution of the sensors is estimated to be better than 0.5mm for position and 0.1° RMS angular orientations.

The output from the control unit provides 90 measurements of position and orientations per second. A recent study by Hummel looked [114] at the potential application for these kind of sensors in endoscopes and guiding wires. Their experimental measurements had largely confirmed these data and suggest many opportunities exist for spatial tracking during medical procedures. For the purpose of this study we consider this level of accuracy and resolution to be sufficient. To compensate for the magnetic field distortions due to the presence of metallic objects we employ two of these sensors per instrument, one distally located at the instrument tip and another proximal in the instrument handle.

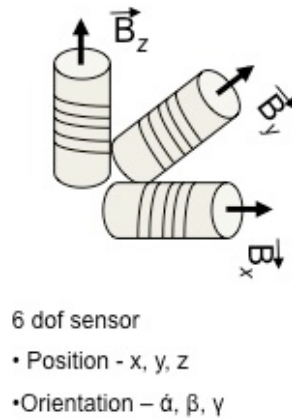


**Figure 8:** Tri-axial fluxgate sensor

The sensors used in this study are miniaturized to a size 4-French equivalent to 1.3 mm in diameter and approximately 5mm in length.

### 3.3.2 Sensor Integration

The goal was to integrate the sensors into the shaft of each laparoscopic tool without affecting their functionality. It was immediately obvious that any wire along the shaft of the instrument would prevent a proper seal between the instrument and the trocar, there. Further, each laparoscopic instrument was disassembled and examined for opportunities to integrate these sensors inside. It was observed that due to their small diameter, there is just enough space to place these sensors between the actuating rod and the inner side of the shaft.

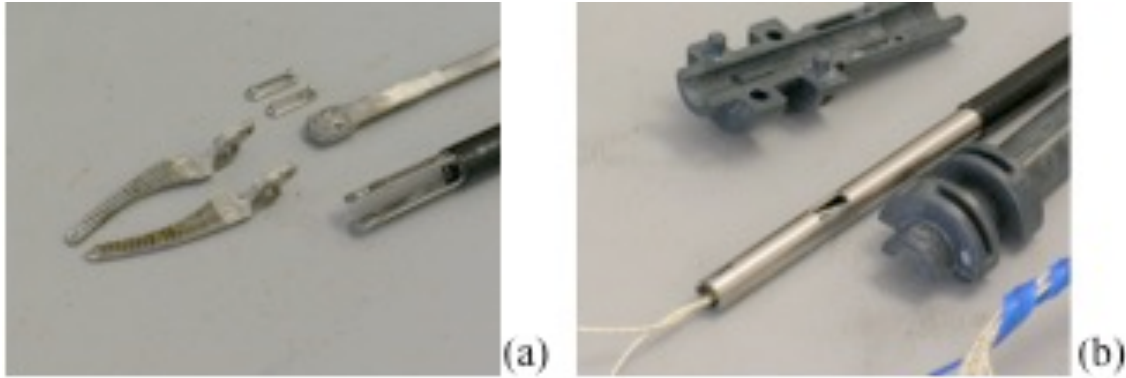


**Figure 9:** (a) Ethicon grasper disassembled and (b) wiring from the sensors pulled through the metal shaft.

Therefore the distal sensor was placed inside the shrouded part of the metal shaft just behind the articulation for the grasping jaws, at a distance of 25 mm from the tip, when the jaws are closed, **Figure 9a**. The proximal sensor is similarly placed 50 mm from the opposite end of the instrument shaft just before the cut in the shaft that locks to the instrument handle **Figure 9b**. The sensor wires are thus contained inside the shaft and are routed through the electrocautery connector of the instrument handle as seen in **Figure 10a**. After about 24 hours, the epoxy holding the sensors is fully cured and the instrument is re-assembled, as shown in **Figure 10b** with only the sensor wiring visible. The wiring is 0.9mm in diameter, due to the nature of its insulation is very flexible, and does not easily make kinks. At 2 m long, it provides enough working space for the surgeons and the trainees.

Before each training session the tracking-system is turned ON and the calibration procedure is initiated by placing the instrument tips in specific positions and orientations when prompted and held steady until procedure is complete.



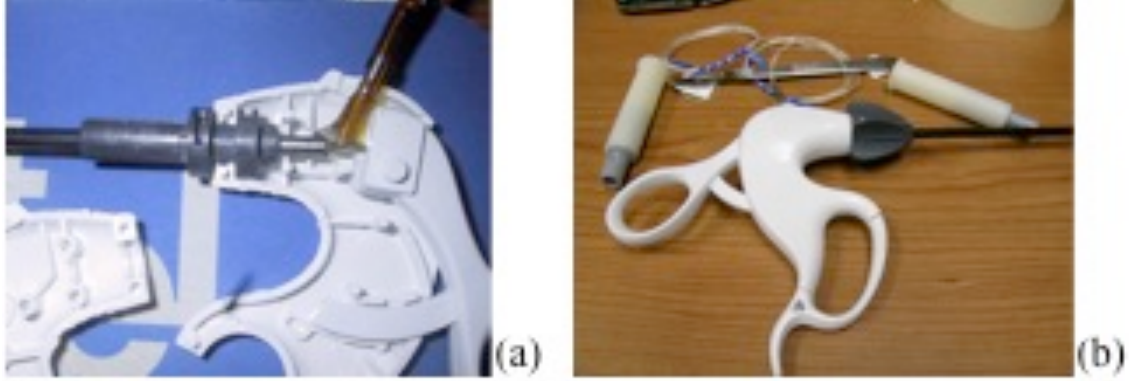


**Figure 10:** (a) Ethicon grasper with the handle disassembled to show the sensor wiring and (b) the assembled grasper handle with the sensors wiring and their connectors to the Bird control unit.

### 3.3.3 The Hardware-Software Interface

Each of the four sensors integrated into the laparoscopic tools provides its position as three words: X, Y, Z and orientation as either a nine words that are the elements of a 3x3 orientation matrix  $M(i,j)$ , the three Euler angles: azimuth, elevation, roll or the four quaternion elements. In this study we used the rotation matrix, expressed in terms of the three angles: roll (R), elevation (E) and azimuth (A) to define the orientation of each sensor with respect to the reference electromagnet.

$$M(i, j) = \begin{bmatrix} \cos(E) * \cos(A) & \cos(E) * \sin(A) & -\sin(E) \\ -\cos(R) * \sin(A) + \sin(R) * \sin(E) * \cos(A) & \cos(R) * \cos(A) + \sin(R) * \sin(E) * \sin(A) & \sin(R) * \cos(E) \\ \sin(R) * \sin(A) + \cos(R) * \sin(E) * \cos(A) & -\sin(R) * \cos(A) + \cos(R) * \sin(E) * \sin(A) & \cos(R) * \cos(E) \end{bmatrix}$$

For the proximal sensor the position and orientation is described by the elements of a standard computer graphics modeling matrix  $P_p(i,j)$ .

$$P_{p(i,j)} = \begin{bmatrix} P_{11} & P_{12} & P_{13} & 0 \\ P_{21} & P_{22} & P_{23} & 0 \\ P_{31} & P_{32} & P_{33} & 0 \\ X_p & Y_p & Z_p & 1 \end{bmatrix}$$

A similar modeling matrix is required to describe the position and orientation of the distal sensor  $P_d(i,j)$ .

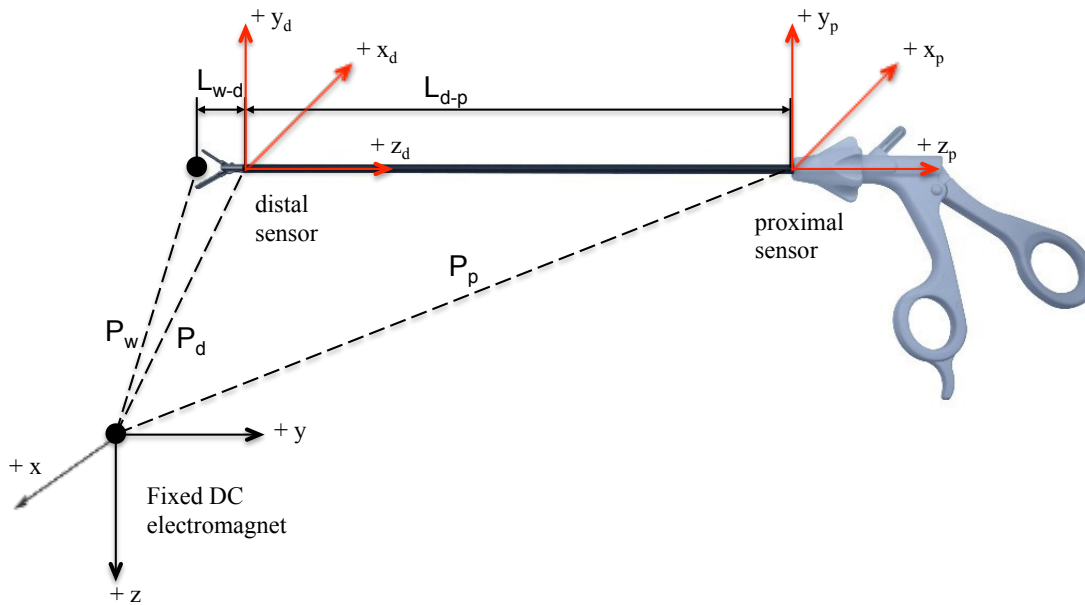


**Figure 11:** Coordinate systems for the fixed reference DC electromagnet and the sensors embedded in the instrument

The standard computer graphics coordinate system for each sensor has the plane XY parallel to the plane of the monitor display, with positive X to the right and the positive Y pointing up, while the positive Z pointing out of plane towards the observer, see **Figure 11**. The reference fixed DC electromagnet is placed distal from the observer at the back of the training box with the positive Y pointing towards the observer.

To have the instrument phantom on the computer screen follow the position and orientation of the surgical instrument, the coordinates measured with respect the fixed reference electromagnet was transformed to the screen coordinates for each sensor. Thus the screen coordinates for the proximal sensor will be  $P_p^s(i, j)$ .

$$P_p^s(i, j) = \begin{bmatrix} P_{11}^s = M_{22} & P_{12}^s = M_{23} & P_{13}^s = -M_{21} & 0 \\ P_{21}^s = M_{32} & P_{22}^s = M_{33} & P_{23}^s = -M_{31} & 0 \\ P_{31}^s = -M_{12} & P_{32}^s = -M_{13} & P_{33}^s = M_{11} & 0 \\ X_p^s = -X_p & Y_p^s = -Z_p & Z_p^s = Y_p & 1 \end{bmatrix}$$

The working end-effector is represented on the computer screen  $P_w^s(i, j)$  as a 325mm translation of the proximal sensor where  $Z_w^s = Z_p^s - 325$ , or 25mm from the distal sensor, where  $Z_w^s = Z_d^s - 25$ .

The software component of the system is comprised of separate interfaces for data acquisition and analysis. Both interfaces make use of a common library for trace analysis written in C++. The acquisition application provides a simple interface using the FLTK windowing library to store new traces in the motion database. The analysis application uses the OpenSceneGraph library to allow real-time, three-dimensional playback and analysis of user traces from the motion database. To assist the user in self-assessment, several performance metrics are computed by the common library and reported via the graphical user interface.

### 3.4 Test Description

The exercises in the training program are designed to train hand eye coordination skills specific to the laparoscopic surgery. These exercises can be standardized or customized for the

individual needs or requirements of a specific student or program as defined by the training supervisor.

Using the console, the mentor defines the appropriate basic skill pathways for the novice surgeon to manipulate his/her instruments, over a set of synthetic tissue models. An immersive training simulation is generated by recording an expert surgeon perform these training tasks. These data are stored in the database and later accessed at one or multiple training stations that are designed to reproduce an operating surgeon's ergonomic experience.

Due to the system design, the specific tasks for a basic training session are independent of the performance metrics. The basic performance metrics are based strictly on kinematic analysis of the instrument motion. This approach offers flexibility for in situ and impromptu designed training tasks as deemed appropriate by the mentor.

For more complex training scenarios or even complete surgical procedures a different set of performance metrics are to be designed that should take into account the transition from a skill based behavior to a rules and knowledge based behavior [115].

In this study we start with a short explanation of the difficulties encountered during laparoscopic surgery: fulcrum effect, the use of long instruments, poor depth perception and disorientation, *etc.* with the goal of mentally preparing the trainee to the difficulty of the task ahead. Following the preparation, the trainee is then introduced to the training task as described in **Figure 12**. This is a peg transfer task that involves both hands in basic skills of tissue grasping and manipulation, all the while keeping the instrument tips in a confined space. The steps described in **Figure 12** show only the transfer of a rubber piece from the right hand peg to the left hand peg. To complete this training task, the steps described above need to be repeated

in reverse order such that the rubber piece is now transferred from the left hand peg back to the right hand peg and again with both instrument tips ending in the central resting position. Each trainee repeats the complete peg transfer 10 times and then we proceed to analyze the kinematic performance parameters for each participant in this study.

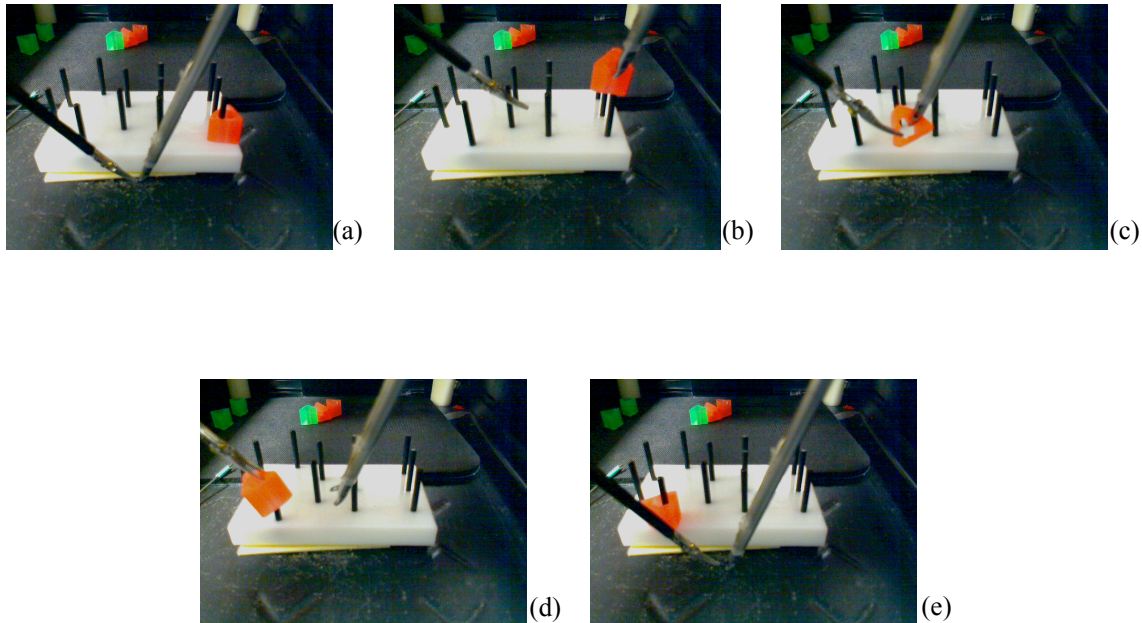


**Figure 12:** Peg transfer training task: (a) start with both instrument tips in a central position, (b) pick the rubber piece located on the right side peg with the right hand needle driver and lift it off the peg, (c) bring it over the training board and pass the rubber piece to the left hand grasper. (d) Using the left hand grasper place the rubber piece over the peg located on the left side of the training board, (e) release the rubber piece and bring both instruments back to the starting point.

### 3.5 Performance Metrics

To develop an adequate training approach we propose specific objective metrics to assist in the evaluation of laparoscopic surgery skills. While a variety of metrics have been suggested by other researchers [116], they have met with various degrees of success [103]. The development of metrics that successfully distinguish motions made by novice trainees from those made by expert surgeons is non-trivial, and their validation is expensive and time consuming.

For these reasons we believe that a systematic and rigorous approach to the development of new metrics should be used. As a first step, we approximate the instrument tip motion of an expert surgeon using the UCLA-LTS to the normal hand end-effector motion, as if the tool has become an extension of the surgeon's own limb, for the purpose of motion planning. This suggests that the neurophysiologic findings characterizing human arm motion should be a rich source of evaluative motion classifiers. Following this principle we propose performance metrics based on current neurophysiologic hypotheses.

To help understand the generated data, we plot the spatial trajectory of the right hand instrument tip, while performing a peg transfer task (**Figure 13**). Knowing the placement of the pegs, we identify on this trajectory the starting and ending positions in the middle of the graph. Approximately 20 mm to the right of the starting position is the right hand side peg, and the instrument trajectory shows the attempt to pick up the rubber piece, and then the transfer to the left hand instrument.

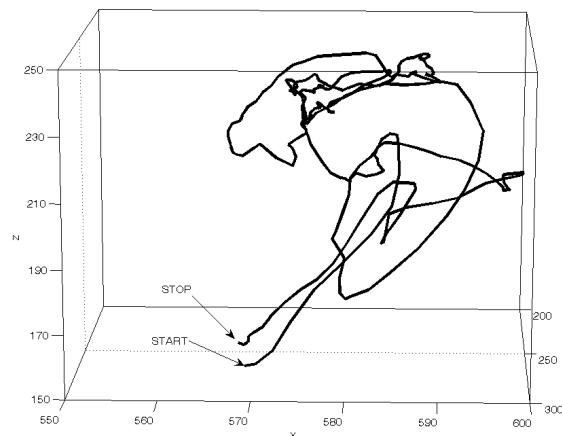


**Figure 13:** Trajectory for the right hand side instrument in the reference coordinates, with (x,y) the horizontal plane, x-axis pointing towards the operator and z the vertical axis.

From these data we are able to extract codified performance metrics, such as time to complete the task, the total path length described by each instrument tip, an approximate volume swept by each trajectory, as well as the estimate for the mechanical work exercised upon each instrument.

### 3.5.1 Smoothness

Early neurophysiologic work found that the speed profile of the natural arm motion is bell-shaped [117]. This finding has been generalized and extended to the general result that human arm motions naturally are as smooth as possible [118]. The smoothness metric is derived directly from the “minimum-jerk” model developed by Flash & Hogan [118]. Maximally smooth motion that minimizes the total of the third derivative of position “jerk” over the course of the task. This metric has been previously suggested [98] and follows our general hypothesis that expert surgeon’s tool-tip motion will resemble the motion of the natural limbs.

$$m_1 = \frac{\frac{1}{2} \int_{t_0}^{t_1} \left( \left( \frac{d^3 p_x}{dt^3} \right)^2 + \left( \frac{d^3 p_y}{dt^3} \right)^2 + \left( \frac{d^3 p_z}{dt^3} \right)^2 \right) dt}{t_1 - t_0}$$

### 3.5.2 Total Path Length

This heuristic metric aims to measure laparoscopic skill objectively. The assumption is that novice users will have poor economy of motion compared to the experts. This has been independently verified in previous studies [119]. The metric used here is the line integral along the path of motion

$$m_2 = \int_{t=t_0}^{t_1} \sqrt{\left(\frac{dp_x}{dt}\right)^2 + \left(\frac{dp_y}{dt}\right)^2 + \left(\frac{dp_z}{dt}\right)^2}$$

The path length implicitly captures other common user errors, such as dropping the rubber piece during the peg transfer task, because it would subsequently require additional tool-tip travel distance to correct, such as retrieving the dropped object. From the position vector, a total path length value is determined as the sum of the incremental displacements:

$$P_x = \sum_i \Delta p x_i = \sum_i |x_{i+1} - x_i|$$

$$P_y = \sum_i \Delta p y_i = \sum_i |y_{i+1} - y_i|$$

$$P_z = \sum_i \Delta p z_i = \sum_i |z_{i+1} - z_i|$$

### 3.5.3 Time to completion

Time to completion is an intuitive measure and has been previously shown to be a good distinguisher of skill [119]. Nonetheless, over-emphasis on this metric encourages trainees to learn speed over precision. We suggest that the time-to-completion metric, as the easiest to measure, has been overemphasized in practice. To correct this we adjust the relative weighting of the time-to-completion in the total score. Time to complete the given task is computed from the time stamp vector as the difference between the last time reading and the initial time reading.

$$m_3 = T = t_{final} - t_{initial}$$



### 3.5.4 Volume described by the instrument tip

Volume described by the instrument is calculated from the maximums and minimums of the tip trajectory along each axis

$$m_4 = Vol = |x_{i\ max} - x_{i\ min}| * |y_{i\ max} - y_{i\ min}| * |z_{i\ max} - z_{i\ min}|$$

### 3.5.5 Specific Kinetic Energy

The specific kinetic energy (KE) is the ratio of the kinetic energy and mass,

$KineticEnergy / mass = \frac{1}{2} * Velocity^2$ . Between two consecutive position readings, the incremental work is  $\Delta ke_i = \frac{1}{2} \Delta v_i^2$  therefore, for the entire trajectory, KE is the sum

$$m_4 = KE = \sum_1 \Delta ke_i$$

### 3.5.6 Scoring

The total score, S, for a task is an affine sum of the relevant metrics  $m_i$ , scaled by the weighing constants  $k_j$  such that  $\sum k_j = 1$ ,

$$s = \sum_i k_j m_i$$

The weighing factors serve to both normalize the metrics to a common abstract unit and to provide a relative measure of importance. To compute the total score, each metric was multiplied by a constant  $k$ . The corresponding constant for each metric was the maximum expert measurement attained, times an affine weighing factor of 0.5 for path length, 0.2 for time-to-completion and 0.3 for smoothness.

### 3.6 Test Data

A small number of trials were performed using the described system to illustrate its utility at performance evaluation. Two traces of recorded motion, one from an expert (a) and a second from a novice (b) are shown in **Figure 14**.

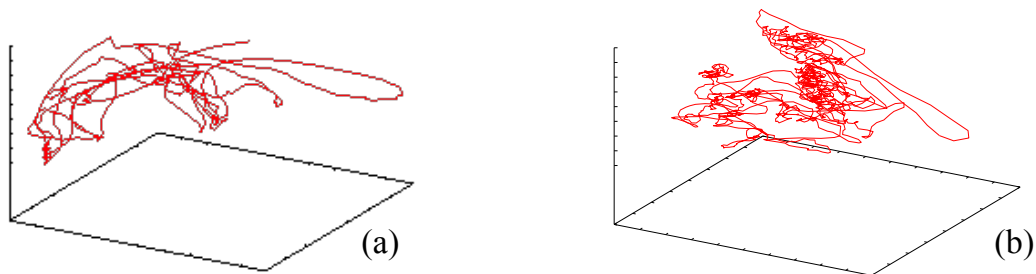


**Figure 14:** Two examples of motion traces for the peg-transfer task showing clear differences in the character of motion tracked between an (a) expert surgeon, and (b) a novice trainee.

Although contained in about the same physical volume, the expert surgeon produces a smooth and efficient instrument tip pathway. The novice trainee on the other hand wanders around as he/she repeatedly attempts to grab the rubber piece, or to pick it up from the floor of the training box after it dropped from the grasper. A clear difference is qualitatively visible from the graphical representation alone.

Average acceleration measured at the tip of the instrument held in the right (R) and the left (L) hand is shown in **Figure 15** for both experts and novices for each of the 10 test runs. It is immediately obvious from both (a) and (b) panes of **Figure 15** that for each test run the instruments experience much larger accelerations while in the hands of the novices. For the instrument in the right hand, the average acceleration is about 3 times as large when manipulated

by the novice. Also in the hands of the expert instrument tip acceleration is steady across the 10 test runs, with very small error bars as shown in the (b) pane. An intriguing observation relates to the acceleration experienced by the instrument in the left hand vs. the right hand. For both experts and novices, there is a significant difference in between the two hands. The instrument in the left hand experiences almost twice as much acceleration as the one in the right hand for both experts and novices.

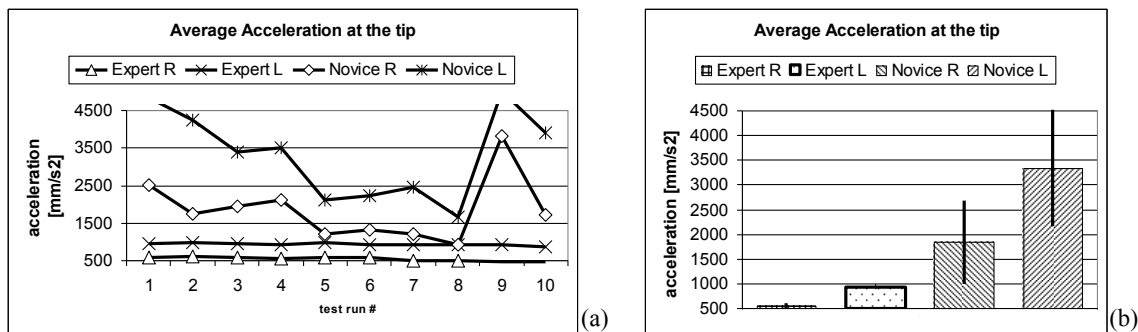


**Figure 15:** Average acceleration at the tip of the instrument held in the right (R) and left (L) hand for both expert and novices.

The smoothness metric, as seen in **Figure 16**, directly compares the amount of “jerk” during a peg-transfer task, and provides a measure of the amount of change in acceleration at the tool-tip during the training task. The novice user’s motion is substantially less smooth than the expert performing the same task. Note that the expert trace shows high “jerk” at the beginning, middle and end of training task. These instances correspond to the rapid motion of the tool tip from the neutral position to the first peg and peg, and show a purpose-driven motion of an expert. In contrast, the novice user shows a far less patterned motion though; with much larger changes in instrument accelerations as it attempts to grab the rubber piece. The two anomalous spikes are due to dropping the rubber piece on the floor of the training box.

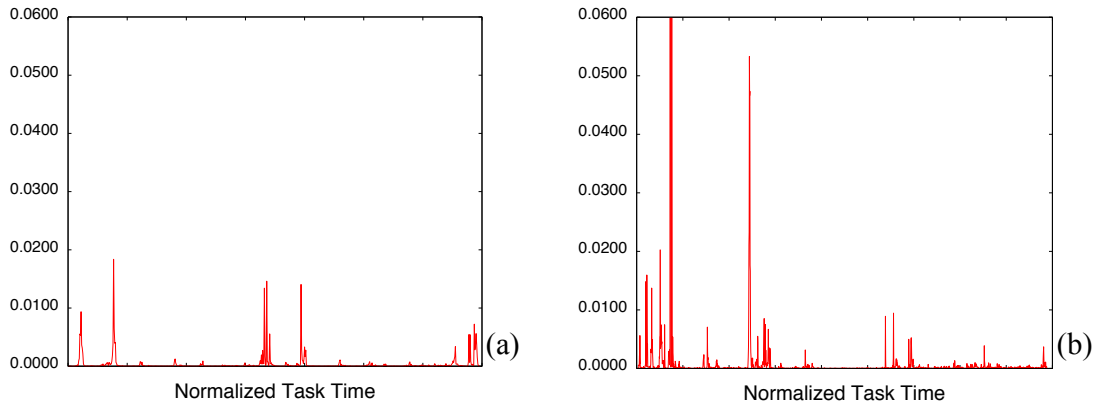


**Figure 16:** Smoothness for (a) expert surgeon, and (b) novice trainee

Over the 10 test repetitions of this task we see that the time to completion appears to be more or less constant at about 25 seconds, see **Figure 17b**. As expected, the novice trainees need about three times as long to complete the task and more significantly the error distribution is about 10 times as much.

Another interesting feature is revealed in **Figure 17a**; while the expert's learning curve is almost flat, the novice shows a sharp slope over the first 5-6 test runs. We hypothesize that for simple tasks such as the peg transfer, novices quickly learn the basics of laparoscopic instrument manipulation. Then, towards the end of the test runs their time to completion increases sharply. We hypothesize that novices are either getting fatigued from the intense mental effort to orient themselves in the environment of the laparoscopic training box, or possibly are trying out new approaches at instrument manipulation. Operator fatigue seems to be the more interesting hypothesis because the increased time to complete the task correlates with a sharp increase in instrument tip acceleration as seen in **Figure 15**. A potential experiment to test that hypothesis would have the participants monitored for physiological stress response such as heart rate, skin sweat, *etc.*

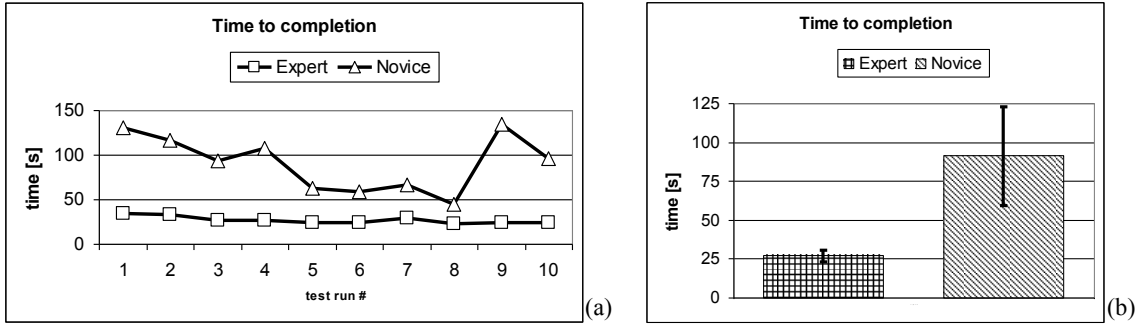


**Figure 17:** Time to completion performance metric (a) over the 10 test repetitions and (b) aggregated.

Although rigorous validation is outside the scope of this study, **Figure 18** shows that even for the small numbers of subjects tested thus far, each metric is able to distinguish novice from expert motions. The score bars show that affine sum of the metrics of novice and expert users and demonstrate the potential for performance evaluation.

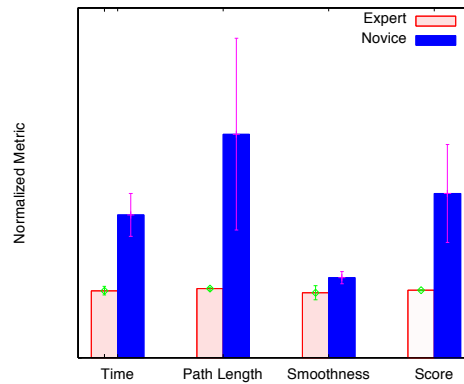


**Figure 18:** Baseline metrics and total score for the expert and novice user. The error bars indicate the standard deviation for each metric (for expert,  $n=2$ ; for novices,  $n=3$ ).

### 3.7 Conclusion

The UCLA-LTS is built around the idea of using actual laparoscopic instruments on a personal computer (PC) based training environment, thus combining the simplicity of the

training boxes currently approved by SAGES (Society of American Gastrointestinal and Endoscopic Surgeons) with the advances in computer-based virtual reality trainers currently available on the marketplace. An important development is the integrations of the motion tracking sensors into the shaft of the actual laparoscopic instruments thus preserving full instrument functionality. As a consequence, these instruments can be used for collecting kinematic data while performing actual surgeries, and not just basic training sessions over a synthetic tissue model. This presents the opportunity for high fidelity training in actual surgical cases and the exposure to a large number of cases from that same simulator/trainer and without unnecessary risk to the patient.

An obvious advantage when compared to either the classical training boxes or the PC based virtual reality based trainer is the increased variety of training material. By having an expert surgeon design each and every task the training simulation is not limited to the prepackaged simulations. Training tasks can be retrieved from the database of standardized curricula or can be designed by the training expert specifically to meet the needs of each trainee in part or for a specific upcoming surgery. The capability to design training drills for any skill deemed necessary by the expert is unlimited, from basic skills to complex surgery without the need to buy the additional software simulation package.

Expertise from several sources and therefore different technical approaches can be accessed on this trainer. This enables not only more depth to trainee teaching, but equally important allows expert surgeons to exchange technical information for the betterment of surgical education. We envision a future where medical schools will have a database of surgeries performed with this kind of instruments. These databases can become public knowledge to be exchanged for the good of the society, among the physician body, as a means of

communicating and improving upon surgical knowledge and competency, just as other published research material.

The electromagnetic motion sensors have been used previously to track motion for assessment of surgical skills, either by tracing instruments [120] or surgeons hands [121]. Since the magnetic fields experience no attenuation in the human body, there is no requirement for “continuous line of sight” as in other instrument tracking technologies. The major drawback, magnetic field distortion due to metallic instruments nearby is addressed here through the use of specific pulsed DC signals in the active source fixed electromagnet [38]. After each source coil is activated with the DC current, the system waits for the eddy currents induced in nearby metallic objects to die out before taking a measurement. By using only a small volume to track the instruments and therefore the magnetic sensors we overcome the drawback of position and orientation resolution degrading as the fourth power of separation distance [38]. This also minimizes latency issue normally associated with the need to use the filter noise of the signal.

Given the large variety of training tasks that form the basis of the UCLA-LTS we couldn't rely on the performance metrics normally used on the PC based VR trainers. The other approaches to assess the performance of training on SAGES approved laparoscopic training boxes needs the presence of an expert on site. We addressed the challenge of giving meaningful performance metrics for the impromptu designed training tasks through the use of kinematic analysis of instrument tip. An overall score defined as their affine sum complements metric, such as smoothness, total path length, graphical display and time to completion analysis. Within the limitations of this study, these performance metrics were able to reveal the differences of surgical skill among the participants and therefore segregate novices from expert surgeons.

## **4 Quantification of Intraocular Surgery Motions with an Electromagnetic Tracking System**

Chapter 4 is a version of the article published by J Son, JL Bourges, MO Culjat, V Nistor, EP Dutson, GP Carman, JP Hubschman, Quantification of Intraocular surgery motion with an electromagnetic tracking system, MMVR 17, 2009, [3]:

### **4.1 Abstract:**

Motion tracking was performed during a combined phacoemulsification (PKE) and pars plana vitrectomy (PPV) procedure on a pig eyeball. The UCLA Laparoscopic Training System (UCLA-LTS) which consists of electromagnetic sensors attached to the surgical tools to measure three-dimensional spatial vectors was modified to enable quantification of intraocular surgery motions. The range of motion and time taken to complete the given task were successfully recorded.

### **4.2 Introduction**

Intraocular microsurgery uses minimally invasive surgical technique in which finger-controlled probes and forceps are inserted into the eyeball through small ports at the eye surface. Various intraocular surgical procedures are commonly performed such as lens extraction, vitrectomy or pre-retinal membrane peeling. To achieve dexterity and precision required by intraocular surgery, ophthalmologists require several years of training. A shortage of ophthalmologists at hospitals both in the US and worldwide especially in developing countries



has become a growing concern [122]. Improved intraocular training and mentoring systems may enable more rapid and more effective training of ophthalmologists. Intraocular telementoring systems may provide further benefits by providing remote training of eye surgeons in underserved countries or in rural settings with minimal access to ophthalmologic specialists [123].

Currently two objective ophthalmic surgical evaluation protocols known as the Objective Assessment of Skill in Intraocular Surgery (OASIS) and Global Rating Assessment of Skills in Intraocular Surgery (GRASIS) revised by a panel of surgeons are in place to assess surgical competency in cataract surgery and improve surgical outcomes of ophthalmic residents during training [124]. While these systems have proven beneficial to training quantitative measurement of surgical motions would provide a more objective and standardized assessment of surgical skills. Quantitative measurements of intraocular surgical procedures may also enable mentoring and telementoring of novice surgeons. This paper describes an intraocular surgical tracking system adapted from a laparoscopic tracking system previously developed at the UCLA Center for Advanced Surgical and Interventional Technology (CASIT) and can quantify the movements of ocular surgical tools [2].

### 4.3 Tools and Methods

An intraocular surgical tracking system has been developed that can track the spatial position and orientation of surgical instruments using magnetic sensors. DC magnetic tracking sensors were attached near the tool tips so not to compromise the functionality of the tools to continuously monitor their (x,y,z) positions. A hardware-software interface was developed that transforms the coordinate data points into instrument pathways. These data were recorded and

saved in a database for subsequent immersive training and training performance analysis. Three DC magnetic trackers of 1.3mm diameters, each tracking six degrees of freedom (DOF) were used.



**Figure 19:** Referential sensor mounted on the pig eye

Motion tracking was performed during a combined phacoemulsification (PKE) and pars plana vitrectomy (PPV) procedure on a pig eyeball. A referential sensor was placed on the surface of the pig eyeball as shown in **Figure 19**. On each tool, PKE hand piece, chopper, vitreous cutter and light probe a sensor was placed at the extra ocular part of the tip next to the entry site and another on the handle of the tools. Five successive surgical steps were identified during the procedure: the lens sculpture (X); the lens emulsification (PKE); the cortex aspirations (IA); the core vitrectomy (PVD); and the 360 peripheral vitrectomy (360). The data from each sensor was recorded and the offset from the tool tip to the sensor was found using

$$\begin{bmatrix} X_s \\ Y_s \\ Z_s \end{bmatrix} = \begin{bmatrix} X_b \\ Y_b \\ Z_b \end{bmatrix} + \begin{bmatrix} X_o \\ Y_o \\ Z_o \end{bmatrix} [R]$$

Where  $(X_b, Y_b, Z_b)$  are position outputs from the sensor with respect to the transmitter's center;  $(X_o, Y_o, Z_o)$  are the offset distances from the sensor's center to the tip of the surgical instrument;  $(X_s, Y_s, Z_s)$  are the coordinates from the instrument's tip with respect to the transmitter's center;  $R$  is the rotation matrix. Offset was calculated for every surgical tool. The offset was incorporated into the data obtained from the sensors to find the path of the instrument tip.

## 4.4 Results

The mean ranges of motion for each tool in each step of vitrectomy are outlined in **Table 2** and **Table 3** for each step of the phacoemulsification and pars plana vitrectomy.

**Table 2:** Phacoemulsification range of motion and time

	X		PKE		IA
	Hand piece	Chopper	Hand piece	Chopper	Hand piece
X [mm]	11.46±1.46	12.18±248	18.02±3.29	8.82±1.29	13.59±4.93
X [mm]	13.14±0.87	15.45±3.53	10.32±1.84	15.70±11.52	15.08±1.75
X [mm]	9.78±1.53	13.13±2.46	16.90±5.84	5.75±0.30	10.09±2.69
Time [s]	69.02±6.94		47.80±16.86		101.86±30.15

**Table 3:** Vitrectomy range of motion and time

	PVD		360	
	Hand piece	Chopper	Hand piece	Chopper
X [mm]	30.66±6.28	7.88±3.37	12.65±6.84	7.96±1.11
X [mm]	25.48±5.08	9.63±1.10	12.14±4.17	14.99±7.02
X [mm]	29.47±2.34	8.94±3.24	9.88±5.17	4.82±1.28
Time [s]	128.83±38.59		112.11±16.55	

**Figure 20** shows the capabilities of the electromagnetic tracking system to graphically demonstrate the intraocular surgical motions.

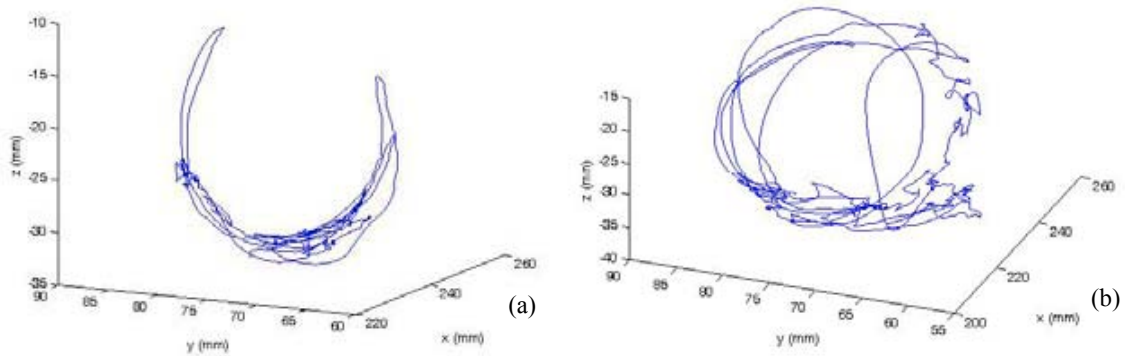


**Figure 20:** Tool tip pathway for the (a) PVD procedure and (b) the 360 vitrectomy

## 4.5 Conclusion

Quantification and recording of the motions of intraocular surgery were possible using the magnetic tracking system. This system provides essential data required to enhance training and mentoring of surgeons and to better design intraocular tools and robotic intraocular surgical systems.

# **5 Identification of Surgical Skills Specific to Laparoscopic Porcine Cholecystectomy**

## **5.1 Introduction**

Cholecystectomy is a procedure that surgically removes an inflamed gall bladder, a condition called cholecystitis, biliary colic, or gallbladder that presents pancreatitis-causing gallstones that block the common bile duct. Laparoscopic cholecystectomy is the prevalent procedure with open cholecystectomies performed only when other severe systemic illness prevents a successful laparoscopy. Everhart's [125] study on the prevalence of gallbladder diseases in the United States estimated that 6.3 million men and 14.2 million women between the ages of 20-74 were affected in 1999. Out of that population Lozano-Ponce [126] estimated 550,000 received an elective cholecystectomy. The Healthcare Cost and Utilization Project (HCUP) [127] estimates that cholecystectomy is by far the most common operating room procedure with a total of 6.2 million, excluding the maternal and neonatal hospital visits.

Laparoscopic cholecystectomy greatly reduces physical suffering of the patient and at the same time significantly reduces healthcare cost. This procedure requires just three-four small incisions of about 1.2-1.5cm in length and avoids cutting the abdominal muscles. Soper et al [128] reported that following laparoscopic cholecystectomy most patients return home the same day and can return to any physical activity within a week after surgery. A meta-analysis of randomized controlled studies by Gurusamy et al [129] found no statistical differences in reported pain, complications rate and hospital readmissions between the group that had a day-case surgery vs. the group that received overnight stay surgery. This is in obvious contrast to the

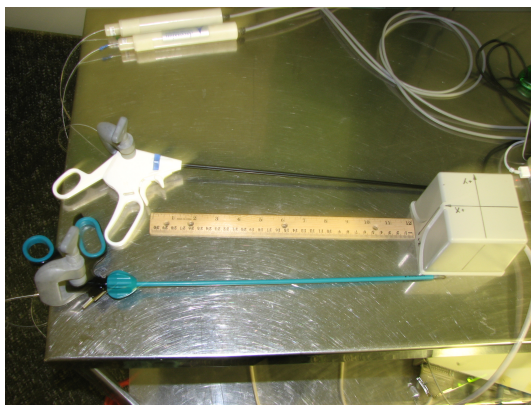
open cholecystectomy procedure that uses a large incision of 10-15 cm length just below the right ribcage. Recovery from this procedure requires a five-day hospital stay followed by approximately six-week convalescence period [130].

The NIH Consensus Statement on Gallstones and Laparoscopic Cholecystectomy [130] found that the single most important variable that determines the safety and efficacy of this procedure is the laparoscopic skill and experience of the surgeon performing the procedure. It further states that it is imperative that detailed guidelines be established for surgeon training, determination of competence, certification and continuous quality monitoring.

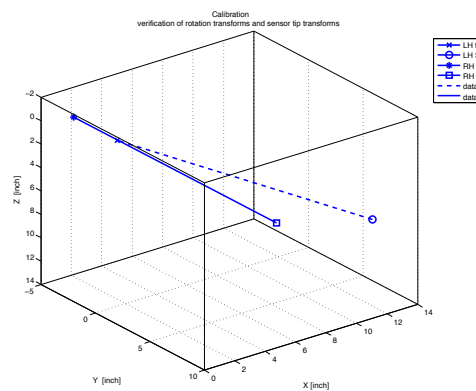
In addition to training in dry box and on virtual reality systems [31] in vivo porcine laparoscopic cholecystectomy is a most valuable tool. The biliary anatomy of the pig closely resembles that of humans both in spatial positioning and size. It is therefore expected that porcine and human laparoscopy will make use of similar procedures and require similar laparoscopic skills on the part of the surgeon. Our hypothesis is that using a combination of video and instrument motion recording we can identify a set of skills that are essential to the successful execution of the laparoscopic cholecystectomy. The porcine gallbladder removal study reported in this section, focuses on recording and quantifying the motion of the laparoscopic instruments during the various stages of this procedure. The goal of this study is to identify the critical skills required for a safe and efficient porcine laparoscopic cholecystectomy, using a combination of video and instrument motion recording.

## 5.2 Methods

The instruments used in this procedure had the electromagnetic motion tracking sensors clamped on the handles as shown in **Figure 21** using surgical clamps. Following sensor clamping, the instruments were placed on the surgical table in the calibration position next to the fixed reference electromagnet. The connector for each sensor was then attached to the control unit and the calibration software application completed the procedure on the laptop. Once this step was executed, the long axis of each instrument was displayed on the laptop screen, as seen in the perspective view from **Figure 21(b)** to verify the rotation matrix and the tip transforms.



(a)



(b)

**Figure 21:** Instruments used in the porcine test have motion sensors clamped to their handle and are placed on the surgical table next to the reference electromagnet for the calibration procedure (a) Axes are plotted on the right pane to verify the transforms for orientation and sensor tip location (b).

Animal use was in compliance with the guidelines for care of laboratory animals at the UCLA David Geffen School of Medicine. This study was conducted on a female pig of 30-40 kg, at the same time as the regularly scheduled porcine laboratory for surgical residents. The animal receives a full anesthesia and then the first trocar is inserted to create a pneumoperitoneum by insufflation with carbon dioxide. This trocar will be later used for the

endoscopic camera and four additional trocars are inserted as shown in **Figure 22** and **Figure 23(a)**.

The expert surgeon inserts the two instruments in the trocars situated on the left side of the pig and the assisting surgeon inserts the endoscopic camera in the upper medial trocar for the best visualization of the gallbladder (**Figure 22**). Before he confirms he is ready to start the procedure, the expert surgeon investigates the pneumoperitoneum using the two instruments, while visualizing the surgical field on the video monitor situated at the top of the instrumentation rack. At this point the video camera starts recording the procedure to capture both the surgeons and the monitor for the endoscopic camera.



**Figure 22:** Surgical team is in position and ready to start. Expert surgeon handles the instruments with sensors and the assistant surgeon handles the endoscopic camera. Surgical field is visible on the monitor sitting on top of the shelf carrying the other instrumentation.

The software application running on the laptop also starts recording the motion tracking data of the two sensors **Figure 23**.



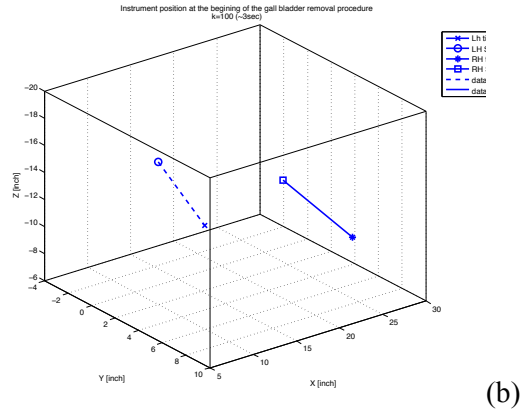
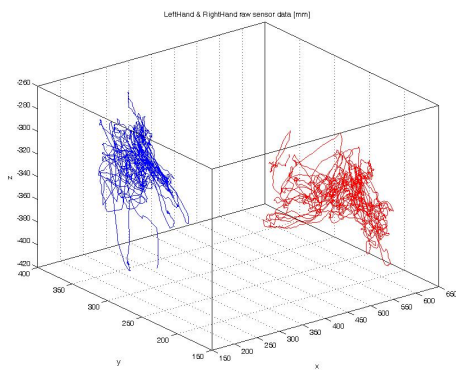


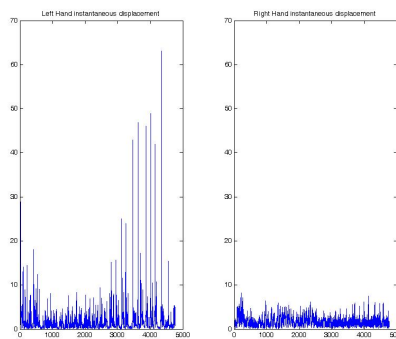
**Figure 23:** Instruments in position and ready to start the gall bladder procedure. Assistant surgeon operates the endoscopic camera (a); instrument axes are displayed in right pane (b)

### 5.3 Analysis

All pathways of instrument tips captured during the procedure are displayed in **Figure 24(a)**. The right hand instrument is shown in red and the left hand instrument in blue. The instantaneous instrument tip displacements between two consecutive data points shown in **Figure 24(b)** demonstrate distinct differences between the movements of the two instruments.



(a)



(b)

**Figure 24:** Pathways for the left (blue) and right (red) hands (a); and the instantaneous displacements between two consecutive readings (b)

The procedure results in a relatively large data set. To explore and analyze the data set we divided it into smaller segments that could be properly interpreted using two separate strategies: (a) time-segmentation using fixed duration time segments or (b) task segmentation by identifying specific steps of the surgical procedure.

The time-segmentation breaks down the whole data set into data chunks of predetermined length of time, for example one-minute long segments. The resulting pathways (**Figure 25**) are shorter and easier to visualize and analyze. This strategy has the advantage that it can be easily automated for subsequent kinematic motion analysis of the surgical instruments. The major disadvantage is that by automatically segmenting the larger data set into smaller chunks of arbitrary length, data interpretation loses its connection to the specific steps of the surgical procedure and the skills required to safely complete this procedure.

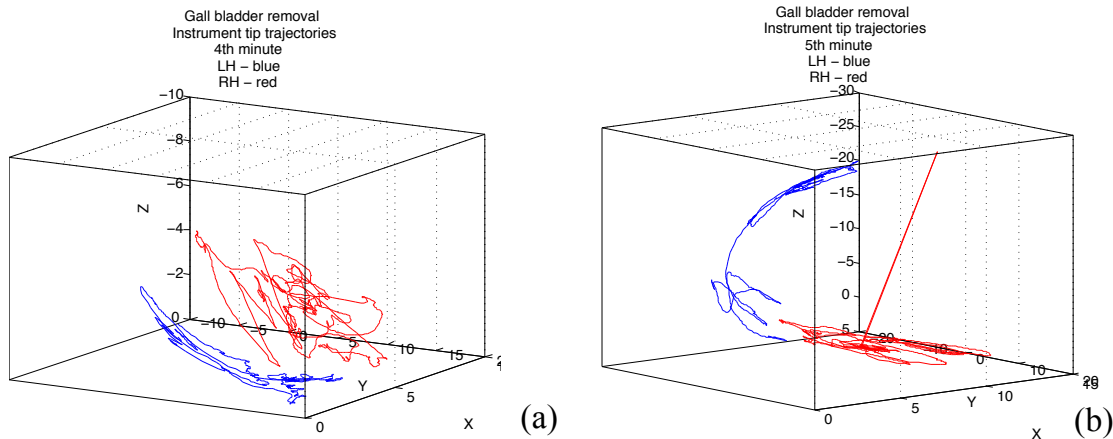


**Figure 25:** Pathway segmentation in one-minute long time increments: (a) 4th minute data, (b) 5th minute data

The task-segmentation is currently performed manually and requires coordination between the video recording and the instrument motion data recording. The two separate

recordings had their time stamps synchronized; then specific steps are identified using the video recording. For example, the video recording shows (**Figure 26**) that at the 10:13am time stamp, the surgeon positions the liver out of the way to expose the hepatocystic triangle. The left hand instrument grasps and pulls on the cystic duct while the right hand instrument uses the scissors to dissect the surrounding tissue. After about one minute the cystic duct is separated from the surrounding tissue, see the **Figure 26(a)**.

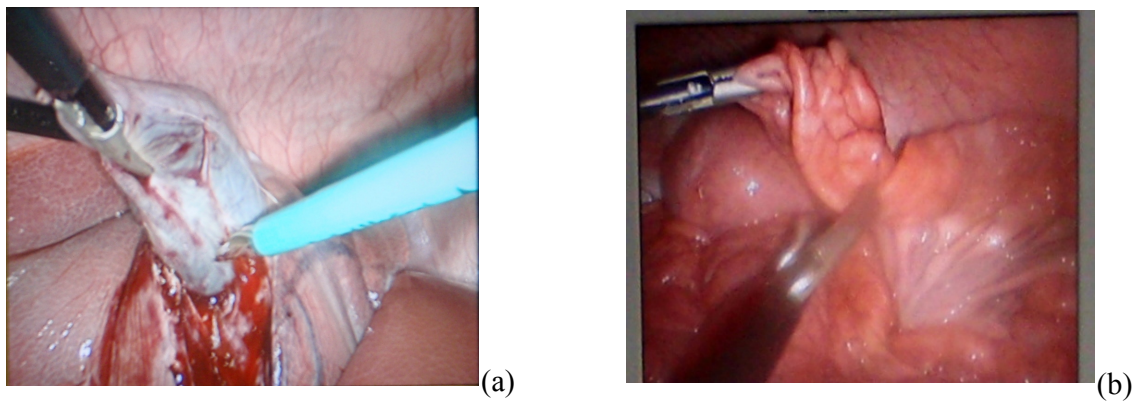


**Figure 26:** Task segmentation from the video recording: (a) clearing the tissue around the cystic duct, (b) inspection of the colon passing it from the right hand to the left hand grasper

Task-segmentation of the dataset isolates a chunk of instrument trajectories specific to the skill set required to separate the cystic duct from the surrounding tissue. This chunk of motion data from the instruments yields the pathways shown in **Figure 27**. The reference electromagnet is positioned on the surgical table between the legs of the pig. The positive z-axis points down towards the ground, positive x-axis is aligned with the spine and points towards the head, while the y-axis points towards the left side where the surgeons are located. It clearly identifies the two phases of this crucial step. In the first phase, shown in **Figure 27(a)** both instruments push

around the liver to provide direct observation of the cystic duct. The motion data also captures the insertion (straight red line) of the right hand instrument in the pneumoperitoneum.

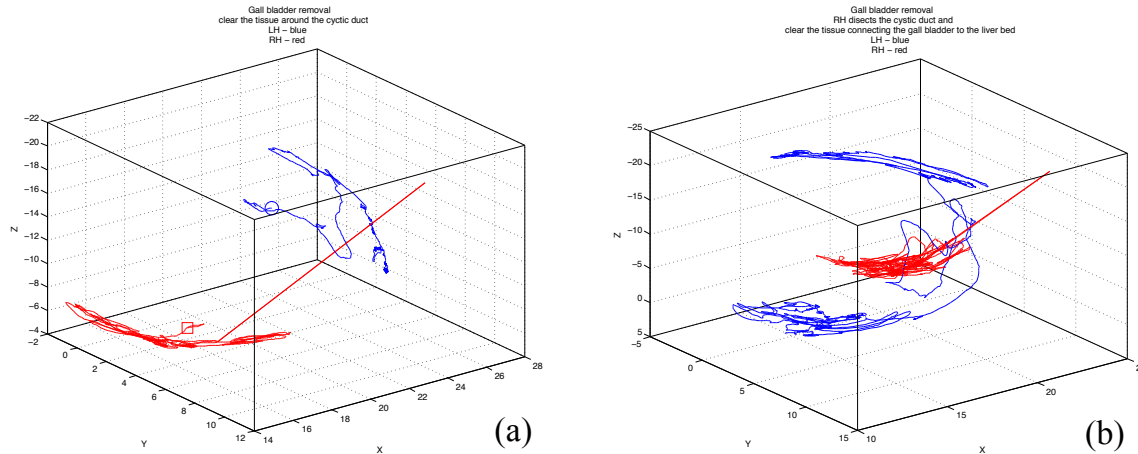


**Figure 27:** Pathway segmentation by tasks: (a) both hands push the liver around the cystic duct and (b) right hand dissects around the cystic duct while the left hand clears the tissue connecting it to the liver bed

In the second phase shown in **Figure 27(b)**, the left hand instrument (blue trace) is shown pulling at the gallbladder, while the right hand instrument is clearing the connective tissue around the cystic duct, before it is pulled out of the pneumoperitoneum (straight red line).

A minute later at the 10:14am time stamp, the right hand instrument is pulled out and is replaced with a stapler. There is no motion data for the stapler because this instrument does not have motion sensors attached to its handle. However the instrument that was just pulled out is now sitting idle on the instrumentation table next to the pig. At the 10:15am time stamp, the stapler goes in, and while the cystic duct is stapled closed, the left hand instrument dissects it. Afterwards, the stapler is pulled out and the right hand instrument is inserted back in the pneumoperitoneum. At the 10:17am the gall bladder is repeatedly lifted off the liver bed by pulling it high up with the left hand instrument, while the right hand instrument stays in an

almost fixed position where it dissects the connective tissue to separate it from the liver. Gall bladder is pulled out at 10:18am.

In preparation of the bowel inspection the right hand instrument is pulled out and tissue scissors are replaced with a tissue grasper instrument. This instrument does have motion sensors attached to its handle either. Inspection of the bowel begins at the 10:18 time stamp by passing it between the two graspers, as shown in **Figure 26(b)**. At 10:23:30 the entire colon is inspected and a second pass is performed in the opposite direction. This second pass is completed at 10:26:30. Note that full and safe inspection of the colon is an essential skill for all abdominal laparoscopic surgeries.

In this study the suturing procedure is divided into two specific time segments: (a) expert and (b) trainee. The expert surgeon executed five knots first before passing the instruments to the assisting surgeon to complete the rest of the suture, with another assisting surgeon handling the endoscopic camera. The expert surgeon starts the running suture at 10:28:30 and completes five knots about every minute and 20 seconds. At 10:35 the expert surgeon pulls both instrument out and handles them to the assisting surgeon, a novice laparoscopist in training. The needle driver is refilled with suture and both instruments are inserted into the pneumoperitoneum at 10:36:45 at which point the novice surgeon starts a running suture. This suture is finished after 6 minutes with two knots completed.

## 5.4 Discussion

The resulting data set for a simple surgical procedure such as cholecystectomy is relatively large. It spans over a time period slightly over 30 minutes and it contains close to

400,000 data points. In order to properly analyze these data we proposed two separate strategies to segment them into more manageable chunks. The time-segmentation is the simplest approach whereby data are automatically segmented into chunks of fixed duration. This approach would have the advantage of being easily automated, however has the potential for significant pitfalls. For instance, our analysis of the video recording of the procedure shows significant time periods when at least one of the instruments is not in the surgical field while switching between the steps of the cholecystectomy. Automated time segmentation would likely not recognize these events. Additionally, the stapler, one of the instruments critical to the success of the surgery, the stapler was not equipped with motion sensors, and therefore its movements were not captured by the dataset. More significantly however, automated segmentation into data chunks of fixed length would result in arbitrary partitioning of instrument movement data without regard for distinctively different phases of the surgery. That would produce a system that fails to identify specific skills, to measure how well those skills are performed and furthermore to give the mentor the opportunity to suggest specific pathways for improvement on those skills.

To address these deficiencies we propose task-segmentation, an alternative segmentation strategy that starts by analyzing the video recording for the procedure and synchronizes the time stamps for the video recording and the motion-tracking recording. Using this strategy we identified and collected data for several critical skills of the laparoscopic cholecystectomy. One of the first steps was the complete exposure of the hepatocystic triangle (**Figure 27a**) to visualize and positively identify the cystic duct and the single artery entering the gallbladder. Once identified with certainty the next critical step is to completely dissect the lower part of gallbladder off the liver bed (**Figure 27b**). Once the gallbladder is clear off of the liver bed, both the cystic duct and the artery are clipped. Our motion data recording did not fully capture that

because the instrument used to place the clips was not equipped with motion tracking sensors. In addition to these specific skills we captured the instrument motion relating to inspection of the colon and for running a suture line.

Overall, task-segmentation allows for identification of specific surgical skills related to each surgical step. Furthermore each one of these steps can be measured and analyzed independently of each other. We have seen that universal specific laparoscopic skills such as suture are already practiced in dry-box training environments. The present study paves the way for identifying skills that are more specific to cholecystectomy and then devising training drills for each and every one of them, either in a dry-box, in a virtual reality system or more likely a hybrid training systems such as the UCLA-LTS.

Further, using the task-segmentation strategy gives the opportunity to measure the skills of different competency populations. As an example, the last step in the cholecystectomy was running the suture with one suture completed by the expert and the second suture completed by the trainee. The expert surgeon completed a knot about every minute and 20 seconds, without mistakes. The novice surgeon completed the first knot in approximately the same amount of time, but pulled on the wrong end of the suture while completing the second knot. Correcting that mistake and completing the knot required almost 4 minutes. A task-specific segmentation is capable of capturing these errors and therefore has the potential to analyze them and gives the mentor opportunity to provide advice.

In addition to manual post-procedure synchronization using video recordings, there is also the potential for automatic segmentation of data by task. One possibility is for the surgeons, both novice and experts to give out clear verbal cues during the surgical procedure thus marking

the beginning and the end of specific tasks. For example during the suture step, the surgeon could begin by saying loud and clear “begin knot number one”. Once the knot is completed the surgeon would then say: “knot number one completed”. These audible clues could then be picked up from the video recording by a voice recognition enabled machine-learning algorithm. This algorithm could then segment both the video recording and the synchronized motion-tracking recording into skill-specific or task-specific chunks of data. These varying length but skill-specific data chunks could then be analyzed for kinematic parameters of performance, such as time to complete the task, smoothness of motion, among others.

## 5.5 Conclusion

The electromagnetic motion-tracking system was successful in recording the pathways of the instruments during the surgical procedure in the electromagnetically noisy environment of the surgical room. We have identified a viable strategy for segmenting the recorded data into skill specific data-chunks. These skill-specific data chunks could be simulated in the hybrid training-environment of the UCLA-LTS and then further analyzed for competency level of the different users.



## 6 Construct Validity for the UCLA-LTS

Chapter 6 is a version of the article published by V. Nistor, B. Allen, P. Faloutsos, E. Dutson, G.P. Carman, Construct Validity for the UCLA-LTS, *Medicine Meets Virtual Reality (MMVR)* 16 [4]

### 6.1 Abstract

*Background:* this study aims to establish the construct validity of the UCLA-Laparoscopic Training System (LTS). Many studies have established the need for an objective assessment of the Minimally Invasive Surgery (MIS) skills and techniques required to ensure safe and high quality treatment [89, 91, 131]. In light of the increasing demand for this surgical approach, it is no longer feasible to train MIS techniques using the apprenticeship model. In addition, training in the operating room exposes the patient to relatively inexperienced surgical residents. This problem is compounded by the current legislation that effectively reduces the number of practical training hours.

*Methods:* Construct validity evaluates whether the UCLA-LTS with kinematics-based performance metrics, time to completion, path length, smoothness, *etc.* [2] can discriminate between the experienced surgeon and the novice trainee. For this study we analyze the performance scores of test subjects (n=29) with two levels of experience, expert (n=4) and novice (n=25). A set of three different training tasks, previously validated in other studies [132, 133], with progressively increasing difficulty were performed in sequential order by all test participants. The “peg transfer” consists of picking up a rubber piece located on a peg, with one instrument; transfer to the second instrument and the place it on the opposite peg. An

increasingly more difficult task “pass the rope” consists of passing a rope from the right hand instrument to the left and reverse, by grasping it at specific points marked at one-inch intervals. Finally the most difficult task is the “cap the needle” test, which requires the subjects to grab the needle with the right hand instrument, then the cap with the left hand instrument and place the needle in the cap, while in the air.

*Statistical Analysis:* the Man-Whitney U test was used to estimate the differences between the two groups. Significance was considered for a values of  $p < 0.05$ .

*Materials:* the UCLA-LTS described previously [2] is a modular system consisting of a traditional laparoscopic training box and a DC electromagnetic motion tracking system, with the sensors directly embedded in the instruments. A desktop PC collects all the motion sensing data and provides the visual feedback.

*Results:* Construct validity was demonstrated for the UCLA-LTS according to the previously stated expertise and the performance scores. The individual kinematic parameters show that novice test subjects require on the average about three times as long to perform a given task while the instrument tip travels about twice as much. More importantly the volume described by the instrument tip is significantly larger for the novice test subjects reflecting an increased risk of injury due to unintended collisions with the surrounding anatomy. Learning curve is almost flat for the expert subjects, whereas the novice subjects experience a sharp slope for the first 5-6 test runs before it flattens out, consistent with observations from previous studies [133]. We observed significant performance differences between the left hand and the right hand for both experts and novice. The overall score for the novice subjects was normalized to that of the experts with a low score indicative of high skill.

*Conclusion:* this is the first study to establish the construct validity of the UCLA-LTS. Kinematics based parameters are employed in the assessment of performance as a means to both automate the scoring process, but more importantly to provide an objective measure to the otherwise subjective, observation based scoring of MIS training. This system thus represents a useful training device for the MIS.

## 6.2 Construct Validity Tests

Construct validity in general measures the degree to which a training tool can distinguish between different levels of expertise and skill for a given task. In this study we used three different training tasks of increasing difficulty, peg transfer, pass the rope and cap the needle.

The “peg transfer” task uses the SAGES approved plastic board with metal pegs of 1-inch height sticking upright, identical to the one used for the Fundamentals of Laparoscopic Surgery (FLS). It is placed in the dry box of the UCLA-LTS, within normal reach for the instruments. This task consists of picking up a rubber piece located on a peg with one instrument, transfer it to the second instrument and subsequently placing it on the other peg, see **Figure 12**. Test participants start by bringing the instrument tips in the spot marked as central starting position **Figure 12a**. Once the instruments are set in the starting position, we initiate the data recording for the test. The test participant proceeds to move the right hand instrument within reach of the rubber piece placed on the right side peg; picks up the rubber piece within the jaws of the grasper and lifts the rubber piece off the peg **Figure 12b**. At this point both instruments need to come towards the center and above the board in order to transfer the rubber piece from the jaws of the right hand instrument into the jaws of the left hand instrument **Figure 12c**. The left hand instrument places the rubber piece over the left side peg and release it **Figure 12d**. The motion

is complete when both instrument tips are back to the starting position. This is the halfway point for the peg transfer. To complete the task the previous steps need to be repeated in reverse order, thus transferring the rubber piece from the peg on the left side to the one on the right side and again with instrument tips in the starting position. At this point the data collection application is stopped and the test data is recorded into a computer file.

The “pass the rope” task simulates the inspection of the intestines for any signs of bleeding. It consists of passing a rope from the right hand instrument to the left hand instrument and reverse, by grasping it at specific points marked with blue ink in 1-inch intervals as shown in **Figure 29**. The rope is of soft cotton, ¼” diameter and 10’ length.

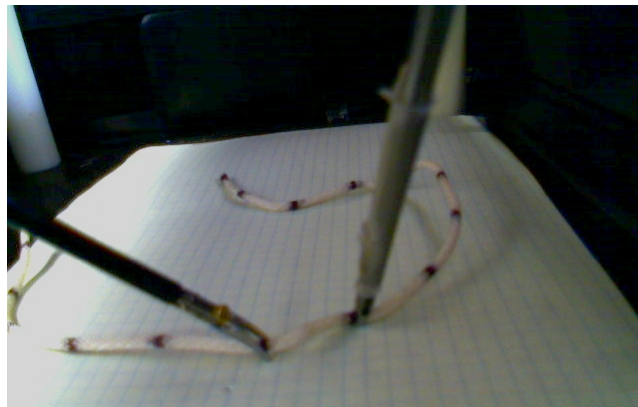


**Figure 28:** Pass the rope with the right hand instrument at the 3 inch mark and the left hand instrument at the 2 inch mark

From the same starting position defined for the peg transfer task, initiate the data collection application and then test subjects start by using the left hand instrument to grasp the left most mark at the end of the rope and the right hand grasp the rope at the first one inch mark **Figure 29a**. Then the right hand releases the rope from the one inch mark and grasps the rope at the two inch mark **Figure 29b**, immediately followed by the left hand releasing the end of the

rope and grasping it at the one inch mark **Figure 29c**. Test subject will continue in this fashion until the end of the rope and then proceed in reverse order to the beginning position at which point data collection is stopped and the motion data is recorded in the database file.

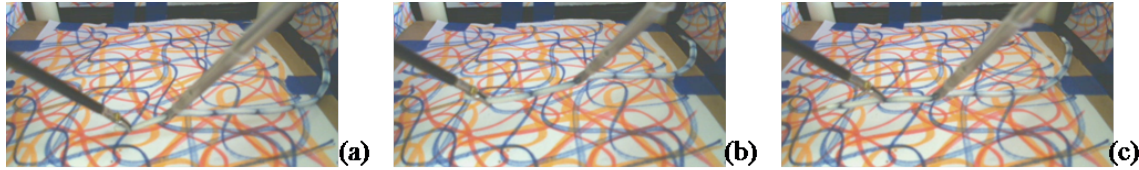


**Figure 29:** Pass the rope task: (a) start with each instrument grasping at the left side of the rope on the first two markings; (b) release the jaws of the right hand instrument and then grasp at the third marking on the rope: (c) now release the jaws of the left hand instrument and then grasp at the second mark on the rope.

The “cap the needle” test requires the test subject to grab the needle with the right hand instrument while the left hand instrument grasps the cap and then places the needle in the cap while floating above the floor of the text box (**Figure 30**). As seen in **Figure 31** the task starts with the tip of the instruments touching the floor of the training box in between the cap and the needle and data collection application is initiated.



**Figure 30:** Cap the needle task

Then the right hand instrument grabs the needle, while the left hand instrument grabs the cap and are both lifted off the floor. Once in the air the test subject aligns the cap with the needle

and inserts the needle inside the cap. Then the right hand releases the needle and pushes on its end until it is fully inserted inside the cap. The task is complete when the left hand places the cap and needle in its rest position and the left releases its grasp; both instruments return to the starting position and the data collection application is stopped.

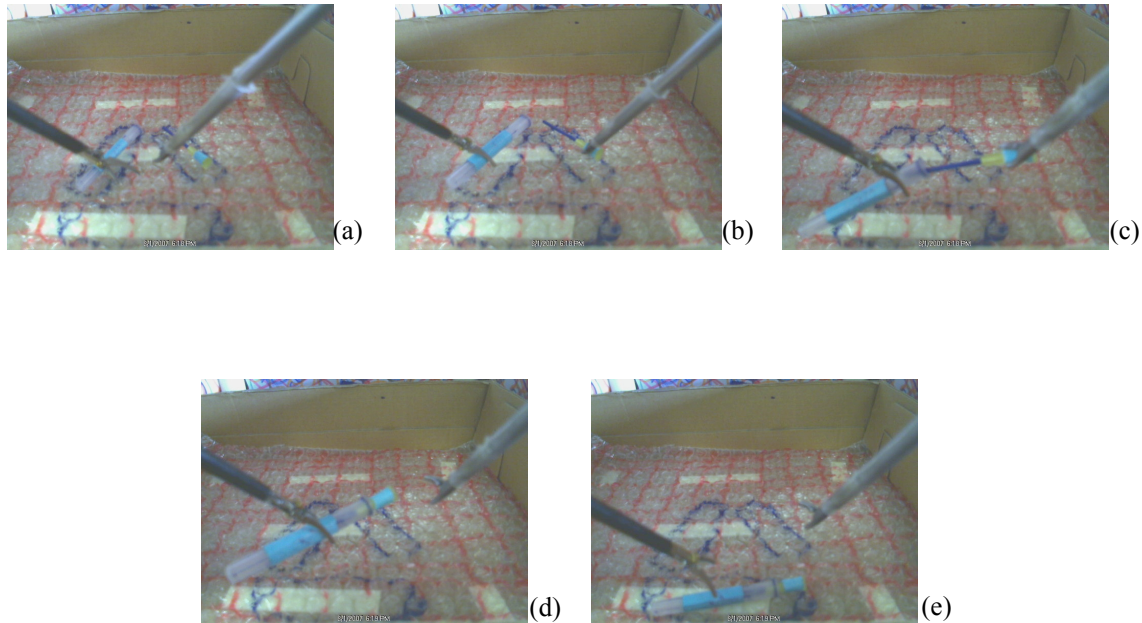


**Figure 31:** Cap the Needle; (a) start by placing the instruments in a central starting point; (b) grab the cap with the left hand instrument and the needle with the right hand instrument and lift them off the floor of the training box; (c) while in the air, align the cap and the needle and insert the needle in the cap; (d) release the needle and use the right hand instrument to push the needle completely inside the cap; (e) use the left hand to place the cap and needle in their rest position and release.

### 6.3 Test Subjects Recruitment

For this study we recruited a total of 32 test participants. Seven of them (n=7) were expert laparoscopic surgeons from the UCLA Medical Center and twenty-five (n=25) others from the graduate student program in the UCLA Mechanical and Aerospace Engineering Program.

### 6.3.1 Inclusion/Exclusion Criteria

All healthy subjects that can provide written consent will be allowed in this study. The graduate students who conduct research will determine availability by answering a few questions. Only students below the age of consent will be excluded from this study.

### 6.3.2 Method and Subject Identification and Recruitment

The four expert laparoscopic surgeons were recruited directly by Dr Erik Dutson MD, from the surgeons at the UCLA Medical Center. All expert surgeons had performed at least 50 laparoscopic procedures prior to participation in this study. The novice group was recruited from the graduate student body at the UCLA Mechanical and Aerospace Engineering. A recruiting poster was created, see Appendix A, and distributed at the research groups throughout the engineering campus as well as posted on the walls.

### 6.3.3 Methods and Procedures Applied to Human Subjects

All test participants were strictly voluntary and there was no payment associated with participation in this study. After establishing initial contact with the test participants an appointment was scheduled with each of them for at least one hour in the research laboratory of Boelter Hall 7673 and we proceeded to test according to the Test Plan in Appendix C. Each test participant whether novice or expert was then instructed in person on what to expect according to the Questionnaire see Appendix 0, prepared and agreed upon in advance. We start by describing the purpose of this study and then actual test procedure. We will describe the potential risks and discomforts associated with participation in this study and then conclude with a description of potential benefits to them as well as to the human society.

The expert laparoscopic surgeon answers two additional questions relating to previous laparoscopic training and previous laparoscopic procedure at the day of the study. Then each of the test participants will sign this document before we move on to discussing the actual testing procedure.

Each test participant will listen to a short power point presentation that explains the difficulties surgeons encounter during the laparoscopic surgery, with the goal of mentally preparing him or her for the difficulty of the task ahead. In this presentation we discuss the fulcrum effect, the use of long instruments, the poor depth perception and spatial disorientation associated with visualizing the surgical field indirectly on a computer monitor. Then we introduce the two surgical instruments used in the test, we will emphasize the lock and release mechanisms of the needle driver and grasper. We conclude with a live demonstration when we will then perform the three training tasks. At this point we ensure that we answer all the questions coming from the test participants. After this description the test participants will get them familiarized with the instruments and the UCLA-LTS and then proceed to performing the actual training task. There is no data collection at this stage and there are no time constraints either, the only requirement is that each test participant performs each training tasks at least three times.

#### 6.3.4 Data Collection, Storage and Confidentiality

Kinematic motion parameters data will be collected for each training task performed by the test subjects and stored on computer files in the computer running the other software components associated with the UCLA-LTS. As seen in **Table 4**, each test data file is a software generated spreadsheet that contains the time stamp in column #1 and the position and orientation



coordinated for each of the four sensors in the following columns. For each sensor the data acquisition interface collects three bod coordinate (x,y,x) and the three successive elemental rotations around the coordinate axes of the reference electromagnet

**Table 4:** Kinematic data collected from the four magnetic tracking sensors

Time stamp [sec]	Sensor #1				Sensor #2				Sensor #3				Sensor #4			
	Distal Left hand				Proximal Left hand				Distal Right hand				Proximal Right hand			
	x <sub>1</sub>	y <sub>1</sub>	z <sub>1</sub>	φ <sub>1</sub>	θ <sub>1</sub>	ψ <sub>1</sub>	x <sub>2</sub>	y <sub>2</sub>	z <sub>2</sub>	φ <sub>2</sub>	θ <sub>2</sub>	ψ <sub>2</sub>	x <sub>3</sub>	y <sub>3</sub>	z <sub>3</sub>	φ <sub>3</sub>

No names or other identifying clues will be recorded and numbers that specify only the date of participation will identify this data. Only the researchers will have access to this data. After the study is complete this data will be transferred to a separate computer used by researchers for data processing.

Each of the test participants will be identified through a six-digit number assigned according to the date and order of testing: MMDDNN (MM-month, DD – day, NN – order of testing on that day). For each test participant, the testing personnel create a data folder, named MMDDNN to store the data files generated for each test-iteration. Test results from each test run are stored in a spreadsheet data file, named MMDDNN-MM, where the last two digits MM identify the run number for each test. If for some reason a data file is corrupted and needs to be rejected, that file will be identified as MMDDNN-MM-abort.

The computer that runs the UCLA-LTS is password protected to restrict access only to the two test personnel named above. Password protection ensures that test data is only accessible

to the test personnel. Any changes to this test plan need prior approval from the project PI, Dr Greg Carman PhD.

### 6.3.5 Potential Risks and Discomforts

There are no risks that we can foresee and the UCLA IRB office on a related project has confirmed this evaluation.

### 6.3.6 Potential Benefits

The individuals participating may learn some concepts of minimally invasive surgery. Society may benefit and training techniques may be improved

### 6.3.7 Personnel Inviting Participants

Only researchers involved in this study will solicit participation. They will briefly describe the project and give instructions. The description and instructions will also be given on the recruiting poster. The researcher include UCLA professors, clinicians and graduate students: (1) Greg P Carman PhD - Professor, MAE; (2) Erik Dutson MD – Asst Professor of Surgery; (3) Petros Faloutsos PhD – Asst Professor, Computer Science; (4) Vasile Nistor – Graduate Student

### 6.3.8 Process of Consent

The consent forms will be provided at the location of the experimental setup in Boelter Hall 7673. This is a spacious, comfortable laboratory with chairs provided for the waiting participants. The subjects will have the option of taking the form and returning to the laboratory at a later date.

### 6.3.9 Comprehension of Information Provided

The researcher will talk to the subjects and explain the process, follow up with questions to ensure understanding of the testing procedures

### 6.3.10 Information withheld from subjects

No information will be withheld from the test participants. If they express a desire to know their personal test results we will provide that information but will not discuss the results of other test participants.

### 6.3.11 Consent Access Forms

Only Adult Consent Forms will be used, see Appendix B.

## 6.4 Data Analysis

### 6.4.1 Peg Transfer

Data collected from the motion sensors comes as a time series of position vectors  $(x,y,z)$  and the elements of the rotation matrix with regard to the reference electromagnet. To help understand our data, we plot the spatial trajectories for the left and the right hand instrument tips, side by side for an expert and a novice see **Figure 32**, while performing the simplest of the three training tasks, the peg transfer.

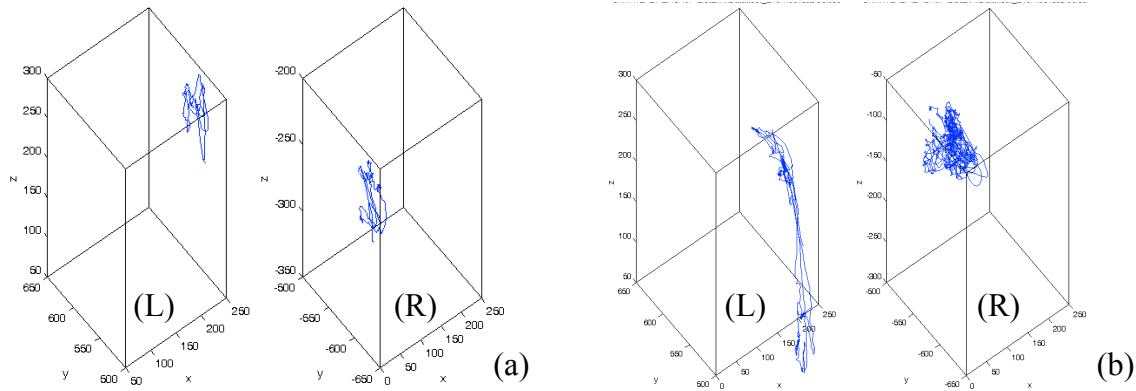


**Figure 32:** Trajectories for expert (a) and novice (b) for the left hand (L) and right hand (R) instrument tips

For the trajectories shown in **Figure 32**, we calculate the performance metrics and can be found tabulated in **Table 5**.

**Table 5:** Performance metrics example

Metric	Expert LH	Expert RH	Novice LH	Novice RH
Time [s]	26.6	26.6	204	204
Path length [mm]	701	697	3310	6637
Volume [cm <sup>3</sup> ]	26	26	330	160
Jerk [m/s <sup>3</sup> ]	2.2	3.2	5.7	2.3
Mechanical Work [mJ/kg]	80	81	1784	700

In this particular test run, the expert required 26.6 seconds to complete the peg transfer task. The path length of the instrument controlled by the left hand is 701 mm, while the instrument manipulated by the right hand travels 697 mm. The approximate volume swept by the tips of the instruments whole controlled by the expert is 26 cm<sup>3</sup>. Experts' hands impart a controlling effort, expressed as specific mechanical work, of 80 mJ/kg for the left hand and 81 mJ/kg for the right hand. Our visual observation of the novice's performance is confirmed by the quantifier metrics. Time to complete the same task is 204 seconds and the instrument tips

travel 6637 mm and 3310 mm respectively. As visible from the trajectory graphs the volume used by the instrument tips is also much larger for the novice: 330cm<sup>3</sup> and 160 cm<sup>3</sup> respectively. Not obvious from the graphical representation of trajectories, but coming out of the kinematics parameters is that the controlling effort is much larger as well: 1784 mJ/kg and 700 mJ/kg respectively.

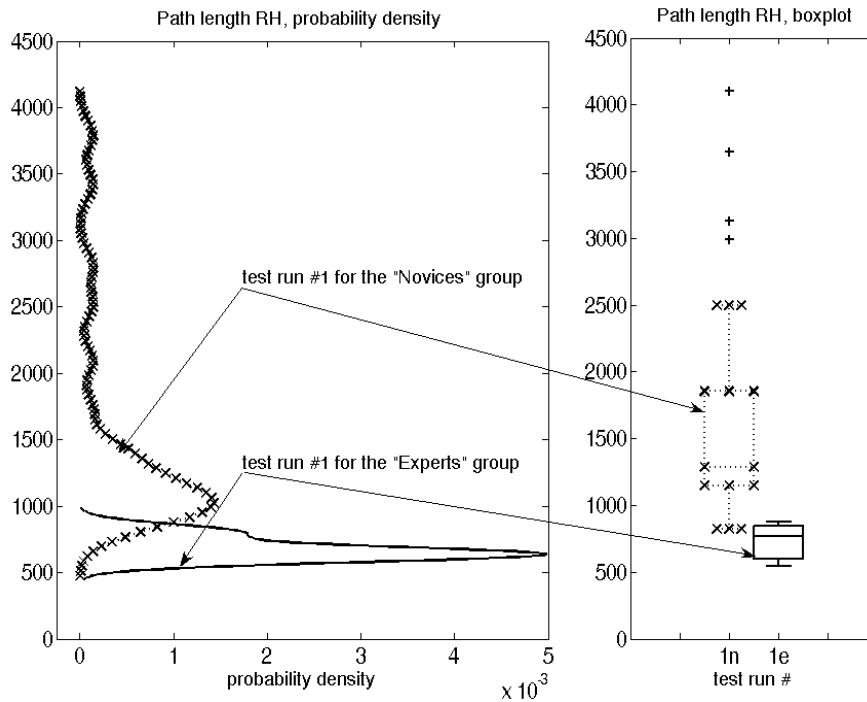


**Figure 33:** Probability density and the box plot. The left pane plots the probability density for the path length of right hand (RH) for the first test run of the peg transfer task, for both the experts group and the novices group.

To summarize the performance of the entire group of experts and compare to the group of novices, we plot the distribution of for that performance metric. For example in **Figure 33**, on the left pane we plot the probability density of the path length metric for the two groups experts and novices on the first run of the peg transfer task. Expert's group has a smaller distribution of path length (continuous line), concentrated in the 500 to 1000 mm range. The novice's group

data (dotted line) distribution is much wider and it shows a lot of data points far away from the apparent median.

The right pane of **Figure 33** is the equivalent representation of the same data, with box plots. Box plot data presentation shows the median value of the distribution as the line in the middle of the box, with 50% of the population distribution within the Inter Quartile Range (IQR). The IQR is defined between the upper quartile  $Q_1$  that contains 25% of the population distribution above the median and the lower quartile  $Q_2$ , containing the 25% of population immediately below the median. When comparing to the probability density function of a normal distribution, the IQR is equivalent to  $\pm 0.6745$  standard deviation. The upper whisker is at  $Q_1 + 1.5 \times IQR$  and the lower whisker is at  $Q_2 - 1.5 \times IQR$ . Data outside of this range are represented as outlier points. Box plot data presentation is a lot more economical and in presenting the results from the large data sets resulting from our construct validity experiments. For the rest of this data analysis we will present our data in box plot form wherever appropriate.

The two populations are of unequal size, the expert group has  $n=7$ , and the novice group has  $n=25$  and hypothesis testing will be done with a two tailed t-test. We show the results for the first test run in each of the training tasks in **Table 6**.

#### 6.4.2 Time to Completion

Time to completion shows that the means of the two populations are significantly different, and the difference is statistically significant as well,  $p < 0.001$ . Mean time to complete the peg transfer task is about 27 seconds  $\pm 4.2\sigma$  for the expert group and about 57 seconds  $\pm 26\sigma$  for the novice group. For the “pass the rope” task the equivalent values are  $70 \pm 12\sigma$  for expert group and  $112 \pm 30\sigma$  for the novice group. Similar differences are observed for the “cap the

needle” task where the expert group takes 33 seconds  $\pm 9\sigma$  and the novice group takes 63 seconds  $\pm 43\sigma$ .

**Table 6:** Time to complete the task for the first test run in the series

	Expert group (n=7)		Novice group (n=25)		
test run #	mean [s]	stdv, $\sigma$	mean [s]	stdv, $\sigma$	significance
Peg Transfer					
1	26.9	4.2	56.9	26	p<0.001
Pass Rope					
1	70	12	112	30	p<0.001
Cap Needle					
1	33	9	63	43	p<0.001

Not only are the mean values almost twice as high for the novice group, but also the standard deviation is much higher as well. This agrees with the visual observation from **Figure 33** that the experts group has a narrow distribution of time to complete the task.

An all-inclusive representation of time to complete the task for all participants (experts and novices) in the peg transfer task is captured in **Figure 34** as box plots. On the horizontal axis we have alternative expert and novice boxplots: test run #1 for the experts is label “01e”, while right next to it the novices test run #1 is label “01n”. The next two box plots present the data from test run #2 for expert group, label “02e”, while the novice boxplot is labeled “02n” and so on until the last test run #10 labeled “10e” and “10n” respectively.

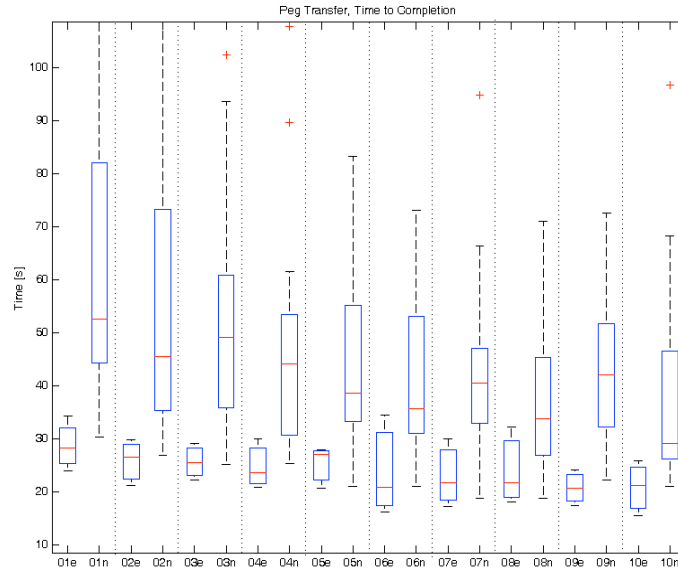


**Figure 34:** Time to complete the task, box plot representation for all test runs and for both expert and novice groups

Throughout all 10 test-runs, the expert group has a mean time to complete the task in the mid to lower 20 seconds with a standard deviation of about 5 seconds.

**Table 7:** Time to completion, t-test

test run #	Experts group		Novice group		Significance
	mean	stdv	mean	stdv	
1	26.9	4.2	56.9	25.7	P < 0.001
5	25.1	5.9	47.3	27.4	P < 0.001
10	21.7	5.2	41.3	20.5	P < 0.001

The novice group starts out with completion time close to 57 seconds and then it reduces that time into the mid to lower 40 seconds, about twice as much time as the expert group. The standard deviation for the novice group however starts at about 26 seconds and even though we see it reduce, it still is about four times as large as that of the expert group at about 20 seconds.



### 6.4.3 Path Length

The total path length for the peg transfer task is shown in **Figure 35**, side by side for both expert and novice groups, with the left hand instruments in the left pane **Figure 35(a)** and the right hand in the right pane of **Figure 35(b)**. Similarly to the boxplot for time to completion in each pane the expert's path length is displayed alternatively with the novice group path length.

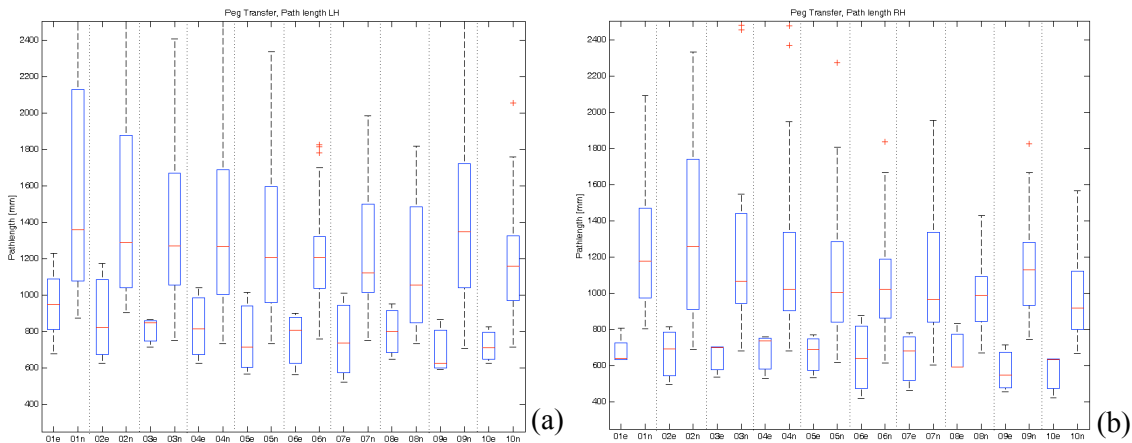


**Figure 35:** Path Length for the Peg Transfer: (a) left hand (LH) and (b) right hand (RH) for both experts and novices

Similar to the time to completion, we observe that the path length is about twice as long for the novice group. We also notice that there are differences in path length between the left hand and the right hand instruments, for both novices and experts groups. Even after 10 runs, the path length for experts 751mm (LH) and 615mm (RH) is significantly less than the novices group 1303mm (LH) and 1118mm (RH) see **Table 8**. The peg transfer task is highly symmetrical and yet even for the experts group the dominant hand is a lot more economical in it's path when compared to the left hand. The path length for the left hand is 22% longer for the experts group and 17% for the novices group.

**Table 8:** Path Length for expert and novice groups, t-test

Test run #	Hand	Experts group		Novice group		Significance
		Mean [mm]	stdv	Mean [mm]	stdv	
1	LH	908	196	1498	586	p<0.001
	RH	669	108	1378	661	p<0.001
5	LH	802	182	1348	556	p<0.001
	RH	678	145	1221	709	p<0.001
10	LH	751	156	1303	555	p<0.001
	RH	615	135	1118	489	p<0.001

#### 6.4.4 Volume swept by instrument tips

Volume used by the instrument tip is shown in **Figure 36** again; side for side experts and novice groups and again with the left hand volume shown in the left side pane **Figure 36(a)** and the right hand instrument in the right side pane of **Figure 36(b)**.

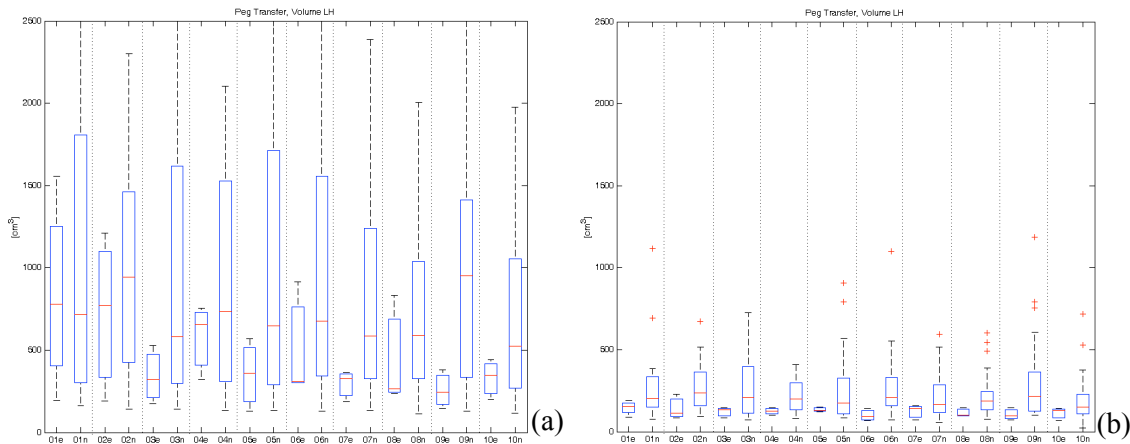


**Figure 36:** Volume used by the tip of the instruments in (a) left hand (LH) and (b) the right hand (RH)

We can see from this metric that not only the instrument tip has a path length twice as long for novice group but that tip also uses a volume about twice as large as well. In the 10<sup>th</sup> test run we see **Table 9** that the dominant hand (RH) for the novice group needs a volume of about 244 cm<sup>3</sup> compared to the experts dominant hand using only 116cm<sup>3</sup>.

**Table 9:** Volume used by instrument tip, t-test

Test run #	Hand	Experts group		Novice group		Significance
		Mean [cm <sup>3</sup> ]	stdv	Mean [cm <sup>3</sup> ]	stdv	
1	LH	701	472	1164	1192	0.036
	RH	135	50	303	341	0.001
5	LH	499	267	1147	1465	0.001
	RH	122	28	251	182	0.000
10	LH	611	468	1156	1488	0.018
	RH	116	35	244	198	0.000

The non-dominant hand (LH) of the experts group however is not that clearly different than the novice group. Even though the significance figure from the t-test is still below the  $p < 0.05$  threshold, we see that the standard deviations are now of comparable size to the mean. In the 10<sup>th</sup> test run the volume used by the experts left hand is 611 cm<sup>3</sup> with a standard deviation of 468, whereas the novices left hand instrument uses 1156 cm<sup>3</sup> with a standard deviation of 1488.

#### 6.4.5 Specific Mechanical Work

The specific mechanical work used to moving the instrument tips along the path when performing the peg transfer task shown in **Figure 37**. Just like for the previous metrics we split the left hand (LH) in the left side pane of **Figure 37(a)** with the alternating box plots for expert and novice groups and for the right hand (RH) instrument in the right side pane of **Figure 37(b)**.

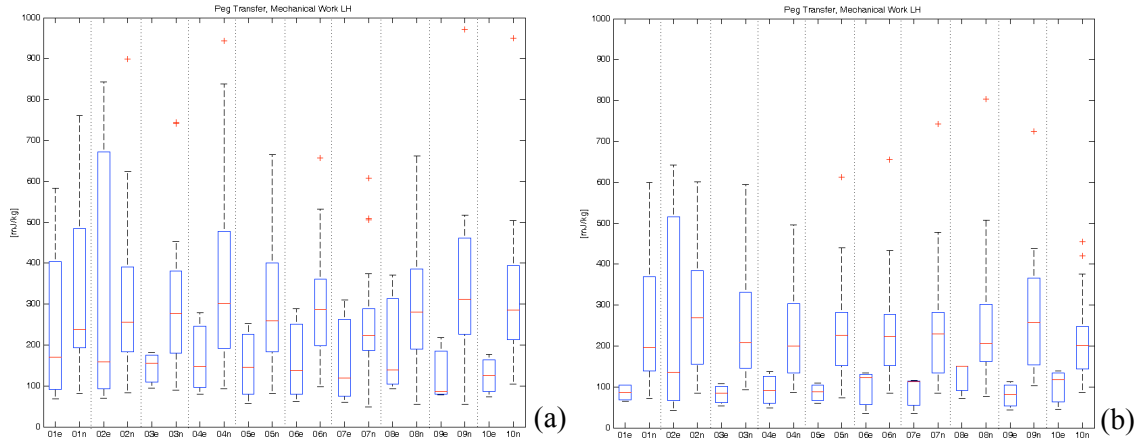


**Figure 37:** Mechanical work at the instrument tips for expert and novice groups for (a) left hand (LH) and the (b) right hand (RH).

We can see that for the dominant hand the specific mechanical is significantly different between the expert and novice groups, see **Table 10**.

**Table 10:** Specific Mechanical Work imparted to each instrument, t-test

Test run #	Hand	Experts group		Novice group		Significance
		Mean [mJ/kg]	stdv	Mean [mJ/kg]	stdv	
1 <sup>st</sup>	LH	269	264	337	232	0.481
	RH	149	187	327	502	0.045
5 <sup>th</sup>	LH	171	92	338	224	0.001
	RH	97	36	282	325	0.000
10 <sup>th</sup>	LH	160	102	583	1335	0.009
	RH	100	43	292	295	0.000

For example in the 10<sup>th</sup> run the experts group right hand (RH) generates about  $100 \pm 43$  mJ/kg, compared to the novice group right hand which generates about  $292 \pm 295$  mJ/kg. The specific mechanical work however highlights that even for the expert group the non-dominant hand (LH) needs a few test runs before it is significantly different that the novice's left hand. For example on the first test run the expert group left hand generates  $269 \pm 264$  mJ/kg, comparable to the novice group's left hand which generates  $337 \pm 232$  mJ/kg and the t-test returns a significance value of  $p=0.481$ . This is not immediately obvious from the other

performance metrics discussed thus far and has the potential to be a more sensitive performance metric than either the path length or the swept volume, when it comes to assessing the training level for the non-dominant hand of surgeons and trainees.

# 7 Motion Parameters of Surgical Instruments for the Assessment of Laparoscopic Psycho-Motor Skill

## 7.1 Abstract

Using motion-tracking sensors, subjective assessments of economy and fluidity of motion can be quantified with objective kinematic measures. We build on the previously validated metrics for measuring surgical dexterity: time to completion and path length, and contribute two new metrics: volume covered by instrument tip, and the mechanical power output expended while controlling the instruments. We compare a group of expert surgeons to a group of novice trainees. Time improves rapidly with each test run, while path-length and volume at the instrument tip shows a markedly slower improvement. Power output increases for both groups but more so for the expert group.

*Objective:* Our hypothesis is that using motion-tracking sensors attached to surgical instruments the subjective assessments of economy and fluidity of motion can be quantified using kinematic motion parameters.

*Summary of Background Data:* Most assessments of surgical skill are made using subjective global scores gathered from a panel of observers. These methods have been shown to be reliable, but this is an expensive process, both in manpower and time, and is often more suitable for research projects.

*Methods:* Experts (n=7) and novices (n=25) participated in trials consisting of three training tasks: peg transfer, pass the rope and cap the needle. Instrument motions were recorded

and reduced to four performance metrics: time, path-length, volume and power output. Results from experts and novices were then compared using the two-tailed null hypothesis t-test assuming normal distributions for the two populations of different and unknown variance.

*Results:* Data analysis demonstrated statistically significant differences between the two groups for all performance metrics. For the peg transfer-training task, the novice group took more time (experts 26.9 sec vs. novices 56.9 sec) to complete the same task, and novices used a longer path-length (experts 669 mm vs. novices 1378 mm). Volume containing the tool tip is significantly larger as well (experts 135 cm<sup>3</sup> vs. novices 303 cm<sup>3</sup>). The power output at the surgeons' hands while guiding the instruments is about 2.1mW among the expert group and 4.3 mW for the novice group. Similar differences were observed for the other training tasks.

*Conclusions:* using this novel way of collecting motion data for the surgical instruments we build on the previously validated metrics for measuring surgical dexterity: time to completion and path length. Two new metrics, namely volume containing the instrument tips and the mechanical power output while controlling the instruments add to the assessment of minimally invasive surgery skill.

## 7.2 Introduction

Extensive training is required to achieve proficiency in minimally invasive surgical techniques. Currently employed training methodologies include didactic sessions, dry-box and virtual reality simulators, complemented by the actual surgical operations. Traditional apprentice-mentor model of training during actual surgical procedures is time consuming [91] and does not obviate the need for additional skills-acquisition training [92]. Furthermore,

training in the operating room (OR) exposes the patients to risk and the opportunities for this training model have been further diminished by the recently mandated reduced working hours for surgical trainees [91]. There have been several attempts at creating virtual reality (VR) based trainers for laparoscopic surgery [32, 93, 112, 134, 135]. MIST-VR[90, 103, 136] has been the most extensively studied and validated [103, 107]. Other systems proposed and studied include the Procedicus MIST [119], LapSim [95], Xitact [99, 100], VESTA [117] and CELTS [102, 103]. When addressing psychomotor skill acquisition, these simulators have not been proven to be superior to far less expensive techniques, such as watching videotape [113], or basic trainer boxes [111]. Therefore, there still exists a need for a laparoscopic trainer that teaches psychomotor skills as well as provides performance feedback to the novice laparoscopic surgeons. The purpose of this study is to investigate the role of kinematic motion parameters as evaluator of surgical dexterity using the laparoscopy trainer developed at UCLA [2].

### 7.2.1 System Description

As described in previous chapter 3, section 3.3: System Overview, the UCLA-LTS consists of a training box, a set of laparoscopic instruments with position sensors and a software interface. The laparoscopic training box has a top porthole plate cut from an opaque polycarbonate plate. Visual feedback is provided by a USB based web-cam at 640x480 resolution and 30Hz refresh rate, attached to the front of the training box. For the purpose of this study we chose two commonly used instruments, a tissue grasper (Ethicon Endosurgery, Cincinnati OH) and a needle driver (KARL STORS GmbH & Co. KG, Tuttlingen, Germany). Both laparoscopic instruments are fitted with magnetic position and orientation sensors, which provide real-time spatial tracking. The tracking system (Ascension technology, Burlington, VT,



USA) consists of an active source electromagnet, a controller box and the position sensors. An electromagnet is attached to the far side of the training box, away from the surgeon, to provide a fixed reference frame for the recording the motion of the instruments. Two sensors of 1.3mm diameter (4 French) and 7 mm length are incorporated into the instruments, inside the long tube between the handle and the end effector grasper. The working distance for the distal sensor (the one close to the tip of the instrument) is less than 0.3 m. Under these conditions the static resolution for the three orthogonal axes is less than 0.5 mm for position and  $0.1^\circ$  rms for orientation, at 60 measurements per second. Data collected from the position sensors comes as a time series of Cartesian coordinates (x,y,z) and the Euler angles (Azimuth, Elevation and Roll), with regard to the reference electromagnet. There are two software interfaces, one for data acquisition, and another one for data analysis. Both interfaces make use of a common library for trace analysis written in C++. To assist the user in self-assessment, several performance metrics are reported via the graphical user interface.

## 7.3 Methods

### 7.3.1 Test Subjects

Thirty-two individuals participated in this study as described previously chapter 4, section 6.3 Test Subjects Recruitment. The expert group consisted of four practicing laparoscopic surgeons with more than 100 procedures each and three MIS fellows. The remaining 25 subjects were novices that had no prior training with laparoscopic instruments. All participants, experts and novices are right handed. Each participant conducted ten trials on three

separate evaluation tasks. A two-tailed t-test for two populations of unequal size with different variance is used for evaluating the test data.

### 7.3.2 Testing Method

This study examines three training tasks of increasing difficulty described in chapter 4, section 6.2: Construct Validity Tests. These are the Peg transfer, Pass the Rope and Cap the Needle, with each task being repeated 10 times. The peg transfer task uses the FLS peg transfer board and consists of picking up a rubber piece located on the far right hand side peg with one instrument and transferring it to the second instrument which will then place it on the far left hand side peg. The previous steps are then repeated in reverse order thus transferring the rubber piece from the left hand side peg back to the right hand side peg. The pass the rope consists of running the length of a soft cotton rope of 6mm diameter and 25 cm in length by transferring it between the two instruments, grasping it only at specific points marked with blue ink at 25 mm intervals. The cap the needle test requires that subjects pick a needle and a cap laying on the floor of the training box, and then place the needle inside the safety cap.

### 7.3.3 Performance Metrics

Time  $T$ , required completing the task is calculated by taking the difference between the final time stamp reading and the initial time reading for a given test run:

$$T = t_{final} - t_{initial}$$

Path length,  $P$  is the discrete line integral along the path of motion for the tips of the surgical instruments. The path length is calculated as the sum of incremental displacements between consecutive measurements:

$$P = \sum_i \Delta p_i$$

With

$$\Delta p_i = \sqrt{(\Delta x_i)^2 + (\Delta y_i)^2 + (\Delta z_i)^2}$$

Where incremental displacement for each axis are defined by

$$\Delta x_i = (x_{i+1} - x_i),$$

$$\Delta y_i = (y_{i+1} - y_i),$$

$$\Delta z_i = (z_{i+1} - z_i)$$

where  $(x_i, y_i, z_i)$  are the consecutive Cartesian coordinates of the instrument tips at the time  $i$ . The position tracking apparatus collects data samples at 60 times per second and when divided among the four data channels, the resulting time resolution is 67 milliseconds between consecutive position data points.

Volume  $V$ , is defined as the smallest rectangular box containing the instrument tips throughout the task.

$$V = \Delta x_{max} \Delta y_{max} \Delta z_{max}$$

Where,

$$\Delta x_{max} = (x_{max} - x_{min}),$$

$$\Delta y_{max} = (y_{max} - y_{min}),$$

$$\Delta z_{max} = (z_{max} - z_{min}),$$

Power output, Power, is the time rate of mechanical work done by the surgeon's hands on to the surgical instruments

$$Power = \frac{Work}{T}$$

work done on the instruments is the stepwise change in kinetic energy as measured by the embedded position sensors. For the entire trajectory the total work is the sum of incremental changes in kinetic energy, ke, between consecutive measurements.

$$Work = \sum_i \Delta ke = m \sum_i \left| \frac{1}{2} \Delta v_{i+1}^2 - \frac{1}{2} \Delta v_i^2 \right|$$

where  $m=0.400\text{kg}$  is the approximate mass of the surgical instrument and  $\Delta v_i = |v_i - v_{i-1}|$  represents velocity changes between consecutive data points:

$$v_i = \sqrt{\left(\frac{\Delta x_i}{\Delta t_i}\right)^2 + \left(\frac{\Delta y_i}{\Delta t_i}\right)^2 + \left(\frac{\Delta z_i}{\Delta t_i}\right)^2}$$

Where  $\Delta t_i$  is the time between two consecutive position readings.

#### 7.3.4 Time to Completion

Time to complete the task for the first test run in the series is shown in **Table 11** for all three training tasks. Judging by this metric the two populations are significantly different with the mean for the novice group almost double that of the expert group and this difference is statistically significant ( $p < 0.001$ ). Mean time to complete the peg transfer is about  $27 \pm 4.2$  seconds for the expert group and about  $57 \pm 26$  seconds for the novice group. For the pass the rope task, the equivalent time to completion are  $70 \pm 12$  seconds for expert group and  $112 \pm 30$

seconds for the novice group. Similarly for the cap the needle task, the expert group needs  $33 \pm 9$  seconds while the novice group requires  $63 \pm 43$  seconds.

We observe that not only the mean values are almost twice as high for the novice group, but the standard deviation is much higher as well.

**Table 11:** Time to Completion for the 1st test run in the series

	Expert group (n=7)		Novice group (n=25)		
Test run #	Mean [s]	stdv, $\sigma$	Mean [s]	stdv, $\sigma$	Significance
Peg Transfer					
1	26.9	4.2	56.9	26	p<0.001
Pass Rope					
1	70	12	112	30	p<0.001
Cap Needle					
1	33	9	63	43	p<0.001

Time to completion for all peg transfer tasks for novice and expert groups was discussed in previous chapter see **Figure 34**. For the equivalent time to completion on the other two training tasks we look at **Figure 38**. As described previously in each of the two panes (a) for Pass the Rope and (b) for the Cap the Needle, there are a total of 20 box plots, arranged alternatively between the expert group pass the rope (11e, 12e, ... 20e) and the novice group pass the rope task (11n, 12n, ... 20n). Similarly in pane (b) for the cap the needle task the expert group box plots are labeled (21e, 22e, ... 30e) while the novice group box plots are labeled (21n, 22n, ... 30n).

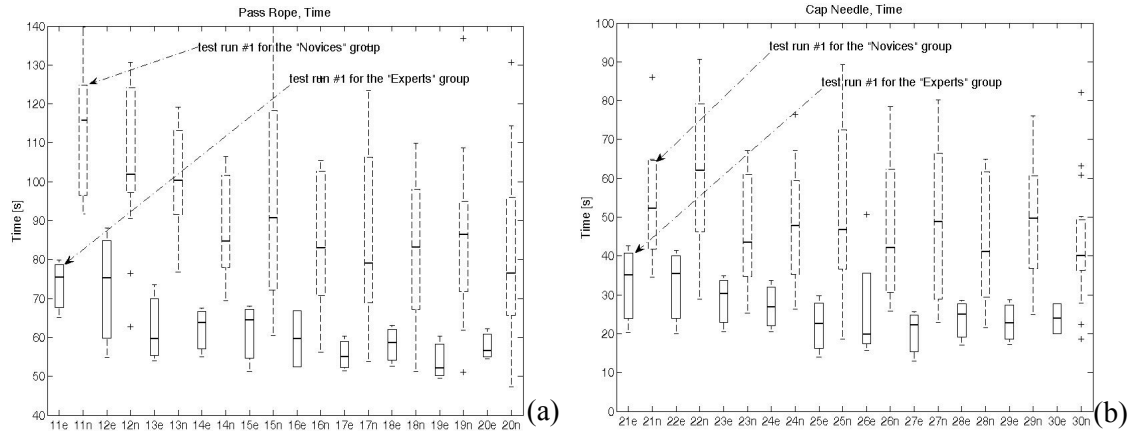


**Figure 38:** Time to completion for (a) Pass the rope and (b) Cap the needle.

Median times for the distribution of time to complete the task are consistently and significantly lower for the expert group. For all 10 of the test runs and across all three training tasks, the novice group, not only has a larger mean value for the time to completion, but also their population distribution is much larger as seen from the size of the Inner Quartile Range (IQR) of the box plot. The t-test confirms that for all 10 test runs, and for all three training tasks, the means of the two populations (expert and novice) are significantly different and that difference is statistically significant as evidenced by values of  $p < 0.001$ .

### 7.3.5 Path Length

Hypothesis testing for the Path Length metric used the same two-tailed t-test. In **Table 12** we look at a snapshot of this metric for the 1<sup>st</sup> test run of the three training tasks. As we discussed in the previous chapter, the size of the distributions for the left hand instrument was more significantly larger than that of the dominant hand instrument.

In the remainder of this study we will focus our data analysis and performance metrics discussion to the instrument in the right hand only because any differences visible for the right hand will be obviously more so for the left hand instrument.

**Table 12:** Path Length for the instrument in the right hand

Test run #	Expert group (n=7)		Novice group (n=25)		Significance
	Mean [mm]	stdv, $\sigma$	Mean [mm]	stdv, $\sigma$	
Peg Transfer					
1	669	108	1378	661	p<0.001
Pass Rope					
1	1240	326	2079	804	p<0.001
Cap Needle					
1	857	196	1475	986	p<0.001

Path length of the right hand instrument to complete the task for the 1<sup>st</sup> test run in the series shows that the means of the two populations are significantly different, and the difference is statistically significant, as evidenced by values of  $p < 0.001$ . For all three training tasks the novice group uses about twice as much instrument travel to accomplish the same task. This is to account for inaccuracies in the trajectory and for the instances where the rubber piece is being dropped and additional instrument travel is required to recover it. For the peg transfer task, mean values of path length are  $669 \pm 108$  mm for the experts group and  $1378 \pm 661$  mm for the novice group. For the pass the rope task, experts group scores  $1240 \pm 326$  mm, and the novice's  $2079 \pm 804$  mm. Similarly for the cap the needle task, experts the experts take  $857 \pm 196$  mm, while novices take  $1475 \pm 986$  mm. Again the larger differences are observed for the standard deviations of the two populations whereas the experts group has a more narrow distribution.

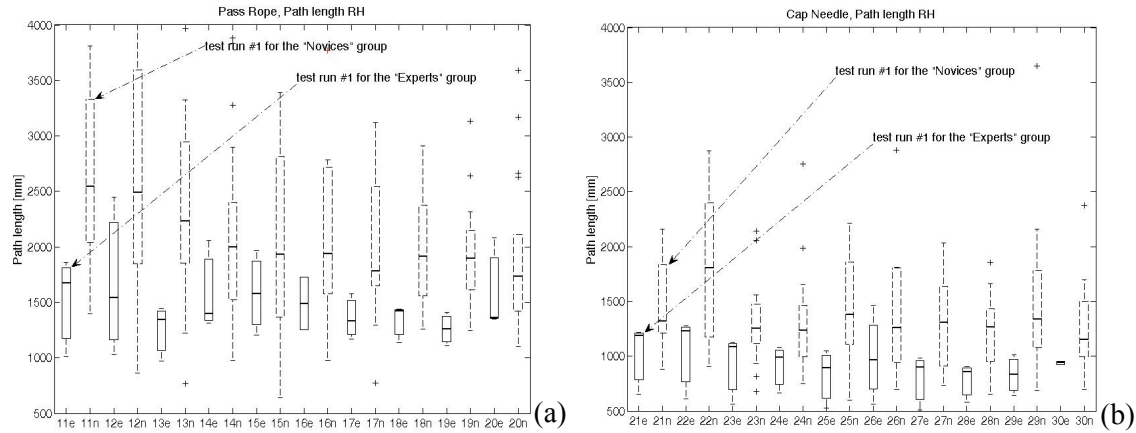


**Figure 39:** Path Length for the instrument in the right hand (RH) for (a) pass the Rope and (b) Cap the Needle.

The path length for the peg transfer task was discussed in detail in the previous chapter. We focus our discussion on the path length for the other two training task (a) pass the rope and (b) cap the needle as shown in **Figure 39**. Similar somewhat to the peg transfer, the path length for these two tasks has a larger mean for the novice groups and again with a much larger IQR.

### 7.3.6 Volume

Similar to the other two metrics, the volume that contains the trajectory of the instrument path is about twice as large for the novice group when compared to the expert, see **Table 13**.

Thus for the peg transfer the experts volume is  $135 \pm 50 \text{ cm}^3$ , whereas the novices volume  $303 \pm 341 \text{ cm}^3$ ,  $p < 0.001$ . In the case of the pass the rope task, experts volume is  $79 \pm 45 \text{ cm}^3$ , whereas the novices volume  $191 \pm 212 \text{ cm}^3$ ,  $p < 0.001$ . And for the cap the needle, experts volume is  $373 \pm 93 \text{ cm}^3$ , whereas the novices volume  $529 \pm 343 \text{ cm}^3$ ,  $p < 0.012$ . It emerges that the means of the two populations are significantly different for this metric as well and just like the other metrics the larger differences are between the standard deviations of the two populations.



**Table 13:** Volume swept at the tip of the right hand instrument for the first test run

	Expert group (n=7)		Novice group (n=25)		
Test run #	Mean [cm <sup>3</sup> ]	stdv, $\sigma$	Mean [cm <sup>3</sup> ]	stdv, $\sigma$	Significance
Peg Transfer					
1	135	50	303	341	p<0.001
Pass Rope					
1	79	45	191	212	p<0.001
Cap Needle					
1	373	93	529	343	p=0.012

Looking at the other test runs in **Figure 40**, the emerging picture is not as straightforward as for the previous metrics. We see that the volume swept by the right hand instrument is not consistently different between the two populations. While the IQRs for the expert group appears to be smaller than that of the novice group, the means for these box plots is not that much different.

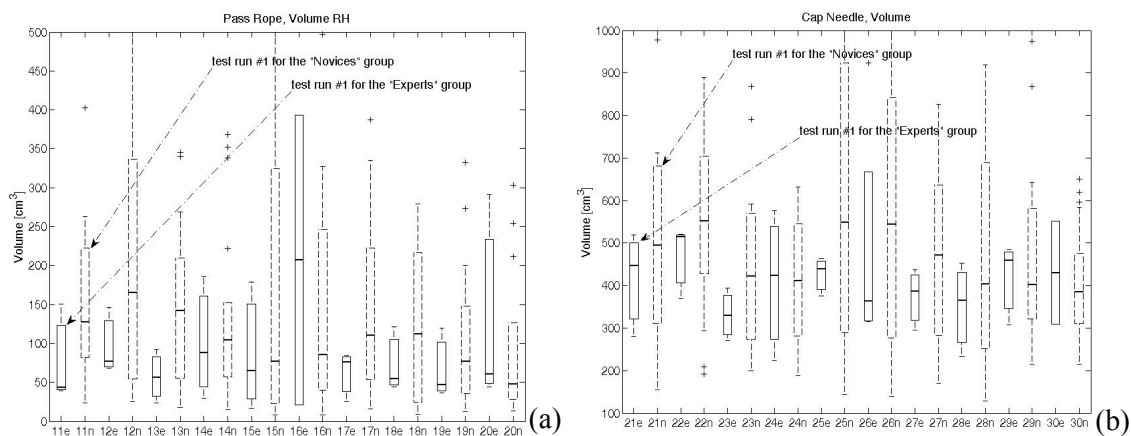


**Figure 40:** Volume swept by the tip of the instrument in the right hand (RH) for the (a) pass the rope and the (b) cap the needle tasks

This may have something to do with that fact that both of these training tasks afford more freedom to the subjects, and that there are very few physical constraints for where the instrument tips need to be during this run.

### 7.3.7 Mechanical Work

Similar to volume swept by the instrument tip, the mechanical work exercised on the instrument is much larger for the novice group during the peg transfer task. However for the other two training tasks, the differentiation between the two groups is not that obvious anymore. For the cap the needle task even for the first test run the difference in means is not significant anymore,  $p < 0.072$ . Thus for the peg transfer the experts mean value of work is 149 mJ/kg, compared to the novices work 327 mJ/kg,  $p < 0.045$ . In the case of the pass the rope task, experts' work is 146 mJ/kg, whereas the novices work 385 mJ/kg,  $p < 0.001$ . And for the cap the needle, experts' work is 151 mJ/kg, whereas the novices work 580 mJ/kg,  $p < 0.072$ .

**Table 14:** Specific mechanical Work exercised on the instrument for the first run in the series

	Expert group (n=7)		Novice group (n=25)		
Test run #	Mean [mJ/kg]	stdv, $\sigma$	Mean [mJ/kg]	stdv, $\sigma$	Significance
Peg Transfer					
1	149	187	327	502	p=0.045
Pass Rope					
1	146	65	385	396	p<0.001
Cap Needle					
1	151	58	580	1614	p=0.072

Just like with the volume metric, the mechanical work for the remainder of the test runs presents box plots with mean values that are consistently lower for the experts group. The t-test

shows that that for all 10 test runs and for a all three training tasks, the means of the two populations are different. However these differences are not as pronounced, nor statistically significant as the time to completion and path-length metrics see **Figure 41**. Occasionally, such as the case of the 4<sup>th</sup> and 5<sup>th</sup> test runs of the pass the rope task the expert group has fairly large IQRs, comparable to those of the novices group. This could be an artifact of the relatively small population size for the expert group (n=7). Additionally, corrupted data files can cause the population size to drop below the minimums required for a valid box-plot, such as the case of the 6<sup>th</sup> test run for pass the rope.

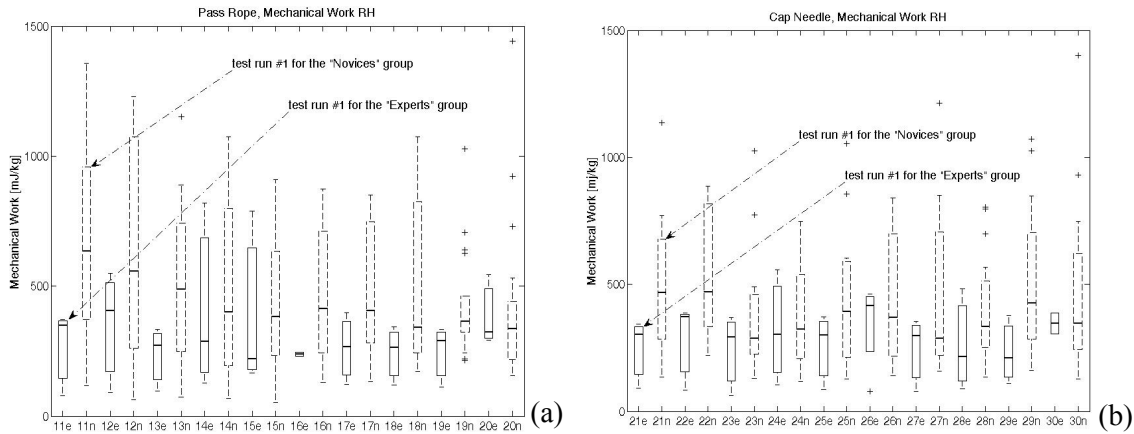


**Figure 41:** Specific Mechanical Work for instruments in the right hand (RH) for (a) pass the rope and (b) cap the needle

### 7.3.8 Power

The power delivered to the instrument takes into account two of the metrics studied so far, the mechanical work required to move the instrument and the time to complete the task. For the peg transfer task we see in **Figure 42** that the power output for the instrument in the right hand (b) is clearly significantly different between the expert group and the novice group. By

comparison to the mechanical output metric (a) we see that the box plot means though visibly different are much closer together for the power output metric.

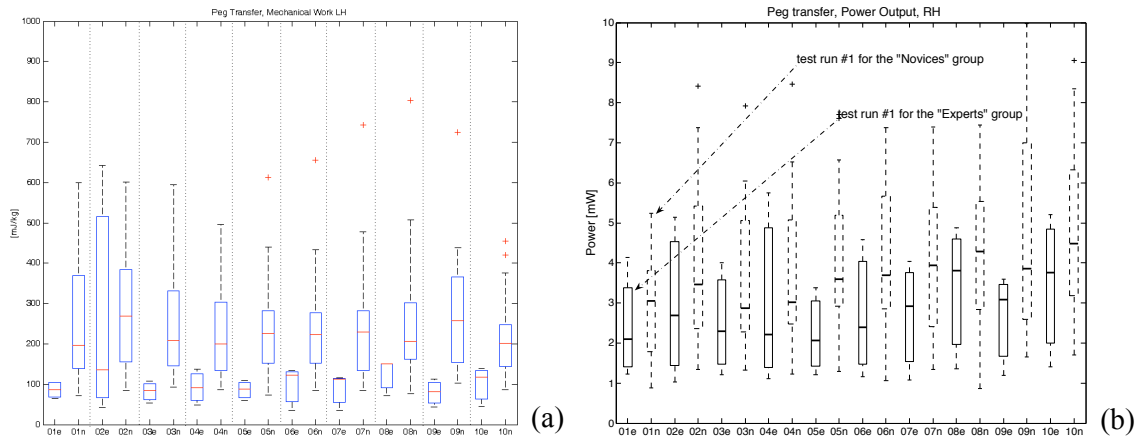


**Figure 42:** (a) Mechanical Work and (b) Power Output for the right hand (RH) of Peg Transfer

For the other two training tasks **Figure 43** the means of the power output metric are just barely different between the two populations but the IRQs overlap to a large extent.

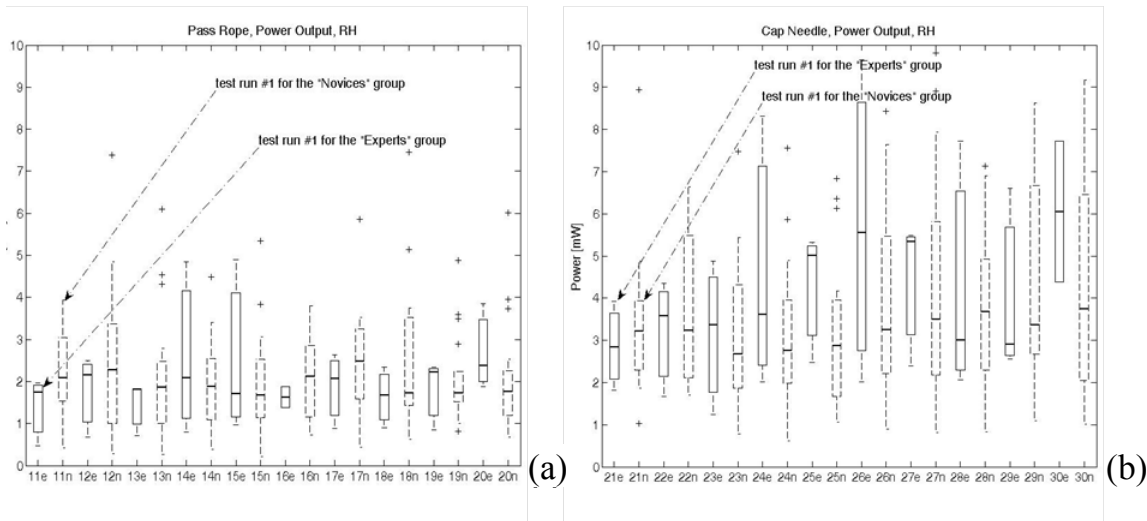


**Figure 43:** Power output for the right hand instruments for (a) pass the rope and (b) cap the needle

### 7.3.9 Learning Curve

All participants in this study repeatedly performed each of the three training tasks and therefore experienced a learning process. The mean time to completion is charted in **Figure 44** for the two populations (a) expert and (b) novice.

Aside from the magnitude differences between the various tasks we notice that the experts' time to completion charts an almost flat curve (slope between -0.7 to -1.1), especially for the most familiar of the tasks the peg transfer and the cap the needle. The pass the rope task is less familiar to the surgeons that specialize in surgeries other than the abdominal cavity. The pass the rope task simulates the inspection of the small and large intestines to check for hidden injuries punctures, bleeding before pulling out all instruments and trocars. As such is a critical skill for abdominal cavity surgery but one that is rarely practiced by the other surgeons. The slope of -1.8 we see associated with this task could be due to the other surgeons in the group catching up with a non-familiar task. The time to completion charts for the novice group exhibits a slope that is about twice as large as the expert population. For the easier tasks peg transfer and cap the needle the slope is -2.3 to -2.5, while the much harder task of pass the rope has a slope of -4.0.

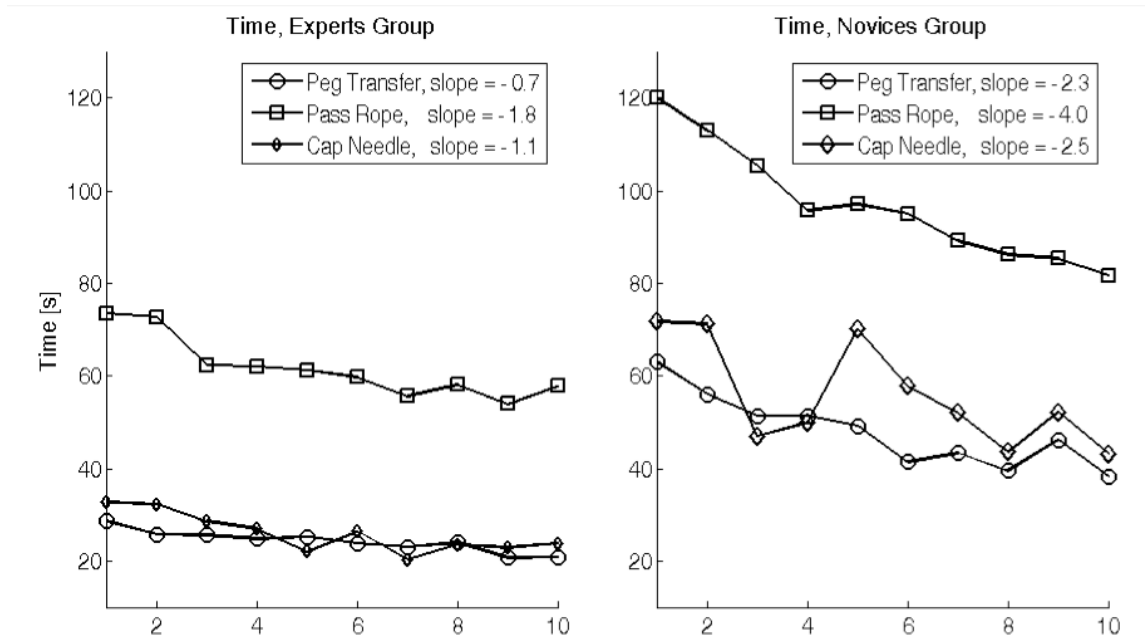


Figure 44: Learning curve for (a) expert group and (b) novice group

For a linear regression fit over the 10 test runs  $y = ax + b$ , where  $a$ , is the slope, the novice population shows a learning curve twice as fast as the expert group. Under the assumption that learning and acquisition of psychomotor skills is a linear process, it is possible to extrapolate that the novice group would require between  $23 \div 28$  test runs to achieve a similar time to completion with the expert population. This does not take into consideration how fatigue may affect skill acquisition process. We have seen from the mechanical work metric that novices tend to use about twice as much energy to perform the same task. Nor does it consider skill retention, namely how much of that newly acquired skill is still available at the beginning of the next training session [137].

The slope of the novice learning curve for the time metric was much steeper than for all other metrics. It comes as a cautionary observation that in the absence of comprehensive feedback trainees will focus on time to completion as they readily observe and appreciate

improvement in this metric and therefore strive for a shorter time at the expense of the other performance metrics.

It is important to note that these psychomotor skills are foundational skill sets that, when properly mastered contribute to a deeper understanding of surgical technique and allows for acquisition of more complex skill sets. These results are in agreement with previous observations [138] using virtual reality simulators, and suggest that training sessions should provide feedback on a complete set of performance metrics such that trainees work to improve all aspects of their performance.

We normalized the means of all performance metrics for the peg transfer task with respect to the first value in the series **Figure 45**. It is immediately obvious that time to completion is indeed the only performance metric that experience improvement. We see that both the path length and the volume swept by the tip of the instrument show no improvement during the 10 test runs. We expect that for the expert surgeons, since their skill set is already in place and should experience just minor random variations from one test run to another. However the novice population does not improve on their path length or on their volume swept by the instrument tip. These suggest that that the novice population is simply repeating the same poorly learned skill, over the next 9 runs but now it does so much faster. This population needs a lot more learning before their critical skill measures are on par with that of the expert group.

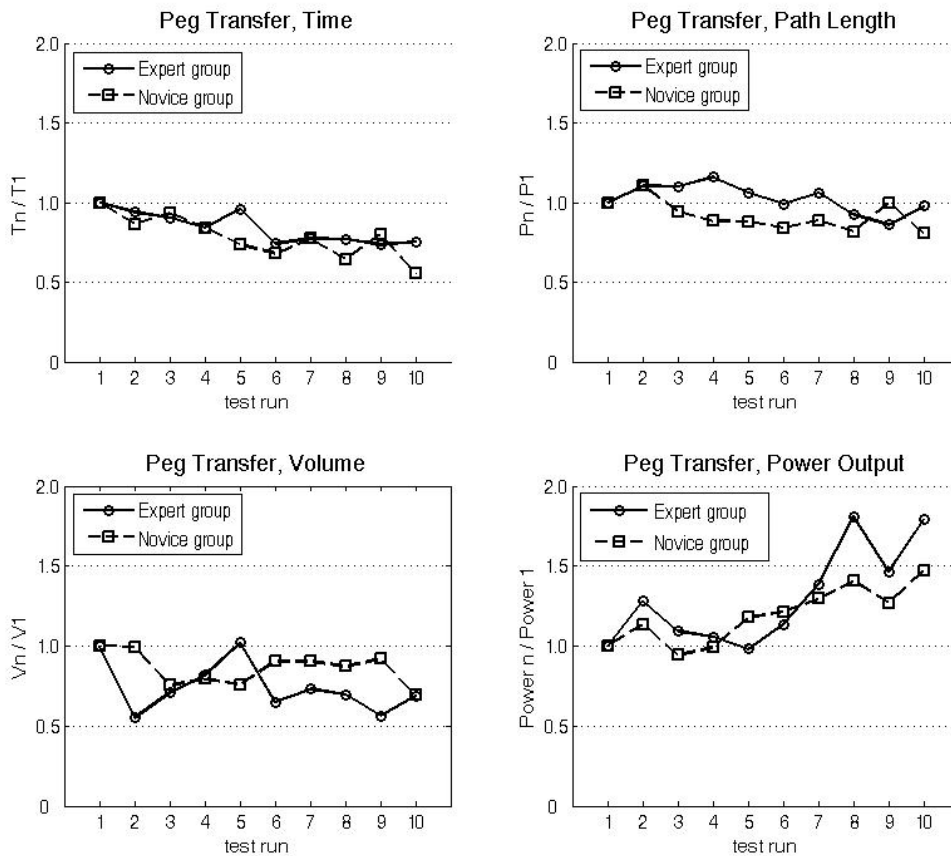


**Figure 45:** Normalized Learning Curves for the peg transfer

It is important to note the normalized chart for the power output metric. We see that expert surgeons power output immediately doubles up starting with the 6<sup>th</sup> or 7<sup>th</sup> of their test runs. It shows that even experienced surgeons, in the absence of an overall performance feedback will focus exclusively on time to completion. We speculate that this is a stimulus for competitive behavior and even experienced surgeons will abandon their cautious approach from the first 5 test runs and race to complete the task faster than the previous time. Again we speculate that improving the graphic user interface to provide real-time feedback on all other performance metrics would be beneficial to the training scenarios tested here. This way we



could channel the competitive spirit of test participants to focus on a holistic approach to surgical skills.

### 7.3.10 Left hand vs. Right hand

All the training tasks in this study were designed to carry an equal load between the left and the right hand instruments. Furthermore all test participants were right handed. In **Figure 46** we chart the path length for both the right hand instrument and the left hand instrument for both populations and across all three training tasks.

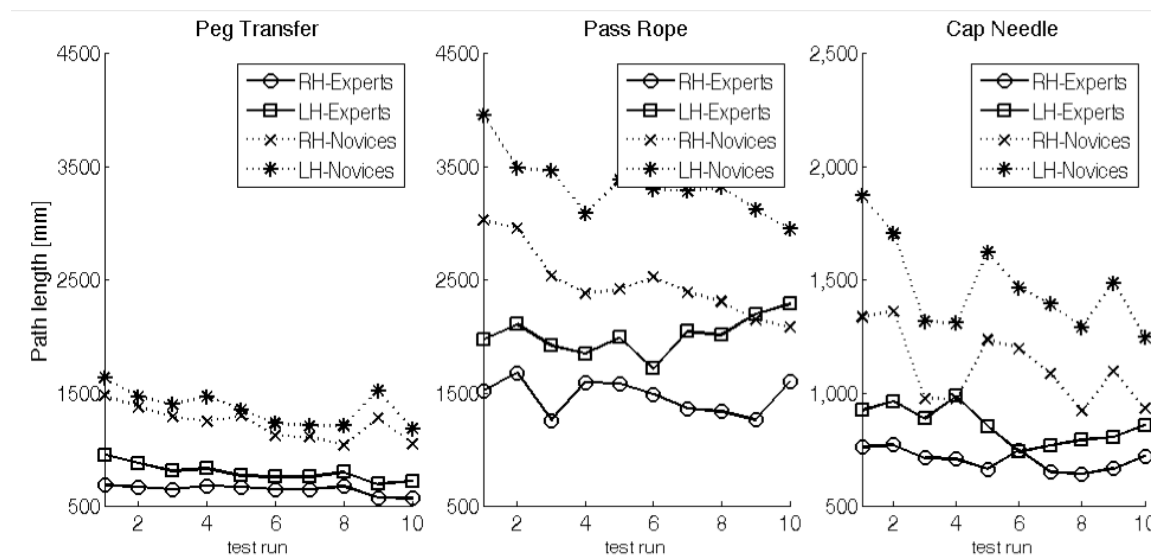


**Figure 46: Dominant vs. non-dominant hand**

Consistently the tip of the left hand instrument travels more than the right hand instrument, even though the task was designed to be of equal path between hands. This observation is valid for both populations and it appears to be somewhat consistent throughout the three training tasks. For the peg transfer task, experts' left hand travels on the average 24% more

than the right hand, while for the novices the difference is on the average about 11%. For the pass the rope task, the left hand travels about 38% more than the right hand, for both experts and novices. On the cap the needle task, experts' left hand travels about 34% more while for the novices the left hand travels about 42% more. These results show significant differences in skill between the dominant and the non-dominant hands. Other researchers [139] have addressed the issue of specialized training requirements for the non-dominant hand. Our experts group when exposed to this observation believed that while it is important to have good control over the non-dominant hand it is equally true that in an actual surgical setting, the two hands will play different roles.

### 7.3.11 Discussion

Well-structured surgical training should provide appropriate instruction and assessment for all levels of training covering cognitive as well as the dexterity requirements. It has been estimated that for the open procedures a skillfully performed operation depends to a large degree, 75% on decision-making skills and only to a lesser degree, 25% on the dexterity of the surgeon [140]. However for the MIS approach psychomotor skills become more important and have to be mastered to advanced level in order to successfully complete a procedure. Situational awareness, accurate targeting and bimanual dexterity while compensating for two dimensional perception in poor lighting situations can take a long time to master, with some specialties requiring as many as 100 procedures before achieving proficiency [141]. Counting the number of surgeries performed to accredit surgeons tells nothing about how the surgeon operates because it invariably accounts for other variables such as patient complexity. Without an objective assessment of deficiencies in training and surgical performance it is difficult to identify those

deficiencies and also quantify training progress [142] however, finding objective criteria for judging good surgical technique is difficult.

Most assessments are purely subjective and use global scores gathered from a panel of experts. Performance is graded using operation-specific checklists, detailed global rating for the economy and fluidity of motion and pass/fail judgments. Subjective methods using structured scoring systems have been shown to be reliable [90] but are expensive [143] both in manpower and time and often more suitable for research projects.

To improve surgical skill assessment many researchers have addressed the problem in laboratory conditions either using training boxes [88, 89] or animal models [144]. By using specialized equipment to track the surgical instruments the subjective assessments of economy and fluidity of motion become objective measures [90, 145]. It is important to observe that for specific tests bench-model simulation gives equivalent results to the use of live animals [90]. Our study suggests that when measured at the tip of a laparoscopic instrument, kinematic motion parameters are indeed a valid assessment of MIS psychomotor skill set.

We examined four different parameters: time to completion, instrument tip path length, volume of space containing the tool tips at all time and tool controlling effort on the part of the surgeon. Time to complete the task is an intuitive and easy to quantify metric and our study agrees with previous results [119] that time correlates with psychomotor skill. A fast surgeon is not necessarily a good surgeon [92, 146] however and emphasizing time performance during training sessions may encourage speed over accuracy [139].

Previous studies [147] show that novice users display poor economy of motion. Total path length traveled by the tool tip is one of the proposed metrics to objectively assess economy

of motion [148] concomitant with the time to completion. Because additional tool tip travel is required to recover from errors, such as dropping the manipulated piece during a peg transfer, using this metric obviates the need for an observer counting such errors. However in certain situations [149] emphasizing the shortest path length may not capture the complexity of the task.

Given the physical constraints of the working space inside the an insufflated cavity we suggest that volume covered by the tip of the instrument is another important measure of the economy of motion and would complement the assessment made by looking at the path length only. An errant tool tip traveling outside the bounds of the insufflated working space can easily results in injury to the surrounding anatomy. Our measures show a statistically significant correlation between MIS experience and these two metrics, with novices using about twice as much space while also traveling a path that is twice as long. The one metric that may best illustrate the level of dexterity is the physical effort required to control the surgical instruments as this measures efficiency of motion that comes with mastered skill.

Economy in motor coordination is a learning phenomenon realized by reduced physiological energy expenditures that also translate into reduced energy output. We use the normalized measure of specific mechanical work to account for the variability in arm and hand size among the test participants. Our experimental data suggests that the controlling effort is a uniform measure across the three different training tasks and seems to be independent of the specific training task. For the experts group the mean values of specific mechanical work is around 150mJ/kg for all three tasks and may therefore represent the energy cost of performing a mastered skill.

Future studies on actual surgeries should investigate whether the intra-operative demands placed on the surgeon during the MIS procedure alter that baseline value of controlling effort. Taken individually all the above metrics show statistically significant differences between experts and novices. Based on these findings we envision a machine-learning algorithm that uses these metrics in order to provide automated real-time feedback to learners. We suggest the use of a compound score that is an affine sum of all these metrics with relative weighing of each metric in the total score,  $S$ .

$$S = \sum_{i=1}^4 \alpha_i \times k_i = \alpha_1 \times Work + \alpha_2 \times Vol + \alpha_3 \times Time + \alpha_4 \times P$$

$$\sum_{i=1}^4 \alpha_i = 1$$

Computing this score for every test run as well as for a given training sessions will help pinpoint specific training needs. A benefit to this setup over other types of laparoscopic simulators is that an expert surgeon would not need to be present to provide feedback to the learner because it is generated automatically. In addition there would be no limitations to the type of or number of training tasks available for learning and evaluation as an expert score can be established for any task based on results from a sufficiently large group of experts.

### 7.3.12 Conclusion

Although there is more to becoming an expert in laparoscopic surgical technique than acquiring adequate psychomotor skills mastery of the basic skills lays the foundation for the expertise. Basic psychomotor skills must become second nature to the surgeon in order to allow the freedom to concentrate on higher cognitive aspects of surgery. Based on these results of this

study we conclude that the motion parameters evaluated here including time to completion, path length, volume swept by the instruments and specific mechanical work are all valid measures of laparoscopic training progress. We must emphasize above all the significance of a constant value for specific mechanical work across all training tasks for the expert as a group. It appears that experts have one average base value of 150 mJ/kg for the amount effort required to perform these tasks.

# 8 Support Vector Machines Improve the Accuracy of Performance Evaluation of Laparoscopic Training Tasks

Chapter 8 is a version of the article published by B Allen, V Nistor, E Dutson, GP Carman, CE Lewis, and P Faloutsos, Support Vector Machines Improve the Accuracy of performance Evaluation of Laparoscopic Training Tasks, Surgical Endoscopy, 2010 [5]

## 8.1 Abstract

*Background:* Despite technological advances in tracking surgical motions, automatic evaluation of laparoscopic skills remains remote. A new method is proposed that combines multiple discrete motion-analysis metrics. This new method is compared to previously proposed metric-combination methods and shown to provide greater ability to classify novice and expert surgeons.

*Methods:* Thirty participants (four experts and 26 novices) conducted a total of 696 trials of three training tasks. The tasks were peg transfer, pass rope and cap the needle. Instrument motions were recorded and reduced to four metrics. Three methods (summed-ratios, Z-score normalization and support vector machine (SVM)) of combining metrics into a prediction of surgical competency are compared. The comparison is based on (1) the area under the receiver-operating characteristic curve (AUC) and (2) predictive accuracy on a previously unseen validation data set.

*Results:* for all three tasks, the SVM method was determined to be superior by both AUC and predictive accuracy on the validation set. The SVM method resulted in AUC's of 0.968,

0.952 and 0.970 for the three tasks, compared to 0.958, 0.899, 0.884 for the next-best method (weighted Z-normalization). The SVM method correctly predicted 93.7%, 91.3% and 90.0% of the competencies of subjects, while the weighted Z-normalization predicted 86.6%, 79.3% and 75.7% accurately, respectively ( $p < 0.002$ )

*Conclusions:* This study shows that a support vector machine based analysis provides more accurate predictions of competency at laparoscopic training tasks than the previous analysis techniques. A support vector machine approach to competency evaluation should be considered for computerized laparoscopic performance evaluation systems.

## 8.2 Introduction

Minimally invasive surgery (MIS) provides significant benefits to the patients, including shorter hospital stays, smaller scars and faster healing. However MIS procedures can be significantly more complex than their open procedure counterparts and MIS thus requires longer training and additional experience.

Educational programs such as the Fundamentals of Laparoscopic Surgery (FLS) from the Society of American Gastrointestinal and Endoscopic Surgery (SAGES) and the American College of Surgeons (ACS) are a significant step toward improved consistency and objectivity in surgical education but many feel that further improvements in both quality and reduced training time are possible, see Aggarwal et al [31] for a summary. In recent years technological advances in motion data acquisition for laparoscopic training such as the virtual reality (VR) based [103, 150], optical (LapVR, Immersion medical, 55 W. Watkins Mill Rd, Gaithersburg, MD) and magnetic [151] tracking systems have provided surgeons and their residents with copious data.



Thus while substantial kinematic data are available to judge the competency of surgeon's performance, distilling useful automated feedback from this information remains difficult,

To meet this challenge motion analysis systems generally reduce the full kinematic record to a small number of scalar metrics such as the time taken to complete the assigned task, or the length of the path taken by the instrument tip over the course of a task. It has been shown that principled combinations of metrics can provide a more powerful discriminator of competent vs. non-competent motions compared to a single metric [102, 152].

This paper proposes a new approach to combining metrics that is based on the supervised machine-learning technique of support vector machines (SVM) [153]. SVMs provide a principled and automatic way to discover complex relationships between motion-derived metrics and the surgeons' level of prior training. The intuition that laparoscopic surgery is sufficiently difficult that individual performance metrics are non-linearly interdependent provides the motivation for examining SVM based approaches.

### 8.3 Methods

To evaluate the proposed technique, motion data was acquired using standard laparoscopic instruments in a training situation. These motion data are compiled into four scalar metrics. The proposed SVM based approach to combining these metrics is compared directly to the strongest previously reported methods: the summed ratios method [152] and the Z-score normalization method [102]. Each of the three approaches is evaluated as to their ability to predict the surgeon's prior level of experience based solely on these metrics computed from the motion data.

### 8.3.1 Subjects

Thirty individuals participants were used in this study. Four were practicing laparoscopic surgeons and the remaining twenty-six were residents without specific training with laparoscopic instruments. Each participant conducted up to ten trials on each of the three evaluation tasks for a total of 696 tasks performances across both populations.

### 8.3.2 Evaluation Tasks

The surgical tasks recorded for this study are based on the Fundamentals of Laparoscopic Surgery (FLS) training system. The participants operated in a standard training box with a grasper instrument (Ethicon Endo-Surgery Inc. 4545 Creek Rd Cincinnati OH) in the left hand and a needle driver (KARL STORZ Endoscopy America Inc, 600 Corporate Pointe Culver City CA) in the right. Visual feedback was provided at 640x480 resolution and 30Hz refresh rate. Using this setup, participants were asked to perform ten iterations of each of three previously validated tasks [132, 154, 155] in fixed order: peg transfer, pass rope and cap needle. A brief description of each is provided bellow.

The peg transfer task required the participants to transfer a small ring made of rubber from one one-inch peg to an identical peg several inches away. The participants were then required to transfer the rubber ring back to the originating peg.

The pass-rope task asks the participants to transfer a ten-inch cotton rope from the right hand instrument to the left and then back left to right. The rope is marked at one-inch intervals indicating allowable grasping points.

The cap-needle task requires the participants to pick up a needle with their dominant hand and a needle cap with the other hand. They then fully insert the needle into the cap and place the cap in a fixed position.

### 8.3.3 Motion Tracking System

Both of the laparoscopic instruments were modified to contain two electromagnetic sensors (Ascension Technology Corp. 107 Catamount Drive Milton VT) capable of reporting the instantaneous location and orientation of the instruments. Placement of the sensors within the instruments is shown in **Figure 10**. The sensors are sufficiently small (1.3 mm in diameter) and light-weight (0.2g, 11.8 g with the cable) that the instruments functionality is not impaired. Each of the four sensors reports spatial position and orientation at 10Hz with a linear accuracy of approximately 0.5 mm and orientation accuracy of 0.2 degrees. The position of the instrument's distal tip is calculated from the sensors information and recorded. The recorded motion of the instrument tip is then analyzed to generate the four metrics of task performance described in the next section.

### 8.3.4 Task Metrics

Four task-independent metrics ( $t_c, l, V, c_e$ ) were gathered at each trial in each task. The first three metrics are kinematically derived from the motion data. The final metric, control effort, is estimated by analytically calculating the forces applied to the instrument. All metrics are scalar quantities and computed by finite sums.

Each metric is appropriate to the simple training tasks observed and is expected to have utility in measuring laparoscopic performance, either due to prior reports specific to laparoscopic

surgery; time to completion and path length [156], control effort [102], or by extension from mentor based skills assessments [157].

*Time to completion  $t_c$*  is the total time, measured in seconds, required by the participant to complete the assigned task and return the instrument tips to the starting position.

*Path length  $l$*  is the total linear distance measured in millimeters traveled by the distal tip of the instrument.

*Volume  $V$*  is computed as the volume of the minimal axis-aligned bounding box that contains all samples of the distal sensor's position.

*Controlling effort  $c_e$*  is a metric based on measures of force rather than position. Estimation is possible because the tracking system records the orientation of the instruments and the changes in position as a function of time. This information provides linear and angular accelerations, which coupled with the measured inertial properties of the instrument, are used to calculate applied forces. The calculation assumes the trocar is fixed in space and acts as an ideal frictionless fulcrum. The mass of the peg from the peg transfer task and the rope from the pass rope task are assumed negligible. To calculate the estimated control effort, the net force applied by the surgeon to the instrument handle is summed over the entire time to completion  $t_c$  of the task

### 8.3.5 Combinations of Metrics

In general, it is hypothesized that single metrics alone provide insufficient means to categorize the skill level with which a particular task is performed. In this section we describe three methods that combine multiple metrics to label the subject with a single binary class, either

“competent”  $C_+$  or non-competent“  $C_-$ . The prior level of training (i.e. surgeon or resident) of each participant was recorded and determines if they are “expert” or “novice”. The goal of each of these three methods is to automatically label experts as competent  $C_+$ , and the novices as non-competent  $C_-$  by examining only the motion metrics. The probability of a test, reporting competency  $C_+$  for an expert  $E$  is  $P(C_+|E)$  and is known as the sensitivity  $S_n$  of the test. Conversely, the specificity of a test is the probability of reporting a novice as non-competent,  $S_p = P(C_-|N)$ . The first two methods described bellow, summed ratios and Z-score normalization are derived from the literature and extended where needed. Both of these methods calculate an aggregate score  $s$  which is then compared to the cut-off score  $s_c$  such that competency is indicated when  $s > s_c$ . The third method is based on support vector machines and does not require determination of a cut-off score.

### 8.3.6 Summed Ratios

The summed ratios method [152] computes an aggregate score for an individual by summing normalized metrics. A metric is normalized by dividing the subject’s metric  $m$  by the maximum score  $max_E(m)$  obtained by an expert for that metric and associated task. All metrics are equally weighted:

$$s = \sum_{m \in (t_c, l, V, c_e)} \frac{m}{max_E(m)}$$

The combined scores are classified into competent or non-competent using a cut-off score that maximizes the product of sensitivity and specificity with equal weight,

$$s_c = \arg max_s (S_p \times S_n)$$

### 8.3.7 Score Normalization

The Z-score normalization method [102] calculates the aggregate score  $s$  as the weighted average of Z-scores that are obtained from metric values  $m$  using the mean  $\mu(m_e)$  and standard deviation  $\sigma_e$  of expert data,

$$s = \sum_{m \in (t_c, l, V, c_e)} a_m \left( \frac{m - \mu(m_e)}{\sigma_e} \right)$$

Where  $a_m$  is the scalar weight for metric  $m$ . We extend the treatment of Stylopoulos et al. [102] to find optimal values for the weights. This is done by considering the scalar weights as a single four-dimensional weight factor  $\vec{a}$ . A series of candidate weight vectors is generated with a per-component step size of 0.1 and each is normalized and then evaluated. The weight vector with the best average performance is retained.

### 8.3.8 Support Vector Machines (SVM)

In this section we introduce a new method to classify an individual's motion based on support vector machines. SVMs are a powerful method for automatically generating non-linear functions from a set of labeled examples. One common use and the one we employ here is to generate functions that output a single binary datum – here the competency with which a task is performed. More formally, for each individual in the training data, a vector is constructed containing a dimension for each explanatory variable. Here, each of the metrics is used as an explanatory dimension. A label,  $z \in (E, N)$ , is appended to store whether the measured motion was recorded from an expert or a novice to form the training vector  $x = (t_c, l, V, c_e, z)$ . Once the training process is complete, a new unlabeled vector of metrics  $x'$  is given a label by determining the region where it falls,  $x' \mapsto (C_+, C_-)$ . This label is a prediction of whether the subject is

competent or non-competent. This label is a prediction of whether the subject is competent or non-competent

The SVM is trained by an iterative process of finding support vectors that divide the space of explanatory variables (in this case the individual metrics) into expert and novice regions. Such support vectors are simply hyper-planes that separate training data points of different labels, so that most expert points are on one side of the hyper-plane and most novice points on the other side. Support vectors are chosen to maximize this separation of categories as well as to maximize the distance from the training points to the hyper-plane itself. In this way, a small number of support vectors can efficiently partition the entire space of explanatory variables into separate regions, with each region associated with one of the labels (i.e. E or N).

If the data are related in a linear manner, simpler methods, such as the Z-score normalization described above are sufficient. SVMs however, are able to handle nonlinear relationships between explanatory variables by employing kernel functions  $K(x,y)$ . The kernel defines the distance function (i.e. the inner product) between two vectors of explanatory variables. A nonlinear kernel allows the linear separating hyper-planes to distinguish nonlinear relationships between explanatory variables. The kernel can be understood intuitively as deforming the space containing the training points. When successful, this deformation permits the linear separating hyper-planes to effectively account for nonlinear relationships between the explanatory variables.

The implementation reported here uses libSVM [158], a freely available and open-source implementation of SVM. Prior to training and classification, the input vector  $(x,z)$  is scaled linearly so that all elements are in  $[0,1]$  and the radial-basis function

$$K(x, y) = e^{-\gamma \|x - y\|^2},$$

is used as the kernel. The SVM training process uses a weighting factor  $C$  to scale the importance of errors in classifying the training data. The process of determining values for  $C$  and  $\gamma$  is described in the following section.

### 8.3.9 Evaluating Classification Performance

To compare the three methods of combining metrics described in previous section, we consider two approaches; the first based on receiver-operating characteristic (ROC) curve analysis and the second on validation against previously unseen data.

#### 8.3.10 ROC Analysis

The first approach relies on the receiver-operating characteristic (ROC) curve. The ROC curve is plotted as one minus the specificity vs. the sensitivity. It provides an intuitive way to compare methods that accepts the trade-off inherent in any binary classifier between being too sensitive and being too selective. The total area under their receiver-operating-characteristic curves (AUC) by trapezoidal integration provides a quantitative comparison between the three methods. Intuitively the AUC estimates the probability that an expert chosen at random will score better than a randomly selected novice. Higher AUCs are more useful distinguishers, with an AUC of 1.0 being the ideal classifier and an AUC of 0.5 no better than pure chance. AUC is a common means of comparing diagnostic tests and Hanley and McNeil [159] show that AUC is equivalent to the non-parametric Wilcoxon-Mann-Whitney statistic.

The second approach to comparing the three methods is to measure the accuracy of classification on a previously unseen data set. This validation process simulates the conditions of



an on-line evaluation system deployed for example as a training assistant to provide online objective feedback. This approach is described in the next section.

### 8.3.11 Validation Comparison

The motion data from each task are analyzed separately. The combination score for each trial is computed using either one of the three methods of combination previously described. The following procedure is repeated one-hundred times for each method-task pair:

1. Segment data. The aggregate scores for each trial are randomly divided into two sets: three-fourths are placed into a training set and the remaining one-fourth in a validation set. Trials are drawn with uniform probability but adjusted as needed to preserve the approximate ratio of expert-to-novice trials in the generated sets.
2. Determine method parameters using only the training set.
  - a. For the summed ratios, five hundred candidate cut-off scores are tested across the full range of composite scores. The cut-off with the largest product of sensitivity and specificity is saved as the delineator.
  - b. For the Z-score normalization method both a weight-vector and the corresponding cut-off score must be determined. To find the best weight-vector each unique unit-vector with elements in  $[0,1]$  and with elements spaced by 0.1 is examined. For each of these candidate weight vectors, five hundred candidate cut-off scores are tested over the range  $[-2, 2]$ , encompassing approximately 95% of the observed variance in composite scores. The combination of weight vector and cut-off score that produce the largest product of sensitivity and specificity is saved as the delineator.

- c. For the SVM method,  $C$  and  $\gamma$  are found using an exponential grid search across  $C = 2^{17}, 2^{15}, \dots, 2^{-3}$  and  $\gamma = 2^{17}, 2^{15}, \dots, 2^{-3}$ . Each  $(C, \gamma)$  pair is evaluated by doing five-fold cross-validation using only the training set data. The support vectors producing the highest accuracy rate are used for the classifier.
3. Evaluate against the validation set. The validation set is then classified using the parameters determined in training, i.e.: cut-off score, weight vector and cut-off score, or support vectors. The resulting accuracy and specificity of classification are computed over the validation set.

Significance of the validation-set accuracy is calculated using Welch's t-test [160] and a threshold of 0.05 is assumed significant.

## 8.4 Results

### 8.4.1 Individualized Metrics

Values calculated for each individual metric for each task are summarized in **Table 15** with the peg transfer population of  $n=285$ , 31 expert and 254 novice; pass-rope population  $n=212$ , 29 expert and 138 novice; and cap-needle population  $n=199$ , 30 expert and 169 novice.

All four individual metrics were computed for each subject's attempt at each task. The table provides mean and standard deviation of the collected metrics for the different populations, novices, experts and all participants.

**Table 15:** Mean and standard deviation values for each of the individual metrics applied to each task and for each population sub-group

	All	Expert	Novice
<b>Path Length (mm)</b>			
Peg Transfer	1316.5 ±719.1	701.8 ±138.3	1391.5 ±725.5
Pass Rope	2141.1 ±904.1	1464.8 ±350.3	2248.3 ±918.9
Cap Needle	1456.3 ±920.9	907.2 ±253.1	1553.8 ±961.8
<b>Time (s)</b>			
Peg Transfer	45.44 ±24.54	24.41 ±5.22	48.01 ±24.74
Pass Rope	92.18 ±31.62	61.77 ±9.59	97.00 ±31.22
Cap Needle	50.99 ±34.93	26.07 ±8.98	55.41 ±35.96
<b>Volume (cm<sup>3</sup>)</b>			
Peg Transfer	2.559 ±2.442	1.279 ±0.392	2.715 ±2.539
Pass Rope	1.634 ±2.176	0.923 ±0.842	1.753 ±2.300
Cap Needle	5.025 ±3.025	4.133 ±1.350	5.184 ±3.210
<b>Control Effort (m<sup>2</sup>/s<sup>2</sup>)</b>			
Peg Transfer	10.51 ±16.71	3.58 ±2.08	11.36 ±17.50
Pass Rope	15.07 ±12.47	9.62 ±6.77	15.93 ±12.95
Cap Needle	12.08 ±12.99	6.63 ±4.17	13.04 ±13.78

A histogram of the four performance metrics for the peg transfer task is summarized in **Figure 47**. Similar histograms are plotted for the other two training tasks, pass-the-rope in **Figure 48** and cap-the-needle in **Figure 49**.

Each combination of training task and performance metric is shown as two super-imposed histograms. The two histograms are derived from disjoint distributions, one from the expert performances and the other from the novice performances. The vertical axis measures the number of performances in each bin, with metrics in the range indicated on the horizontal axis. The vertical dotted line in each graph indicates the score, which optimally separates the novice and expert populations. This separating score is determined by maximizing the product of specificity and sensitivity for the entire sample.

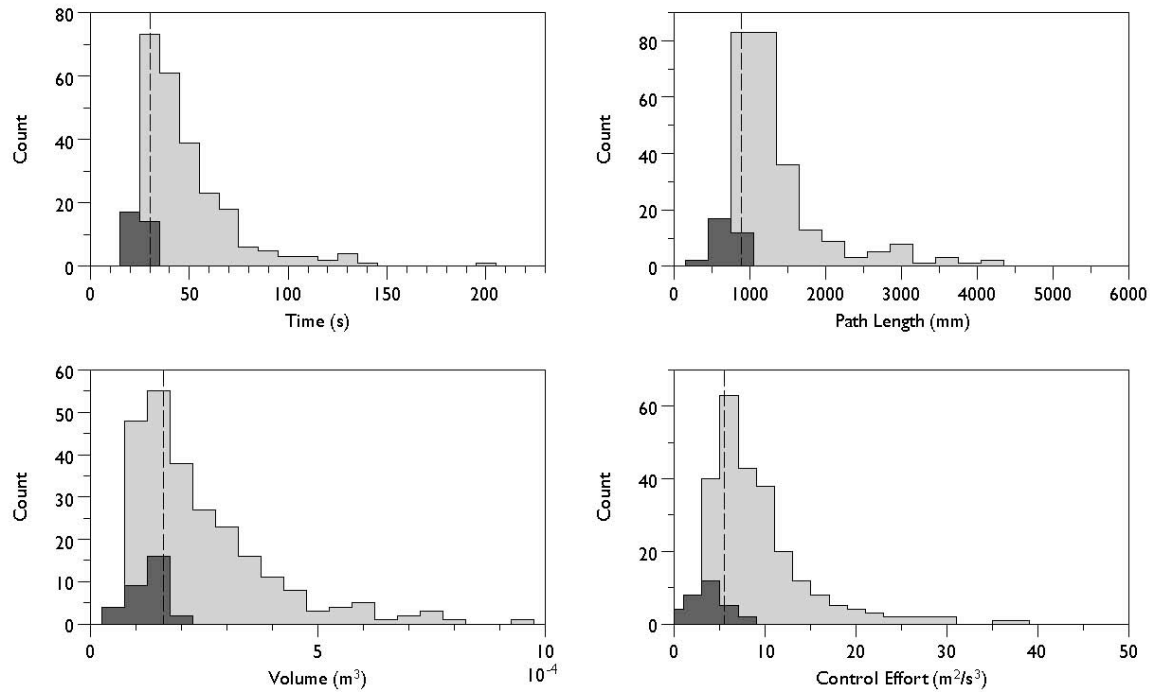


**Figure 47:** Histograms to compare the frequency distribution of observed metrics for the peg transfer task. The dotted vertical line indicates the optimal separating score.

Ideally all expert performances should fall to the left of that score and the novice performances to the right of that score. The histograms illustrate that for each metric-task studied the optimal separating line fails to cleanly divide the novice from the expert. Although the distributions are qualitatively different the significant overlap reduces the usefulness of the metric distinguishing novice from expert. Note also that the separating power of a single metric varies with task. For example the control effort has little ability to distinguish between the two sample groups for the cap-needle and pass-rope tasks but it is quite effective for the peg transfer task.

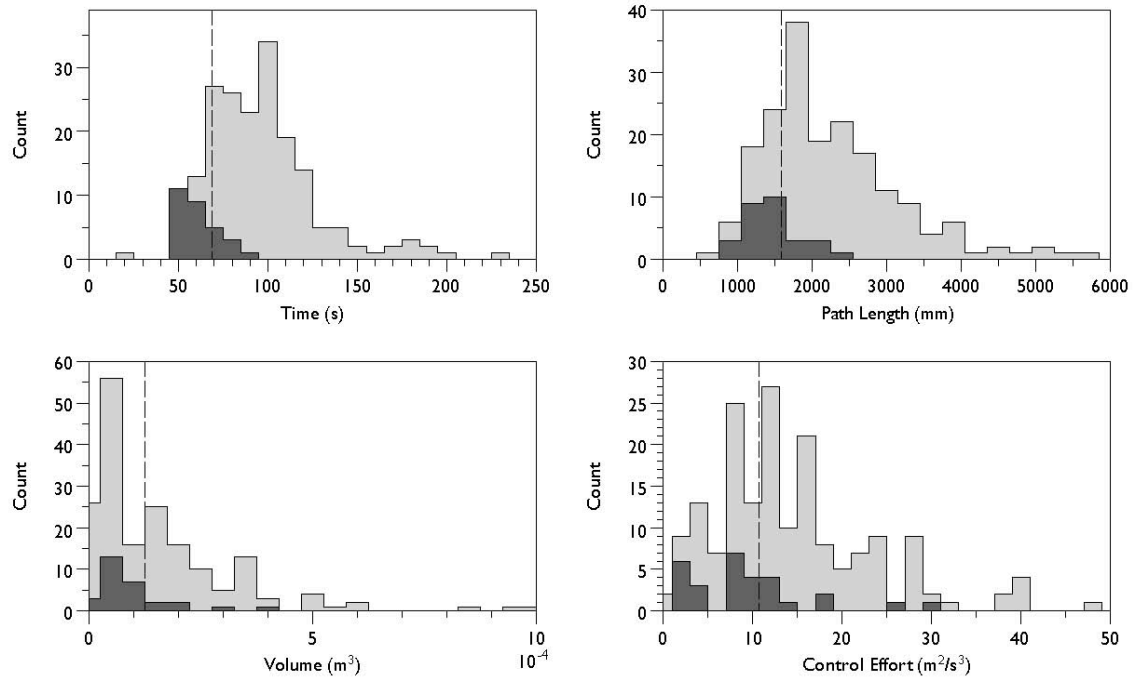


Figure 48: Histograms to compare the frequency distribution of observed metrics for the pass the rope task. The dotted vertical line indicates the optimal separating score.

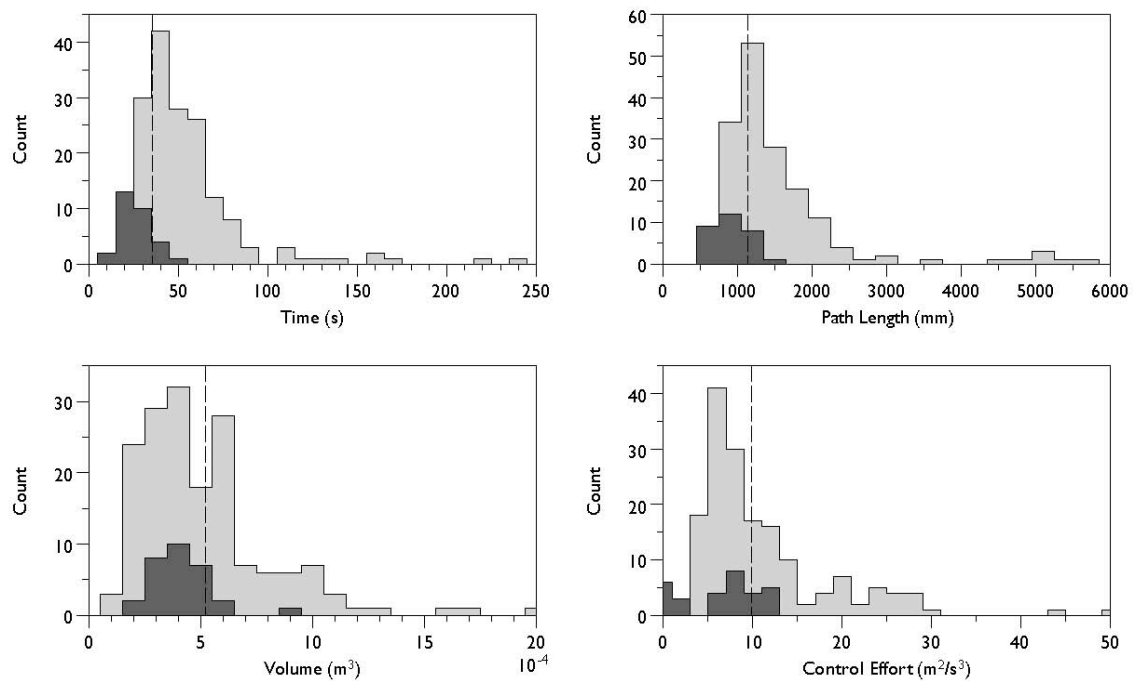


Figure 49: Histograms to compare the frequency distribution of observed metrics for the cap-the-needle training task. The dotted vertical line indicates the optimal separating score.

## 8.4.2 Combinations of Metrics

The methods of combining metrics are first compared by AUC. The AUC measurements for each task and each method are provided in **Table 16**. Values closer to 1.0 indicate better ability to distinguish novice from expert. The tree methods of metric combination are ordered consistently by AUC over all three tasks; the SVM method outperforms weighted Z-normalized method, which in turn outperforms the summed ratios method

**Table 16:** Comparison of area under the ROC curves (AUC) for each method of combining individual metrics

Method	Peg Transfer	Pass Rope	Cap Needle
SVM	0.9682	0.9520	0.9704
Weighted Z-Norm	0.9582	0.8994	0.8840
Summed Ratios	0.9444	0.8356	0.7834

The SVM method is consistently the best classifier as measured by AUC. The cap-needle task shows the largest difference with an area of 0.9704 for the SVM method compared to 0.884 for the Z-normalized method's or the summed ratios method's of 0.7834. The Z-normalized method has the largest mean AUC using a mean best-performing weight vector of (0.965, 0.0, 0.033, 0.002). The best weight vectors for the peg-transfer task and pass-the-rope task are (0.034, 0.865, 0.005, 0.096) and (0.883, 0.086, 0.0, 0.032) respectively.

The second approach to comparing the methods of combining metrics is by their accuracy in classifying previously unseen data, which shows the SVM-based method to be more accurate and yield a smaller variance. **Table 17** shows the mean accuracy  $\mu(Acc)$  and standard

deviation of the accuracy  $\sigma(Acc)$  over the data for each training task. The accuracies of the SVM predictions are significantly better than the next best method, weighted Z-normalized for all three training tasks (peg-transfer  $p < 0.001$ ; pass-rope  $p = 0.001$  and cap-needle  $p = 0.002$ ).

The receiver-operating-characteristic (ROC) is a graphical comparison of the three methods of combining metrics. In **Figure 50** we capture the ROC curves for each of the three methods of combining metrics and for all three of the training tasks. In all three tasks, the SVM method dominates both alternatives. That is, for each given sensitivity the SVM method provides equal or higher specificity shown as a curve above and to the left of the other curves. We that as the complexity of the training task increases from peg transfer to pass-rope and onto the most complex, the cap-needle motion analysis becomes less useful in distinguishing different competencies. However the SVM method suffer markedly less performance degradation than either the weighted Z-normalized or the summed-ratios methods.

**Table 17:** Mean accuracy  $\mu(Acc)$  and standard deviation of the accuracy  $\sigma(Acc)$  for each task and method pair is calculated over 100 repetitions of classification on a randomly selected validation set. The mean cut-off score  $\mu(s_c)$  is the mean score used to divide predicted expert from

Method	$\mu(Acc)$	$\sigma(Acc)$	$\mu(s_c)$
Peg Transfer			
SVM	93.7%	2.6%	N/A
Weighted Z-Norm	86.6%	7.0%	1.405
Summed Ratios	83.2%	5.1%	3.783
Pass Rope			
SVM	91.3%	4.3%	N/A
Weighted Z-Norm	79.3%	9.6%	1.071
Summed Ratios	72.2%	7.3%	3.454
Cap Needle			
SVM	90.0%	3.4%	N/A
Weighted Z-Norm	75.7%	13.5%	0.803
Summed Ratios	70.8%	6.9%	3.658

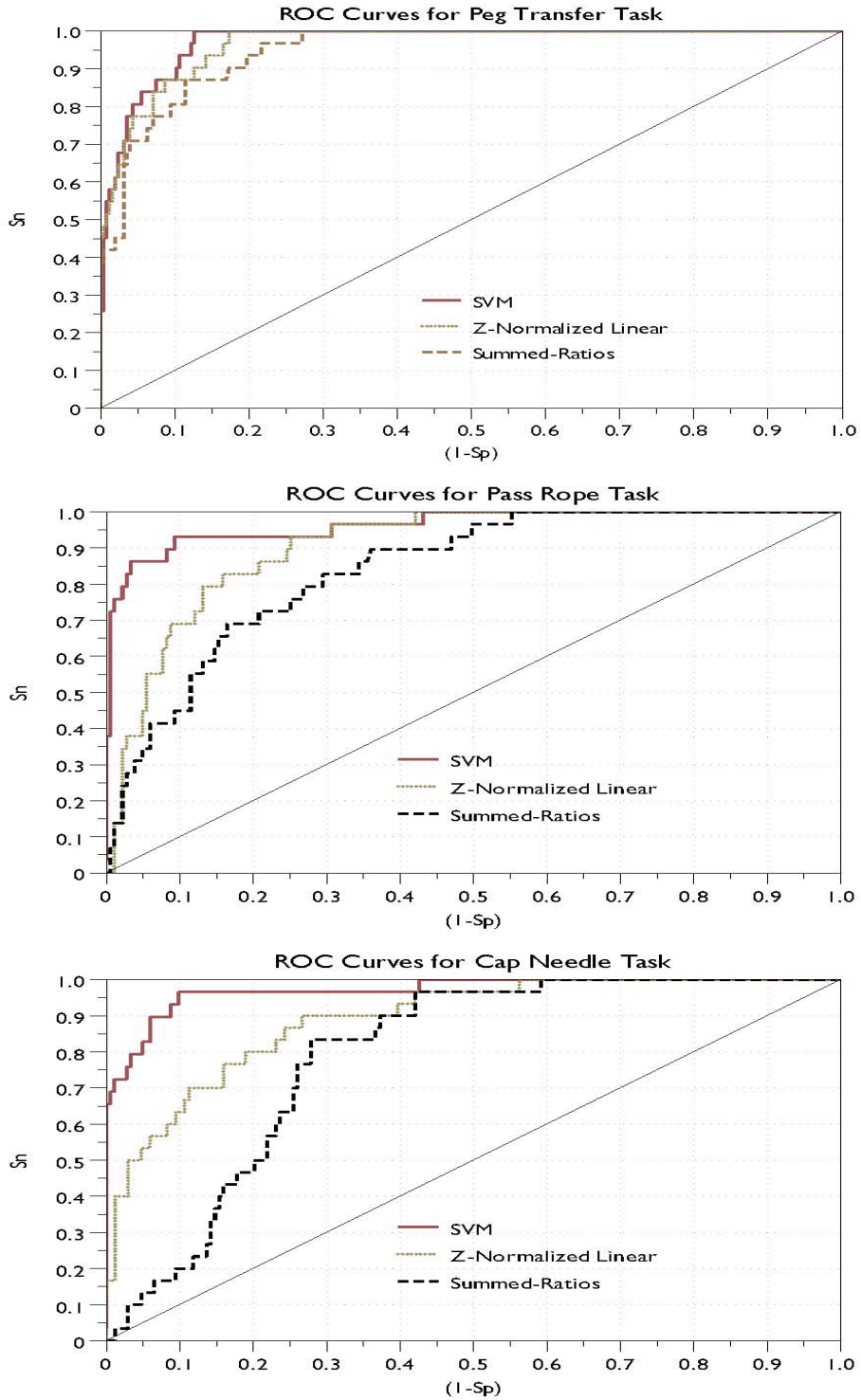


**Figure 50:** Receiver-Operating-Characteristic curves for all three training tasks: peg transfer (top), pass the rope (middle) and cap the needle (bottom). The straight diagonal line represents a theoretical random classifier



## 8.5 Discussion

Our results show that the accuracy of competency prediction can be dramatically improved by 7%, 12% and even 14% for the three tasks examined simply by improving the analysis of motion data. Because this finding builds on standard motion tracking approach it is likely robust to differences in specific technology and platforms and thus widely applicable. To our knowledge this work provides the first direct comparison of aggregation techniques applied to the analysis of laparoscopic motions. It is important to note that our method does not merely rely on linear relationships between metrics, so even if a given metric is poorly correlated with competent performance overall it may add to the analysis as a whole.

Consider the recent study of Chmarra et al. [149] which shows that minimizing the path-length is likely not characteristic of expert surgeons. Merely reporting the raw metric data or a linear combination of such to a student is unlikely to provide practical feedback. It is even possible that presenting overly simplified metrics such as path-length or time to completion directly to the student will encourage the student to maximize those metrics at the expense of overall competency. The characteristics of support vector machines as an analysis tool are well matched to the problem of judging surgical competence based on motion data. Since SVM learn from example motions, the effectiveness of an SVM-based performance evaluator stems from actual differences in the motions of experts and novices. This can be contrasted with attempts to artificially determine the quality or importance of individual metrics. Second, SVM classifiers are able to integrate several orders of magnitude more example motions than used in this study while still providing responses to new queries [153]. Third, as new metrics are devised, they can be trivially added to the evaluator to improve accuracy. To our knowledge, this work is the first

to suggest their use on this domain, although they are becoming a common approach to a variety of difficult diagnostic problems.

Our analysis considers aggregate kinematic information and is only capable of evaluating low-level motor skills. Higher level surgical skills are not examined and approaches based on aggregate metrics are unlikely to provide any significant insight, since by their nature obfuscate the strategies and intentions of the surgeon. However our findings also show that the simplest laparoscopic training task, the peg-transfer has the least benefit from the proposed use of SVMs. Perhaps it is due to some of the novice participants having previously attained a sufficient level of competency at this task to be indistinguishable from experts; in effect a few novices are already experts at the peg transfer task. If so, then the described approach is likely to be most useful to evaluate tasks that are of intermediate complexity, i.e. complex enough to require significant motor skills yet simple enough to not require high-level or strategic surgical abilities. The ROC curves **Figure 50** suggests that motion analysis methods in general have difficulty as task complexity increases. However, the SVM method proves more robust to increased complexity, suggesting that it may be useful for even more complex motor skills, such as knot tying.

A trade-off to the power of the SVM to model nonlinear relationships between metrics are that resulting support-vectors can be difficult to understand intuitively. Thus, it may be difficult to explain to a student precisely why their performance was classified as it was.

In conclusion, the maturation of laparoscopic training systems is providing a wealth of data tracking the movements of trainees. New techniques are needed to take full advantage of the ability of these systems to evaluate surgical performance. This work demonstrates that

improved analysis of motion data can increase the accuracy and discriminatory power of existing and future computer enhanced training systems.

## 9 Laparoscopic Telesurgery and Telementoring

### 9.1 Introduction

Telesurgery is the surgery carried out on a patient that is not physically in the same location as the surgeon. It requires two key ingredients: (1) a master-slave surgical robot and (2) a high speed, high reliability telecommunication link between the master controller and the slave robot manipulator. An evolutionary development of telesurgery is surgical telementoring, whereby an expert surgeon operating at the master console has the ability to mentor a surgical trainee located at the slave side of the surgical robot. Telementoring can be performed during an actual surgery or using some form of virtual reality training simulations.

One of the first successful attempts at robotic surgery, the AESOP (Automated Endoscopic System for Optimal Positioning) [16] was a telepresence application. In this scenario the surgeon had the ability to remotely control, using verbal commands, the position and orientation of the robotic arm driving the endoscopic camera. The laparoscopic instruments were initially manipulated directly by the surgeon. It was cleared for use by the Food and Drug Administration (FDA) in 1994 and became the first robot to assist in surgery. The ZEUS robotic surgical system had three robotic arms, one of which was the AESOP while the other two were driving specialized surgical instruments, and followed the movements of the surgeon now located remotely at a master console. The FDA cleared ZEUS in 2001 and before it was phased out in 2003 in favor of the competing surgical robot, the “da Vinci” it was successfully used in a number of surgical disciplines ranging from general surgery to urology and neurosurgery [17-

19]. Similarly, the “da Vinci” has a master console station and, in the same room, a patient side cart with three or four robotic manipulators.

For telementoring applications, Rosser [13, 14] found that all that is lacking from either of these systems is the ability to reach in and perform the task with the trainee. These surgical robotic systems have real-time videoconferencing systems that simply needed to be adapted for long distance communication between the surgeon mentor and the medical students. Even without being able to directly intervene and touch the tissues themselves, the remote mentors were still able to safely guide trainees through complex MIS procedures. M. Anvari, MD, Director of Centre for Minimal Access Surgery at St Joseph’s Healthcare Hamilton, Ontario, Canada, an experienced laparoscopist, used the Zeus (Intuitive Surgical, Sunnyvale, CA) robotic telesurgical system to assist Dr Craig McKinley, a general surgeon with limited endoscopic experience, as Dr McKinley performed advanced laparoscopic procedures on patients at North Bay General Hospital. These early experiences were so successful that the hospital has since started conducting regular telerobotic procedures [20]. Around the same time, Moore and colleagues at Johns Hopkins in Baltimore conducted a study focusing on telementoring surgical trainees through minimally invasive urologic procedures [15]. In this case, communication was achieved not only through real-time videoconferencing and telestration, but the camera was held by an AESOP robot that could be controlled either locally or by the remote mentor. Their results also suggested that telementoring was a feasible modality for guiding surgical residents through complex endoscopic procedures.

In spite of their significant capabilities the telesurgery and telementoring systems described above have severe limitations. To begin with these systems are extremely costly; each unit cost around \$1 million to acquire and another \$1 million or so for annual maintenance and

consumables. Hospitals that embrace surgical robotics usually acquire at least two units, one used for surgery and another one solely for training. Second, these surgical robots are physically large, have substantial space and energy requirements and are definitely not portable. These factors limit their deployment to large medical centers that already have a large pool of expert surgeons.

Telesurgery and telementoring promise the most benefits to remote locations with sparse population and lack of access to surgical expertise [161]. It is particularly well suited for large military deployments at remote locations and for long periods of time. For example a common procedure to treat gastro esophageal reflux, the Nissen fundoplication has the potential to reduce hospital stay from 6 days to two days when converting from open surgery to laparoscopic surgery, **Table 18**. Convalescence period is reduced by a similar ratio, from 35 to 12 days. It was estimated that with a large deployment such as the 150,000 men serving in the Iraqi Wars in 2004, implementing MIS techniques with telesurgery for this procedure alone has the potential to save 3,360 duty days for convalescence, and an additional 7, 048 days for limited duty days, for a total of almost 11,000 hospital bed days.

**Table 18:** Nissen fundoplication, hospitalization and convalescence time

Nissen fundoplication (gastric reflux)	<b>Open surgery</b>	<b>MIS</b>
Hospital stay time	6.1 days	2.2 days
Convalescence time	35 days	12 days

Deploying da Vinci surgical robots and the surgical experts to such locations is not necessarily feasible. Furthermore, one of the major drivers of cost with the da Vinci system is the need to replace standard MIS tools with the system-specific surgical instruments.

Hence, we have developed a more cost-effective surgical system, the UCLA LapaRobot that has a much smaller footprint and uses existing laparoscopic instruments as much as possible and only with small adaptations where needed. The UCLA LapaRobot can potentially be used for both telesurgery and telementoring applications. These capabilities are enabled using spatial tracking of the surgical instruments held by expert surgeons and, in telementoring applications by mentees as well. Tracking will be accomplished using sensors to monitor the spatial position and orientation of the surgical instruments. Specifically, for telementoring applications, both the mentor and the mentee will be tracked in the process of performing training tasks, as well as during actual surgeries. Data generated by these motion and orientation sensors can then be analyzed using artificial intelligence algorithms to evaluate the progress of mentee training. Finally, these electronic data can be communicated at great distances and have the potential to enable telementoring of MIS students across continents.

## 9.2 The UCLA LapaRobot

The stated goal of the proposed laparoscopic surgical robot (LapaRobot) is to make use of existing laparoscopic instruments with only minor adaptations to reproduce the actions of the surgeon's hands. To that end we start by looking at how existing laparoscopic instruments are currently used. An analysis of surgeon's arm and hand movements [162] while performing a laparoscopic surgery reveals that only five degrees of freedom are required, see **Figure 51**.

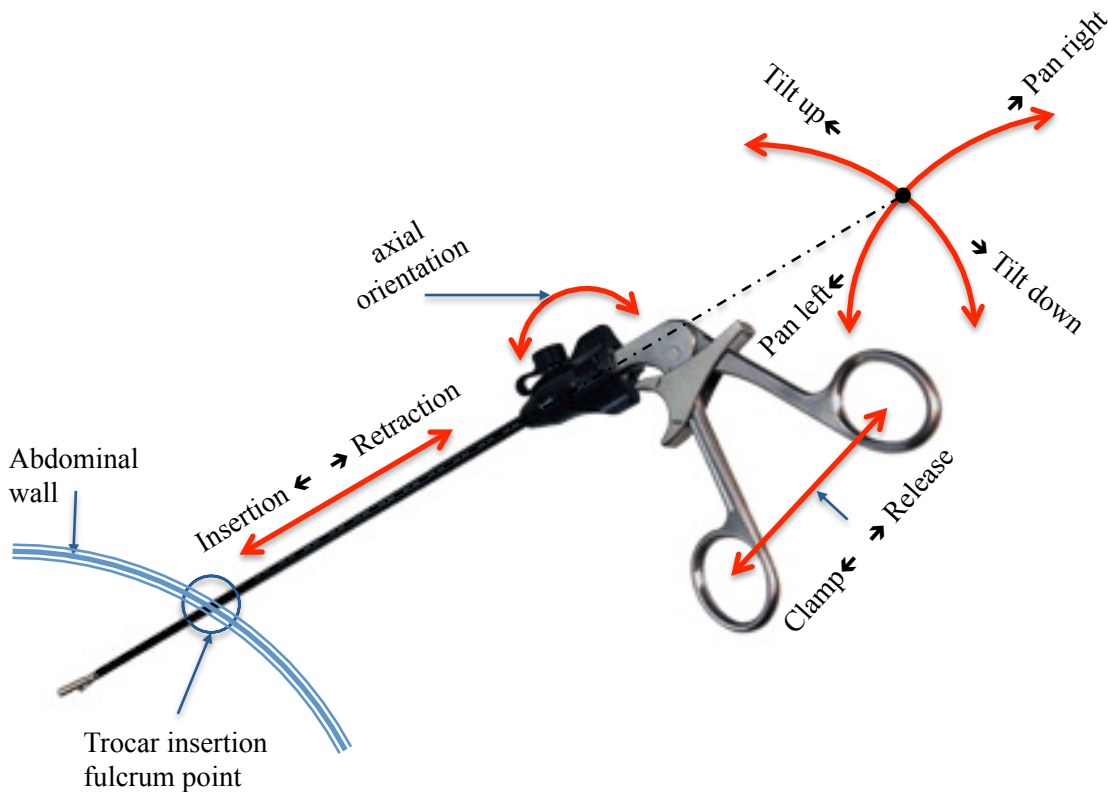


**Figure 51:** Laparoscopic degrees of freedom

There are three translational degrees of freedom (dof) associated with surgeon's arm movement: (1) insertion and extraction out of the trocar along the long axis of the shaft, (2) panning the instrument handle from left to right, (3) tilting the instrument handle up and down. The fourth is a rotational dof, namely the axial rotation about the shaft's long axis. This rotation orients the grasper / scissors jaws for optimal reach to the tissue and is effectuated by the axial rotation knob. Surgeons use their thumb to rotate this knob. Finally the fifth dof is the clamping and releasing of the scissor's blades (grasper jaws) effectuated at the handle with the thumb and the index.

In this study we propose that the three translational-dof are effectuated using a planar mechanism known as the Delta mechanism [163] shown in **Figure 52**



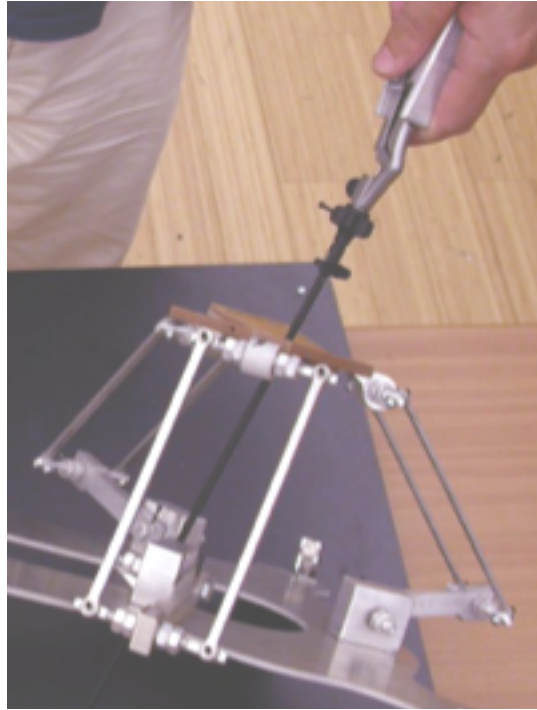


**Figure 52:** Delta mechanism for the three translational degrees of freedom

The Delta mechanism has a fixed bottom plate and a moveable top plate connected to each other by three identical limbs. Each limb consists of a driving link and the upper arm. Each driven link is actuated by a DC electric motor, with the torque amplified in a gearbox and the rotation measured by an encoder, all forming a single unit. This mechanism has shown to be capable to generate forces comparable to those used by the human arms while operating the laparoscopic instruments. Because of its configuration it is also rigid and lightweight.

In this configuration the actuating angles ( $\alpha_1, \alpha_2, \alpha_3$ ) directly drive the three translational dof for the proposed LapRobot, **Figure 53**. The forward kinematics of the delta mechanism maps these actuating angles to the three translational dof: (1) insertion-extraction, (2) pan left right, and (3) tilt up down.

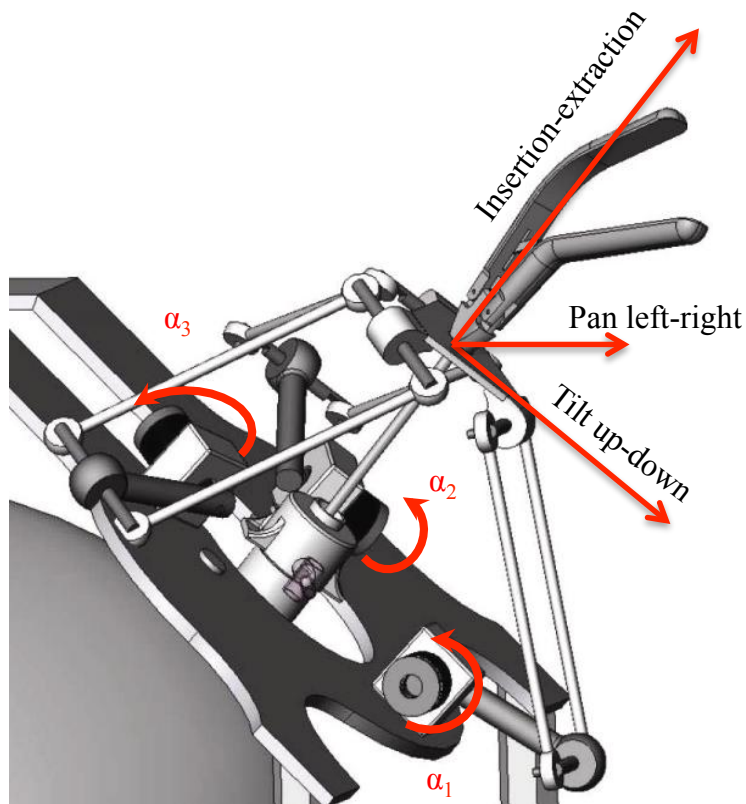


**Figure 53:** Delta mechanism actuating angles

The fourth degree of freedom associated with the action of clamping and releasing the jaws of the grasper, or the scissor blades is enabled by an adaptation of the laparoscopic handle. A separate unit consisting of a DC electric motor with gearbox and encoder is attached to the handle of the instrument while the other handle is being driven by an actuating arm and connecting rod, as seen in **Figure 54**. Thus the fourth dof is effectuated by  $\alpha_4$ , which is the driving angle for the motor actuating the handles of the laparoscopic instrument.

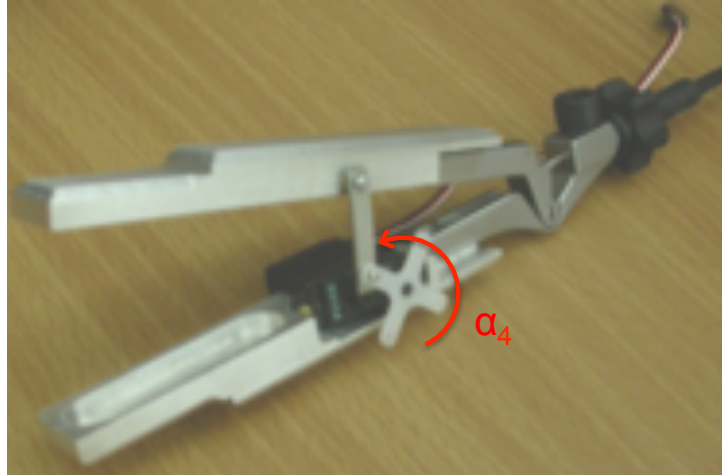


**Figure 54:** Closing and opening of jaws

The fifth degree of freedom orients the grasper or scissor around the long axis of the instrument shaft. This is achieved by modifying the top plate of the Delta to accept another DC motor with gearbox and encoder unit as seen in **Figure 55**, which drives the rotation wheel on the laparoscopic instrument. Thus the fifth dof is  $\alpha_5$ , which is the driving angle for the motor actuating the rotation knob of the laparoscopic instrument.

The laparoscopic instruments move through a fixed location at the fulcrum rotation point of the trocar. There is a secondary moving fulcrum in the top plate of the Delta mechanism. The fixed fulcrum of the trocar allows translation and rotation along and around the axis of the laparoscopic instrument shaft. The moveable fulcrum on the top plate of the Delta actuator is located where the surgeon's hand would normally work. It allows only rotation about the axis of the instrument shaft, equivalent to rotation in the wrist of the surgeon but no translations. All instrument translations are effected with the Delta mechanism, these are the translations normally executed by the surgeon's arms.

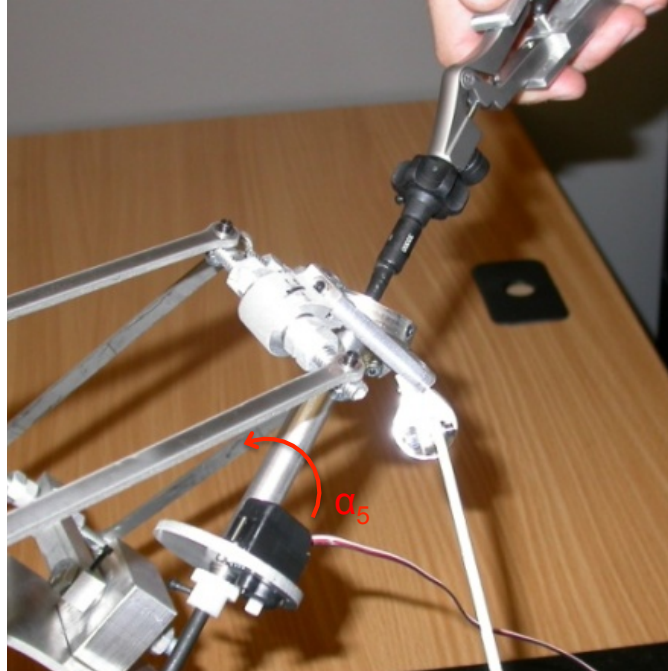


**Figure 55:** Axial orientation for the laparoscopic instrument

In addition to the five dof required to replicate to movements of the surgeon's hand, the system needs to replicate the wrist joint of surgeon's hand and the fulcrum point of the trocar. The wrist joint is replicated with a dual axis gimbal located in the middle of the top moving plate, see **Figure 56**. This gimbal is a passive joint with no motor to drive it or encoders to record its orientation. Similarly the fulcrum point of the trocar needs to be replicated on the master station of the LapaRobot. On the slave side of the LapaRobot, there is an actual trocar inserted in the abdominal wall of the patient, but the fulcrum on the master side of the LapaRobot needs to be replicated. We can achieve this in two ways: (a) place the LapaRobot over a suitable torso model with a trocar inserted in the same position as the slave side trocar or (b) place a spherical joint on an adjustable support to mirror the placement of the trocar on the slave side, as shown in **Figure 56**.

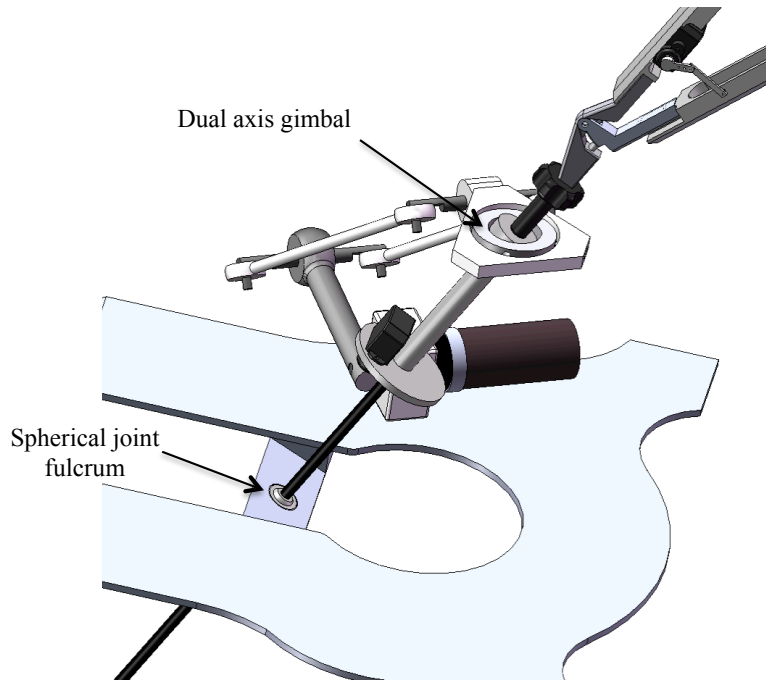


**Figure 56:** Dual axis gimbal at the top plate and sliding spherical axis fulcrum

### 9.3 LapaRobot Kinematic Control

To establish kinematic control of the LapaRobot, we propose an arrangement whereby both the master and the slave sides are identical from a kinematic perspective, with only differences on implementing the fulcrum point of the trocar, as discussed above. Such an arrangement means that measurements for the controlling angles ( $\alpha_1, \alpha_2, \alpha_3, \alpha_4, \alpha_5$ ) for the five dof can be transmitted directly from master station to the slave station, as described in **Figure 57**. At the master station, the surgeon moves his laparoscopic instruments, which results in movement in the controlled joints. Encoders in these joints read the values of the five controlling angles ( $\alpha_1, \alpha_2, \alpha_3, \alpha_4, \alpha_5$ ). These values get acquired by the controllers for their motors and sent by USB (Universal Serial Bus) to the laptop running the application software. In order to communicate to the slave side of the LapaRobot, these five controlling angles values

get transmitted via an Internet connection consisting of 10BASE-T connections locally and an IP - VPLS (Internet Protocol - Virtual Private LAN Service) between the two remote locations. At the slave side these signals get decoded in the application software running on the local laptop and then sent via USB as command inputs to the motor controllers to effectuate the movement along the five dof.

This arrangement bypasses the requirement to have the controlling inputs for those dof run from the control joystick through the inverse kinematics algorithm or mapping dataset. It has the potential to speed up the transmission of data from the master to the slave station. This is very important when transmission time delays create difficulties for the operator.

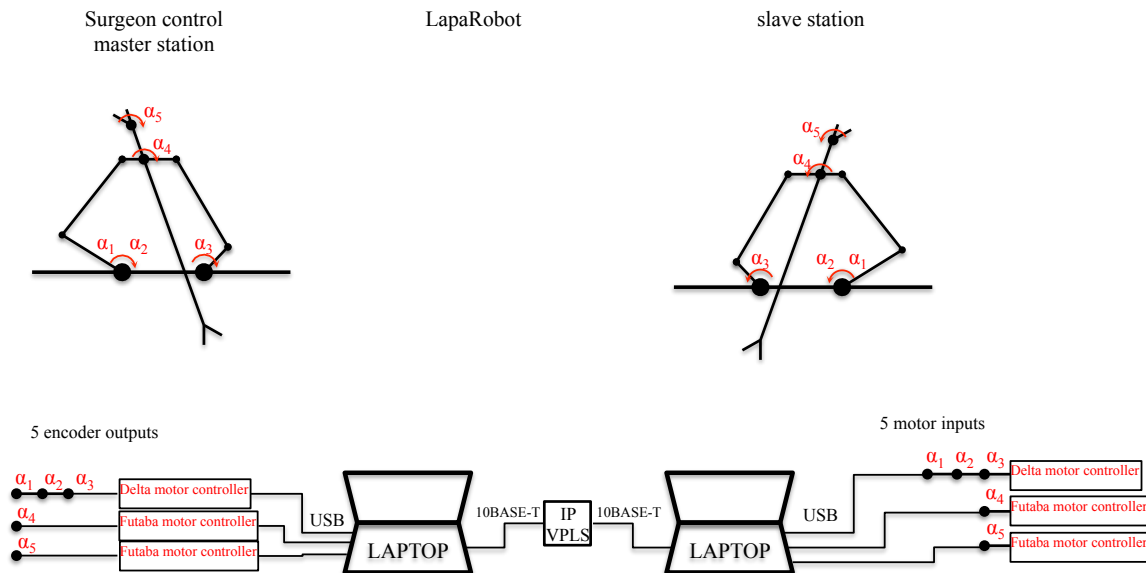


**Figure 57:** LapaRobot kinematic control

## 9.4 Two-handed LapaRobot

The LapaRobot could have any number of paired identical master-slave stations like the one described above. Based on our observations of laparoscopic surgeries and on previous

experience with the ZEUS and the da Vinci, we anticipate that most situations could employ two or three of these pairs: two are generally required to pull and dissect the tissue like in any laparoscopic surgery and the third one would be used to manipulate the endoscopic camera.

In this study we explore a two-handed LapaRobot, where the camera is either fixed or handled by an assistant, like the one shown in **Figure 58**. A fixed platform is designed to support two Delta mechanisms in the position and orientation optimally suited for the surgery or proposed training.

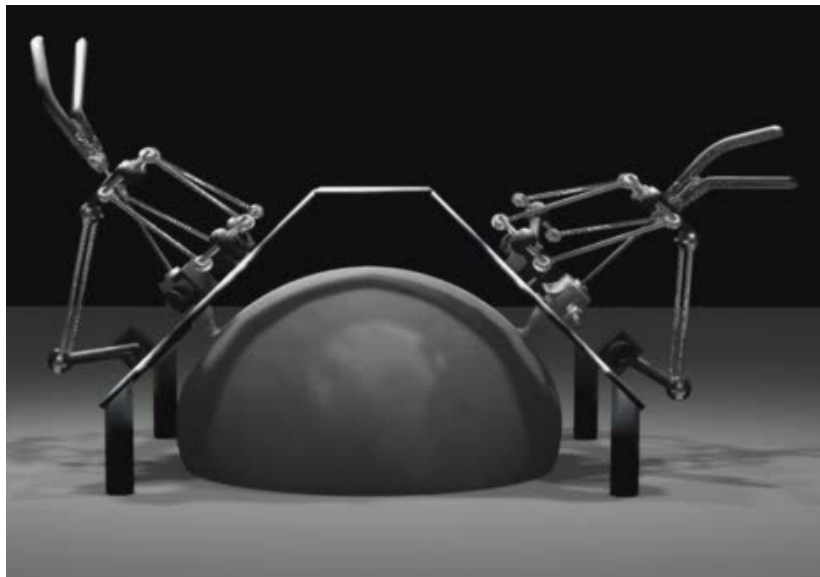


**Figure 58:** Two-handed LapaRobot concept

## 9.5 Reflective Force Feedback

A critical component of telementoring is the ability to provide force feedback. In this study we implement a more basic form of this functionality, described as “no fly zone”, like the one shown in **Figure 59**. The no fly zone would be designated by the expert surgeon and enforced by the control algorithms of the electrical motors as travel limits for the actuators.

Kinematic and dynamic similarity between the two sides of master-slave makes for a linear and transparent force feedback, where the current read on the master side is used to drive the motor on the slave side with an equal torque. In situations where the slave motor requires more torque to achieve its task, it would also require more current from the slave side controllers. The magnitude of this excess current could be measured and a signal returned to the master side of the LapaRobot would provide a proportional but opposite torque to the master motor – in effect creating a reflective force feedback to the surgeon at the master side of the LapaRobot.

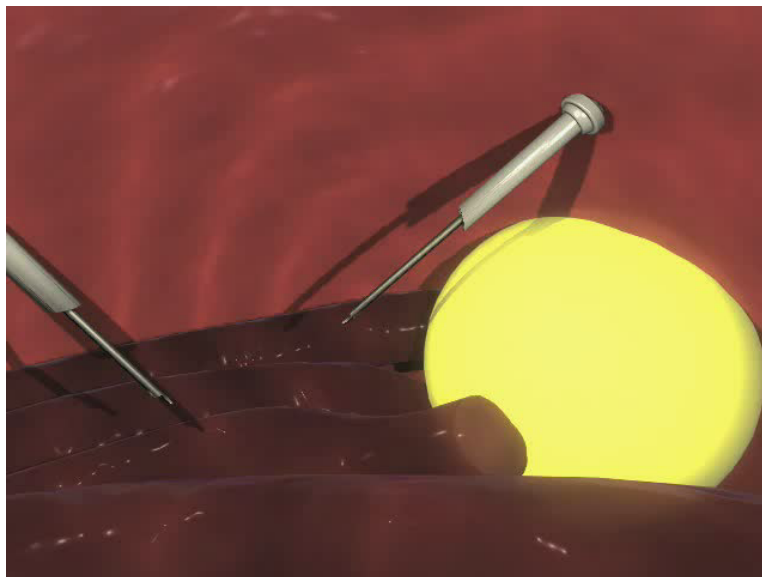


**Figure 59:** UCLA LapaRobot concept “no fly zone” in yellow

## 9.6 Active Guidance in Training with the LapaRobot

The operation of the UCLA LapaRobot was demonstrated in a laboratory experiment. The goal of this experiment was to demonstrate remote teleoperation while performing a training task. For this demonstration we chose the peg transfer training tasks discussed previously in section 6.2 “Construct Validity Tests”



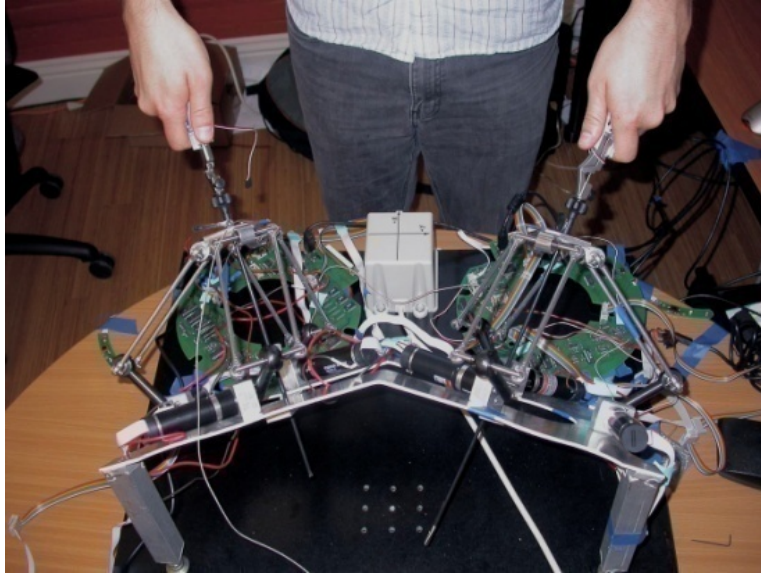


**Figure 60:** LapaRobot master station, ready for the peg transfer

A two-handed LapaRobot was setup for this study. Both the master station (**Figure 60**) and the slave station (**Figure 61**) were setup in the same laboratory, in two separate corners at about 50 feet separation. The two stations communicated with each other over the local Internet network as described in **Figure 57**, using the LAN ports close to them. The communication was routed through the UCLA campus servers. A direct cable of sufficient length was used for the video feedback from the slave station back to the master station. A digital video camera was setup at the slave station to visualize the pegboard and the tips of the instruments. A computer monitor was setup at the master station to provide video feedback to the surgeon. This monitor was connected to the slave station camera with a long USB cable that reached across the room.

The pegboard was placed in the field of view for the slave station camera and the surgeon proceeded to manipulate his instruments at the master station.

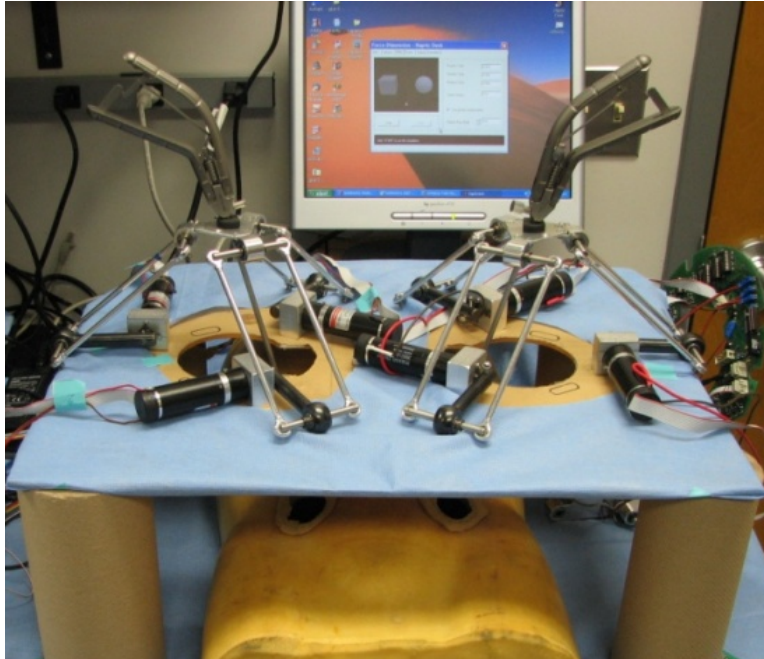


**Figure 61:** LapaRobot slave station with a synthetic human torso in position

At the master station, surgeon's hand moved the laparoscopic instrument along a path (**Figure 62**) that executes the peg transfer task, along with grasping and orientation actions. The motor control software read the data from each encoder and sent the instantaneous angle values for the five dof controlled  $\alpha_1, \alpha_2, \alpha_3, \alpha_4, \alpha_5$  to the application software on the control laptop

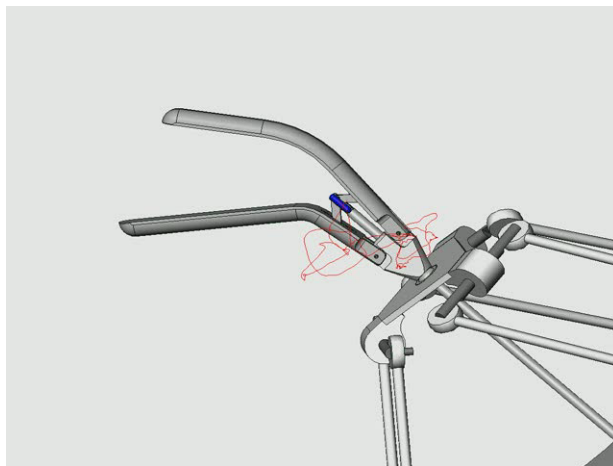


**Figure 62:** Left Hand trace (red) of the master station is recorded

This motion is recorded (**Figure 62**) by the application software running on the laptop controlling the master station. The laptop then transmits these data to the slave station via the local Internet connection.

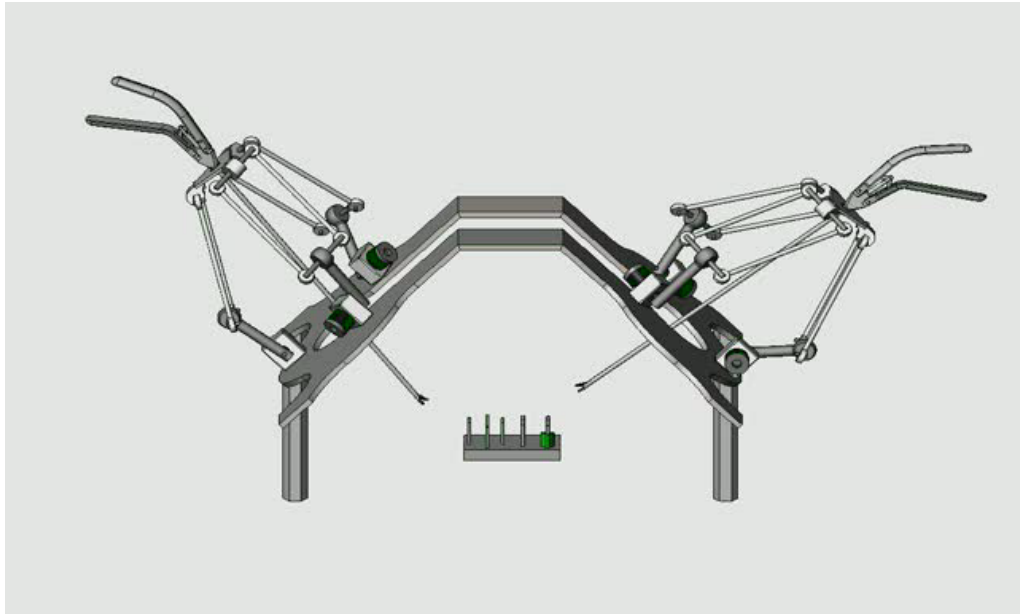


**Figure 63:** Slave station receives the transmitted pathway data from the master station and performs the identical peg transfer

The laptop controlling the slave station then decodes this information and sends the five angle values  $\alpha_1, \alpha_2, \alpha_3, \alpha_4, \alpha_5$  as actuation commands to the motors of the slave station, that executes the peg transfer task at the remote site **Figure 63**.

During this entire procedure the surgeon's only feedback is through the computer monitor in front of him at the master station.

The surgeon successfully executed several passes of the rubber piece between the left and right side pegs. In some instances the rubber piece fell out of the grasper at the slave station, and rolled outside the instruments reach or camera field of view. A local assistant was required to recover it and place it back in the working space of the slave station instruments.

## 9.7 Porcine Laparoscopic Cholecystectomy with UCLA-LapaRobot

The two-handed UCLA LapaRobot was evaluated in the porcine laboratory for its ability to collect motion-tracking data. This study took place at the same time with the study that collected data for identification of surgical skill specific to the laparoscopic cholecystectomy, described in chapter 5 “Identification of Surgical Skills Specific to Laparoscopic Porcine Cholecystectomy”.

The fixed platform discussed in section 9.6 “Active Guidance in Training with the LapaRobot” was designed for telementoring general laparoscopic skills such as suture, pass-the-rope, cap-the-needle, peg-transfer (**Figure 63**). Using the LapaRobot for telementoring the porcine laparoscopic cholecystectomy requires designing a fixed platform suitable for this application.

We performed a study to determine design parameters for a LapaRobot fixed platform suitable for a porcine laparoscopic cholecystectomy. As discussed above in section 9.3 “LapaRobot Kinematic Control”, the design of the UCLA-LapaRobot requires that the master station is kinematically identical to the slave station. This study aimed to evaluate two important variables for the fixed platform: (1) placement of the instrument handles and (2) trocar locations. Instrument handles on the LapaRobot need to be placed in the same location and orientation as those of the surgeon during the free hand laparoscopic cholecystectomy as shown in chapter 5.2, **Figure 23**. Trocar locations on the porcine model create a fixed fulcrum, and need to be replicated on the master station as discussed in **Figure 56**.

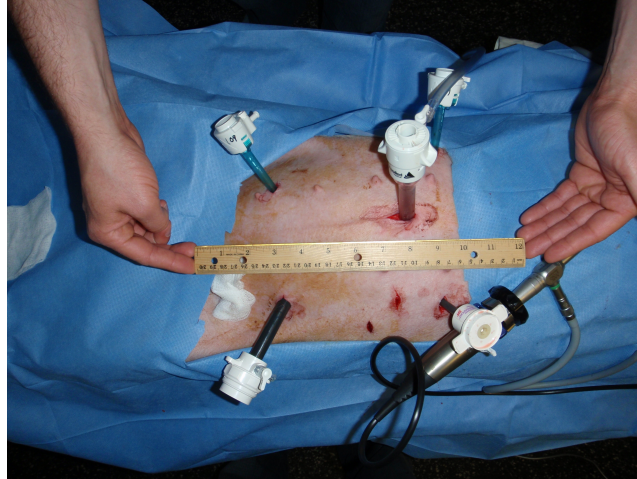


**Figure 64:** Trocar locations for the porcine cholecystectomy

The first set of measurements taken during this study evaluated the placement of the trocars, as shown in **Figure 64**. We measured the location of the trocars used for the tissue manipulation instruments with respect to: (1) the location of the trocar used for the endoscopic camera and (2) with respect to the surgical table.

The second set of measurements evaluated the working space requirements and placement. Working space is affected by placement of the instrument handles and the size and location of the supporting risers. The UCLA-LapRobot was placed over the pig, as shown in **Figure 65**. Measurements were taken again to evaluate the reach of the laparoscopic instruments fitted to the LapaRobot. Other measurements evaluated the location of the surgeon's hand during this procedure, as well as the size and location of the supporting risers. Both sets of measurements need to be expanded to allow for quantitative analysis.

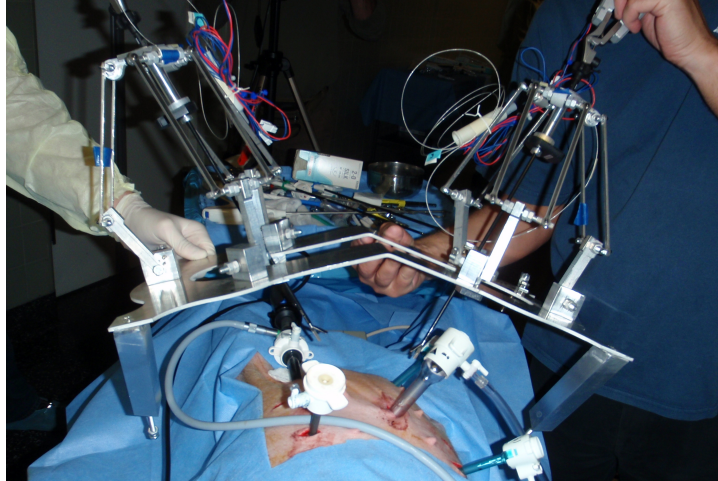


**Figure 65:** LapaRobot working space over the porcine model

## 9.8 Discussion

### 9.8.1 Milestones Achieved

This study built and demonstrated a prototype for a low cost and small footprint laparoscopic surgery robot. It consists of two kinematically identical units used in a master-slave pair. Each unit has a footprint of approximately 24" x 24" x 24" and weighs approximately 50 lbs. It consists of a fixed platform to accommodate the two delta mechanism based actuators and the two laparoscopic instruments, the power supply and motor controllers for the five different motors and the laptop that runs the application software and the telecommunications protocols between the two master and slave units. Given its footprint, weight and low power requirements this can be a highly mobile unit easily deployable to remote locations.

There are two significant breakthroughs in this LapaRobot; first is the use of standard laparoscopic instruments and the second is the use of kinematically and dynamically identical master and slave units. Using standard laparoscopic instruments is a significant step towards

reducing the cost of the surgical robotic units. These instruments are available in a variety of forms from a diverse and large supplier base. We demonstrated that only minor adaptations are required to enable the full five dof required for laparoscopic robotic surgery

The second major breakthrough on this LapaRobot is that it uses two kinematically identical units, one as a master station and the other as a slave station. The significance of this approach is that position and orientation signals transmitted between the two stations bypass the inverse and forward kinematics transforms normally associated with connecting a controller joystick to the end effector manipulators. The traditional approach to remotely control a manipulator such as in the da Vinci or ZEUS, is a two-step process. First, the hand gestures at the master station result in changes of the joint angles ( $\theta_1, \theta_2, \dots$ ). Using the forward kinematics model for this mechanism, the hand positions ( $x,y,z$ ) are then calculated from the joint angles and transmitted to the slave station. At the slave station the reverse process takes place; the ( $x,y,z$ ) position commands then get transformed via the inverse kinematics transform of the end effector manipulator into joint angles ( $\alpha_1, \alpha_2, \dots$ ) for this manipulator. This process of taking the surgeon's hand commands through the forward transforms of the master station, and then through the inverse transforms of the slave station adds time delays between surgeon's movements and actual tissue manipulation, and introduces errors. This is especially concerning if either manipulator operates close to a kinematic singularity [164].

The master and slave stations are also dynamically identical. This has great implications for future implementation of reflective force feedback. Reflective force feedback usually requires force and torque sensors in the slave side manipulator. The output from these sensors, be it current, voltage or digital signal, is then transmitted to the local computer driving the slave station, which then transmits it back to the master station. The forces experienced at the slave

station are reproduced at the master side mechanism, using additional motors that are driving this mechanism against the surgeon's hand. The magnitude of the reflective force is scaled for appropriate feedback perception on the surgeon hand. This requires suitable interpretation of these sensors data in the dynamic model of the slave station and proportional reproduction of those forces using the dynamic model of the master side mechanism.

Implementing the reflective force feedback with kinematically and dynamically identical master slave stations is much simpler than the traditional approach described above. The motors driving the five dof receive a nominal current that keeps the mechanism from changing position and orientation under loading from gravity, at both the master ( $I_{m1}, I_{m2}, I_{m3}, I_{m4}, I_{m5}$ ) and slave ( $I_{s1}, I_{s2}, I_{s3}, I_{s4}, I_{s5}$ ) station. The first three sets of currents ( $I_{m1}, I_{m2}, I_{m3}$ ) drive the delta mechanism at the master station, and are equal to the equivalent currents ( $I_{s1}, I_{s2}, I_{s3}$ ) at the slave station. The other two currents ( $I_{m4}, I_{m5}$ ) drive the axial orientation mechanism and jaw opening-closing mechanisms respectively at the master station and the slave station ( $I_{s4}, I_{s5}$ ). Surgeon's hand movement at the master station changes that balance of currents and the resulting difference in each motor controller is compared between the master station and the slave station. For example, when the surgical instrument at the slave station grasps on the tissue, the local slave station motor controllers increase the driving current ( $I_{s5}$ ) to a predetermined limit. This current increase drives up the motor torque, which insures the tissues stays firmly in the jaws of the grasper, without injury. At this point there is a difference  $\Delta = (I_{m5} - I_{s5})$  between the corresponding currents driving the motor controllers at the master station and the slave station. This difference is then used to calculate the sign and the magnitude of the current driving the master station motor controllers for opening and closing the grasper, to create a reflective force feedback at the surgeon's hand.



This design was implemented in the two-handed LapaRobot platform. We tested it in the laboratory for executing a peg transfer remotely, with the motion data going through the UCLA Internet connection from two distinct locations. The participating surgeon was successful in executing the peg transfer however the video feedback was processed through a direct cable link that did not go through the UCLA Internet servers. It is important to note that even though this was the first time the surgeon worked on this novel UCLA LapaRobot, he was able to successfully execute the tasks.

We anticipate that the next step in the development of the LapaRobot would involve feasibility studies in porcine laparoscopic surgery. For this application the fixed platform supporting the two Delta driving mechanisms needs to be designed to ensure that the laparoscopic instruments are as close as possible to the position used by the surgeon during live demonstration in the porcine laboratory for surgery. Eventually this LapaRobot could be used to develop the concepts of surgical telementoring, and we anticipate the porcine model to be best suited for these studies.

### 9.8.2 Challenges

One of the first challenges that needs to be addressed is the ability to transmit video feedback through the same Internet open ports as the motion data. Video data is a much larger data set than the motion tracking data and it needs to be of fairly high quality to be of any use to telesurgery or even teleoperation.

Relating to that, the next big challenge is to provide communication technologies with low latency, both for the motion data and the video data.

The design and positioning of the fixed platform needs to address two important challenges relating to the workspace available at the slave station. Even with careful selection of the porcine model there is bound to be inherent variability between different animals. This needs to be taken into account in the design of the fixed platform, as well as in the length of the links forming the Delta mechanism, and the length of laparoscopic instruments used in every individual case.

The ultimate challenge however is the acceptance of the paradigm shift in educational methodology that such a system would entail. The surgical community is the ultimate “customer” for this technology and therefore needs to be involved in every aspect of validating not only its ability to perform telesurgery but also its value as a telementoring instrument that has the potential to address the uneven and sparse distribution of surgical expertise in remote locations away from the major population and university centers.

### 9.8.3 Future Work

The immediate work needs to address the quantification of precision and accuracy for placement and operation of the laparoscopic instruments in conditions of controlled latency. This would require a study of each component of the LapaRobot and the quantification of its latency contribution. The preliminary measurements taken during the procedure need to be supplemented to allow for a quantitative analysis. Concomitant with this effort we need to start developing an educational module for surgical telementoring. We believe the porcine laparoscopic cholecystectomy to be a good initial model. The goal of this study would be to discover and address the skills and learning strategies specific to telesurgery and telementoring as well as quantify the specific equipment and software needs for such applications.

## 10 Conclusion

The overarching hypothesis of this dissertation is that telementoring systems in combination with machine learning algorithms and active haptic guidance, can bridge the gap in learning the advanced surgical skills required for the performance of MIS.

This dissertation successfully tested the hypothesis that using motion tracking of surgical instruments via the UCLA – LTS, we could extract a set of kinematically based performance metrics to evaluate the MIS surgical skills of novice trainees. We collected two sets of data, an intraoperative dataset and another one from dry laboratory experiments to identify MIS-specific surgical skills. The intraoperative dataset comes from two separate experiments: (a) a combined phacoemulsification (PKE) and pars plana vitrectomy (PPV) procedure on a pig eyeball and (b) a porcine laparoscopic cholecystectomy. The dry laboratory experimentation on the construct validation of the UCLA – LTS yielded the second data set. It was collected from two populations of test participants, an expert group and a novice group to evaluate the kinematic performance metrics. The datasets present evidence that these performance metrics, when combined with machine learning algorithms, were successful in differentiating between the psychomotor skill of the expert mentors and those of novice.

This dissertation further lays the foundation to test the second hypothesis that, when combined with active guidance from a haptic force feedback mechanism via the UCLA – LapaRobot, these performance metrics have the potential to facilitate the learning of MIS specific surgical skills for remote trainees in a telementoring scenario. From this MIS telementoring we conclude that we can further enhance the deployment of MIS to remote locations in a telesurgery scenario, with medic-trained personnel at the slave station and an

expert at the master station, assisted by the kinesthetic force feedback of the UCLA – LapaRobot.

A. Appendix A: Recruitment Poster for MIS Training System

Needed: Participants for Testing MIS Training System

- **Duration:** up to 1 hour per session. You may NOT participate in more than one session
- **Who:** UCLA Faculty, Staff and Students.
- **Task:** you will manipulate surgical instruments in a MIS Training System in order to determine the effectiveness of the training system itself
- **Location:** Boelter Hall, 7673
- **Email:** vasile@seas.ucla.edu

(This research study is conducted by Prof. Greg Carman, PhD, MAE, Assist Prof Petros Faloutsos, PhD, CS, Assist Professor Erik Dutson, MD, Dept. Surgery, Vasile Nistor GSR, MAE, Brian Allen, GSR, CS, UCLA)

MIS Training System vasile@seas.ucla.edu	MIS Training System vasile@seas.ucla.edu	MIS Training System vasile@seas.ucla.edu	MIS Training System vasile@seas.ucla.edu	MIS Training System vasile@seas.ucla.edu	MIS Training System vasile@seas.ucla.edu	MIS Training System vasile@seas.ucla.edu
---	---	---	---	---	---	---

University of California, Los Angeles

## **Questionnaire**

You are asked to participate in a research study conducted by Prof. Greg Carman, PhD, MAE, Assist Prof Petros Faloutsos, PhD, CS, Assist Professor Erik Dutson, MD, Dept. Surgery, Vasile Nistor GSR, MAE, Brian Allen, GSR, CS, at the University of California, Los Angeles. You were selected as a possible participant in this study because you are a UCLA student, staff or faculty member. Your participation in the research is voluntary.

### **PURPOSE OF THE STUDY**

The purpose of this study is to establish the construct validity of our system as a training tool for the MIS. As such our system must be able to reproduce to certain degree the relevant visual and spatial feel characteristic of the MIS. Moreover, our training system provides automated training-performance score based on the kinematics of the surgical instrument motion through space. This present study will validate our scoring approach as well.

### **PROCEDURES**

If you volunteer to participate in this study, you should expect the following. You will first listen to a short power point presentation that explains the difficulties encountered during MIS/laparoscopic surgery: fulcrum effect, use of long instruments, poor depth perception, and

disorientation, with the goal of mentally preparing for the difficulty of the task ahead. Test personnel will introduce the two instruments used for this test, the Karl Storz laparoscopic needle driver (right hand side), and the Ethicon endoscopic grasper (left hand side). We will emphasize the lock and release mechanism operation of the Karl Storz laparoscopic needle driver. Test personnel will then perform the test itself for you to see what you are expected to do. The researchers will then asks questions to ensure that you understand the procedure, and than you will sign the consent form. You will then proceed to perform the test itself three times in order to familiarize with the test environment. For this stage there is no test data collected, and there are no time constraints. The only requirement enforced is that the test participants complete the entire test procedure ten times. The tests consists of grabbing in each hand the handles of one instrument, and than using the tips of these instruments, grab a rubber piece sitting on a peg and transfer it to another peg, while watching the video feed of the action.

*Testing sessions will last less than 60 min and will be broken down into blocks of 10-15 min. You may not participate in more than one session. Experiments will be conducted in the laboratory at 7673 Boelter Hall.*

#### **POTENTIAL RISKS AND DISCOMFORTS**

There is no risk associated with participation in this study.

#### **POTENTIAL BENEFITS TO SUBJECTS AND/OR TO SOCIETY**

*You will not benefit from your participation in this study. This study will potentially improve the training techniques currently available for practicing MIS.*

**ASSEMENT OF PREVIOUS EXPERTISE**

**1. Previous MIS Training**

What instrument	How many hours total	List the training tasks	

**2. Previous MIS procedures**

What procedures	How many total		



**SIGNATURE OF RESEARCH SUBJECT**

I understand the procedures described above. My questions have been answered to my satisfaction, and I agree to participate in this study. I have been given a copy of this form.

\_\_\_\_\_

Name of Subject

\_\_\_\_\_

Signature of Subject

\_\_\_\_\_

Date

**SIGNATURE OF INVESTIGATOR OR DESIGNEE**

In my judgment the subject is voluntarily and knowingly giving informed consent and possesses the legal capacity to give informed consent to participate in this research study.

\_\_\_\_\_

Name of Investigator or Designee

\_\_\_\_\_

Signature of Investigator or Designee

\_\_\_\_\_

Date

## B. Appendix C: Consent to Participate in Research

University of California, Los Angeles

### **CONSENT TO PARTICIPATE IN RESEARCH**

#### Tactile Perceptual Discrimination

You are asked to participate in a research study conducted by Prof. Greg Carman, PhD, MAE, Assist Prof Petros Faloutsos, PhD, CS, Assist Professor Erik Dutson, MD, Dept. Surgery, Vasile Nistor GSR, MAE, Brian Allen, GSR, CS, at the University of California, Los Angeles. You were selected as a possible participant in this study because you are a UCLA student, staff or faculty member. Your participation in the research is voluntary.

#### **PURPOSE OF THE STUDY**

The purpose of this study is to establish the construct validity of our system as a training tool for the MIS. As such our system must be able to reproduce to certain degree the relevant visual and spatial feel characteristic of the MIS. Moreover, our training system provides automated training-performance score based on the kinematics of the surgical instrument motion through space. This present study will validate our scoring approach as well.

#### **PROCEDURES**

If you volunteer to participate in this study, you should expect the following. You will first listen to a short power point presentation that explains the difficulties encountered during MIS/laparoscopic surgery: fulcrum effect, use of long instruments, poor depth perception, and

disorientation, with the goal of mentally preparing for the difficulty of the task ahead. Test personnel will introduce the two instruments used for this test, the Karl Storz laparoscopic needle driver (right hand side), and the Ethicon endoscopic grasper (left hand side). We will emphasize the lock and release mechanism operation of the Karl Storz laparoscopic needle driver. Test personnel will then perform the test itself for you to see what you are expected to do. The researchers will then ask questions to ensure that you understand the procedure, and then you will sign the consent form. You will then proceed to perform the test itself three times in order to familiarize with the test environment. For this stage there is no test data collected, and there are no time constraints. The only requirement enforced is that the test participants complete the entire test procedure three times. The tests consist of grabbing in each hand the handles of one instrument, and then using the tips of these instruments, grab a rubber piece sitting on a peg and transfer it to another peg, while watching the video feed of the action.

*Testing sessions will last less than 60 min and will be broken down into blocks of 10-15 min. You may not participate in more than one session. Experiments will be conducted in the laboratory at 7673 Boelter Hall.*

#### **POTENTIAL RISKS AND DISCOMFORTS**

There is no risk associated with participation in this study.

#### **POTENTIAL BENEFITS TO SUBJECTS AND/OR TO SOCIETY**

*You will not benefit from your participation in this study. This study will potentially improve the training techniques currently available for practicing MIS.*

#### **PAYMENT FOR PARTICIPATION**

*There is no payment for your participation in the study.*

## **CONFIDENTIALITY**

Any information that is obtained in connection with this study and that can be identified with you will remain confidential and will be disclosed only with your permission or as required by law. We will maintain confidentiality by identifying your data files with a subject number. The only link between the subject number and your name is a file that will be securely stored at the testing laboratory and deleted at the completion of the study.

## **PARTICIPATION AND WITHDRAWAL**

You can choose whether to be in this study or not. If you volunteer to be in this study, you may withdraw at any time without consequences of any kind. You may also refuse to answer any questions you don't want to answer and still remain in the study.

## **IDENTIFICATION OF INVESTIGATORS**

If you have any questions or concerns about this research, please feel free to contact Prof. Greg Carman, PhD, MAE, Assist Prof Petros Faloutsos, PhD, CS, Assist Professor Erik Dutson, MD, Dept. Surgery, Vasile Nistor GSR, MAE, Brian Allen, GSR, CS, at the University of California, Los Angeles.

## **RIGHTS OF RESEARCH SUBJECTS**

You may withdraw your consent at any time and discontinue participation without penalty. You are not waiving any legal claims, rights or remedies because of your participation in this research study. If you have questions regarding your rights as a research subject, contact

the Office for Protection of Research Subjects, 1401 Ueberroth Building, UCLA, Box 951694,  
Los Angeles, CA 90095-1694, (310) 825-8714.

**SIGNATURE OF RESEARCH SUBJECT**

I understand the procedures described above. My questions have been answered to my satisfaction, and I agree to participate in this study. I have been given a copy of this form.

\_\_\_\_\_

Name of Subject

\_\_\_\_\_

Signature of Subject

\_\_\_\_\_

Date

**SIGNATURE OF INVESTIGATOR OR DESIGNEE**

In my judgment the subject is voluntarily and knowingly giving informed consent and possesses the legal capacity to give informed consent to participate in this research study.

\_\_\_\_\_

Name of Investigator or Designee

\_\_\_\_\_

Signature of Investigator or Designee

\_\_\_\_\_

Date

C. Appendix D: Construct Validity Test Plan

**UCLA LTS - Construct Validation Test Plan**

**1. OVERVIEW**

**1.1. UCLA LTS (Laparoscopic Training System)**

**1.2. Rev-April 2007**

**1.3. PROJECT LEADS**

1.3.1. PI: Greg P. Carman, PhD, Professor

1.3.2. Co-PI: Petros Faloutsos, PhD, Assist Professor

1.3.3. Erik Dutson, MD, Surgeon

1.3.4. Vasile Nistor, GSR

1.3.5. Brian Allen, GSR

**1.4. TEST PROJECT STAFF**

1.4.1. Test requirements designers:

1.4.1.1. Vasile Nistor, GSR

1.4.1.2. Brian Allen, GSR

1.4.2. Test case designers:

1.4.2.1. Vasile Nistor, GSR

1.4.2.2. Brian Allen, GSR

1.4.3. Test personnel:

1.4.3.1. Vasile Nistor, GSR

1.4.3.2. Brian Allen, GSR

1.4.4. Documentation reviewers:

1.4.4.1. Greg P. Carman, PhD, Professor

1.4.4.2. Petros Faloutsos, PhD, Assist Professor

1.4.4.3. Erik Dutson, MD, Surgeon

## 1.5. **PRODUCT OVERVIEW**

The aim of this project is to develop a novel training and telementoring system for the minimally invasive surgery. The UCLA-LTS (Laparoscopic Training System) is based around the fundamental philosophy that surgical procedures must be taught on actual surgical devices rather than simulated systems. The UCLA LTS system thus uses two actual laparoscopic instruments containing position-tracking sensors seamlessly integrated into the instruments. The sensing signals are visually produced on a computer screen in real time graphic form as well as recorded for later feedback. The sensing data is fed into a software package to assess the performance metrics of the surgeon as well as provide individual scores on specific metrics as well as a final compound score. In general terms the system consists of a mechanical interface with instruments and tracking sensors, a software interface that acquires the data relating to the motion of each instrument, and a cognitive and psychomotor skills evaluation software, based on analysis of the instruments kinematics. This system combines the advantages of computer simulation with the features and simplicity of the traditional training boxes, which allows it to be easily customized in situ for a wide array of training tasks.

The general configuration of the UCLA-LTS is illustrated in Fig 1. The laparoscopic training box has the porthole plate top covered with opaque material such that operators will see their instruments in action only on the computer monitor. A pegboard from a SAGES approved training set is fixed on the inside using Velcro tape. The active source electromagnet of the tracking system is rigidly attached to the far



side of this box to provide a fixed reference system of coordinates. A USB based web cam fixed to the front of the training box currently provides visual feedback normally coming from an endoscopic camera. Each laparoscopic instrument is inserted into a porthole through a trocar, which forms a friction joint with the rubber of the porthole simulating the friction normally encountered between trocar and abdominal wall tissue. The wiring from the electromagnetic tracking sensors is routed to the control box seen in the background plane; with the control box linked to the PC via a USB port. The computer monitor displays the video feed from the web cam as well as the performance monitoring graphics.

## 1.6. TRACKING AND REPORTING SYSTEMS

- 1.6.1. Each of the test participants will be identified through a six digit number assigned according to the date and order of testing, in order to protect their identity
  - 1.6.1.1. MMDDNN, (MM – month, DD – day, NN - serial number for the participant)
  - 1.6.1.2. For each test participant, the test personnel creates a data folder, named MMDDNN to store the data files generated for each testing iteration,
  - 1.6.1.3. The test results data from each test run are stored in a spreadsheet data file, named MMDDNN-NN, with the last two digits identifying the serial number for the test.
  - 1.6.1.4. If a test-iteration is aborted the data file generated will be identified as MMDDNN-NN-abort.

1.6.1.5. Each test data file is a software-generated spreadsheet that contains the time stamp, in 1<sup>st</sup> column, and the position and orientation coordinates for each of the 4 sensors, in the following columns. For each sensor the data acquisition interface collects three body coordinates, **x, y, z**, and the three successive elemental rotations around these axes, also known as the Tait-Bryan angles, **φ, θ, ψ**.

Time [sec]					<u>Sensor # 1</u>					<u>Sensor # 2</u>					<u>Sensor # 3</u>					<u>Sensor # 4</u>				
	1	1	1	1	1	1	2	2	2	2	2	2	3	3	3	3	3	3	4	4	4	4	4	4

1.6.2. The computer that runs the UCLA-LTS is password protected to allow access only to the two test personnel, named in section 1.4.3. Password protection ensures that test data is only accessible to the test personnel. Any changes to this policy are to be directly approved by the documentation reviewers listed in section 1.4.4.

1.6.3. Any changes to this test plan need prior approval by the documentation reviewers listed in section 1.4.4.

## 2. TESTING SYNOPSIS

## 2.1. Items to be tested

2.1.1. This procedure measures kinematic performance metrics associated with the three dimensional movement of the surgical instrument tips. These metrics are computed by the testing software

2.1.2. smoothness metric, identified in the output spreadsheet as M1,

$$2.1.2.1. \quad m_1 = \frac{\frac{1}{2} \int_{t_0}^{t_1} \left( \left( \frac{d^3 p_x}{dt^3} \right)^2 + \left( \frac{d^3 p_y}{dt^3} \right)^2 + \left( \frac{d^3 p_z}{dt^3} \right)^2 \right) dt}{t_1 - t_0}$$

2.1.3. total path length, identified in the output spreadsheet as M2,

$$2.1.3.1. \quad m_2 = \int_{t=t_0}^{t_1} \sqrt{\left( \frac{dp_x}{dt} \right)^2 + \left( \frac{dp_y}{dt} \right)^2 + \left( \frac{dp_z}{dt} \right)^2}$$

2.1.4. time to completion metric, identified in the output spreadsheet as M3,

$$2.1.4.1. \quad m_3 = t_1 - t_0$$

2.1.5. compound score metric, identified in the output spreadsheet as S,

$$2.1.5.1. \quad s = \sum_i k_i m_i$$

## 2.2. Items *not* to be Tested

2.2.1. This procedure will not test the anatomy and surgery knowledge of the participants.

## **2.3. Glossary**

### **2.3.1.**

## **3. TYPE OF TESTING**

### **3.1. VALIDATION TESTING**

The purpose of this study is to establish the validity of our system as a training tool for the MIS. As such our system must be able to reproduce to certain degree the relevant visual and spatial feel characteristic of the MIS. Moreover, our training system provides automated training-performance score based on the kinematics of the surgical instrument motion through space. This scoring needs to be validated in this setting as well.

The validation process is multileveled.

- Content and face validity examines the relationship between the MIS surgery and the tasks performed on the system under examination.
- Construct validity measures the degree to which the training tool can distinguish between different levels of experience and skill for a given procedure, and forms the object of this test. To show the contrast of expertise among the participants in this study, this test requires the repetition of the training task for a number of times.
- Concurrent/Predictive validity requires the comparison of independent paired tests outcomes using the UCLA LTS and at least one of the already established training tools, such as the SAGES approved training boxes

## **3.2. CONSTRUCT VALIDITY TEST**

Construct validity measures the degree to which the training tool can distinguish between different levels of experience and skill for a given procedure, and forms the object of this test. To show the contrast of expertise among the participants in this study, this test requires the repetition of the training task for a number of times.

### **3.2.1. PRESENTATION INTRODUCTION TO THE TEST**

- 3.2.1.1. The group of test participants is brought to the test laboratory.
- 3.2.1.2. Test personnel will present the Power Point document titled – “Introduction to UCLA-LTS Construct Validity Test”. In this exercise we start with a short explanation of the difficulties encountered during laparoscopic surgery: fulcrum effect, use of long instruments, poor depth perception, and disorientation, with the goal of mentally preparing the trainee to the difficulty of the task ahead.
- 3.2.1.3. Test personnel will introduce the two instruments used for this test, the Karl Storz laparoscopic needle driver (right hand side), and the Ethicon endoscopic grasper (left hand side). Emphasize the lock and release mechanism operation of the Karl Storz laparoscopic needle driver.
- 3.2.1.4. Test personnel will then perform the test itself for the participants to see what they are expected to do, see section 3.2.2.
- 3.2.1.5. The researchers will than asks questions to ensure that the subjects understand the procedure.

- 3.2.1.6. Each test participant will then sign the “consent forms”. The consent form is stored in the folder named “Consent Forms”.
- 3.2.1.7. Each test participant will then proceed to perform the test itself three times in order to familiarize with the test environment. For this stage there is no test data collected, and there are no time constraints. The only requirement enforced is that the test participants complete the entire test procedure three times.
- 3.2.1.8. testing laboratory – room 7673 Boelter Hall
- 3.2.1.9. group size no larger than 5 participants simultaneously

### 3.2.2. TEST DESCRIPTION

- 3.2.2.1. Test personnel prepare the testing software, ready to record a data file.
- 3.2.2.2. Test personnel prepare the instruments to be close to the central neutral position, and the rubber transfer piece to be placed on the right side peg.
- 3.2.2.3. Test participants place themselves in front of the UCLA-LTS in a position that allows them to reach the instruments comfortably, and simultaneously watch the display monitor.
- 3.2.2.4. Test participants then grab one instrument in each hand and bring the instruments tips in the spot marked as the central neutral position, see Fig. 3.2.a.

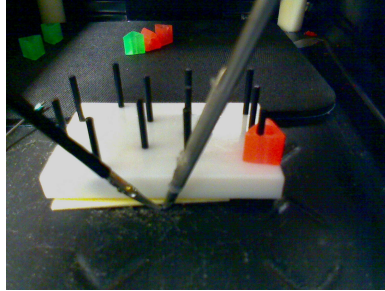


Fig. 3.2.a

- 3.2.2.5. Now the test is ready to start. Test participant tells test personnel “START”, test personnel then clicks the “START” button for the testing software.
- 3.2.2.6. At this point the test participant proceeds to move the tip of the instrument in the right hand to the rubber piece placed on the right side peg.
- 3.2.2.7. Pick the rubber piece within the instrument jaws and engage the lock mechanism.
- 3.2.2.8. Lift the rubber piece off the peg, see Fig. 3.2.b

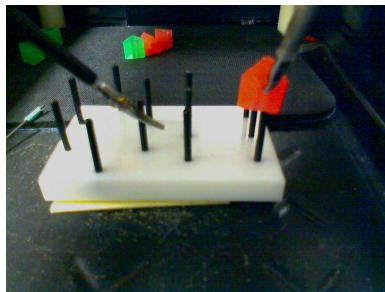


Fig. 3.2.b,

- 3.2.2.9. Simultaneously bring the tips of the two instruments over the pegboard, into the center field of view in order to transfer the rubber piece from the tip of the right hand instrument to the tip of the left hand instrument, see Fig. 3.2.c.

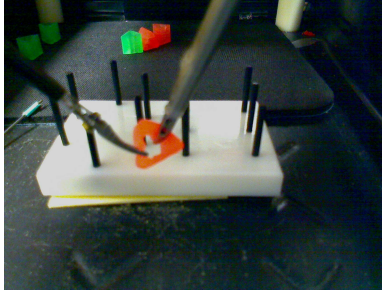


Fig. 3.2.c,

- 3.2.2.10. Grab the rubber piece within the jaws of the left hand side instrument, and when successful release the locking mechanism of the instrument in the right hand.
- 3.2.2.11. Bring the tip of the left hand instrument over the peg on the left hand side and position the rubber piece so that it can be placed over the peg, see Fig. 3.2.d.

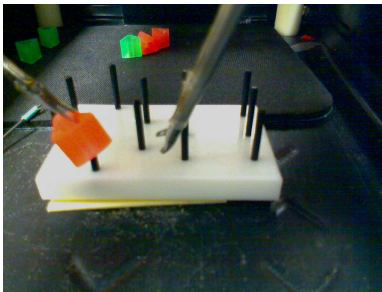


Fig. 3.2.d,

- 3.2.2.12. When placement of the rubber piece is successful, release the rubber piece and bring the tips of both instruments into the central neutral position, see Fig. 3.2.e.

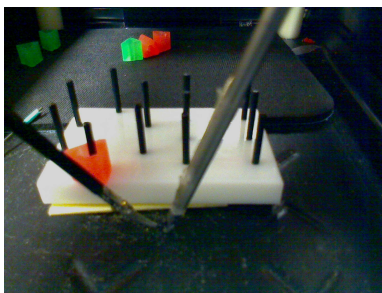


Fig. 3.2.e,

- 3.2.2.13. When both instruments are in place, test participant say out loud “MIDWAY”, and then proceed. This is to ensure that all test participants stop with the instruments in this position for the same amount of time.
- 3.2.2.14. This is the halfway point of the test procedure. To complete this procedure repeat the previous steps 3.2.2.4 to 3.2.2.12 in reverse order, thus transferring the rubber piece from the peg on the left hand side to the right hand side peg, and again end with both instruments in the central location.



- 3.2.2.15. At this point the test participant proceeds to move the tip of the instrument in the left hand to the rubber piece placed on the left side peg.
- 3.2.2.16. Pick the rubber piece within the instrument jaws.
- 3.2.2.17. Lift the rubber piece of the peg, see Fig. 3.2.f

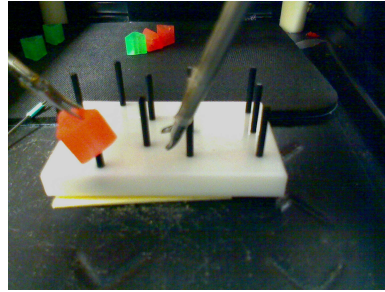


Fig. 3.2.f,

- 3.2.2.18. Simultaneously bring the tips of the two instruments over the pegboard, into the center field of view in order to transfer the rubber piece from the tip of the left hand instrument to the tip of the right hand instrument, see Fig. 3.2.g.

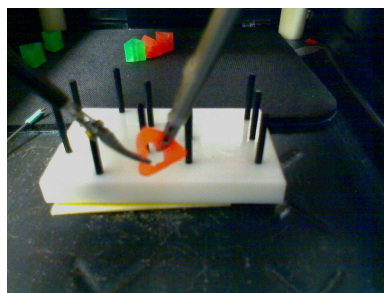


Fig. 3.2.g,

- 3.2.2.19. Grab the rubber piece within the jaws of the right hand side instrument, and when successful release the jaws of the instrument in the left hand.
- 3.2.2.20. Bring the tip of the right hand instrument over the peg on the right hand side and position the rubber piece so that it can be placed over the peg, see Fig. 3.2.h.

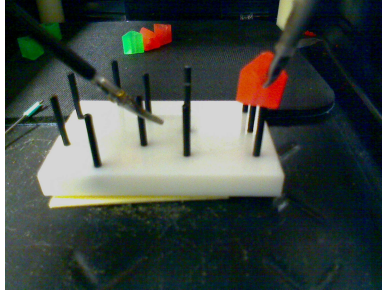


Fig. 3.2.h,

- 3.2.2.21. When the rubber piece is successfully placed over the peg, release the locking mechanism of the instrument in the right hand, and bring the tips of both instruments into the central neutral position, see Fig. 3.2.i.

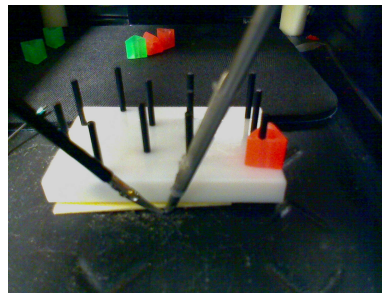


Fig. 3.2.i,

- 3.2.2.22. When both instruments are in place, test participant say out loud “STOP”,
- 3.2.2.23. At this point the test personnel click the “STOP” button on the test software and the data file is automatically saved.

#### **4. TEST SCHEDULE AND RESOURCES**

##### 4.1. Test resources

- 4.1.1. These tests will be administered in Boelter Hall 7673, UCLA.
- 4.1.2. Test personnel consist of Vasile Nistor, GSR and Brian Allen, GSR.
- 4.1.3. There is only one test station that can handle only one test participant at a time.

##### 4.2. Test schedule

- 4.2.1. Each group of test participants will listen to a power point presentation “Introduction to UCLA-LTS Construct Validity Test” – 10 minutes.

- 4.2.2. Test personnel will introduce the two instruments used for this test – 10 minutes
- 4.2.3. Test personnel will then perform the test itself – 5 minutes
- 4.2.4. Each test participant will then sign the “consent form” – 5 minutes
- 4.2.5. Each test participant will then proceed to perform the test itself three times in order to familiarize with the test environment – 10 minutes per participant.

		4.2.2.	4.2.3.	4.2.4.	4.2.5.	4.2.6.	Per session	Per 100 participants
Time per section [min]	10	10	5	5	10	15		
Test participants - one	10	10	5	5	10	15	55	5500 / 92
Test participants - two	10	10	5	5	20	30	80	4000 / 67h
Test participants - three	10	10	5	5	30	45	105	3500 / 58h
Test participants - four	10	10	5	5	40	60	130	3250 / 54h
Test participants - five	10	10	5	5	50	75	155	3100 / 52h

- 4.2.6. Each test participant will then proceed to perform the test itself ten times– 15 minutes per participant.
- 4.2.7. When the group consists of more than one, the test participants will rotate after three consecutive test iterations, to prevent fatigue.
- 4.2.8. For a group of 5 test participants, we require approximately 2 ½ hours, see the table bellow.
- 4.2.9. The total time required to go through 100 test participants under these ideal test conditions is 52 hours.

- 4.2.10. When the groups are four or less, the completion time increases, as shown in the table bellow.
- 4.2.11. Assuming a test session per workday, the time to complete the test range from the ideal 20 days to the worst-case scenario of 92 days.

## Bibliography

### Uncategorized References

1. Nistor, V., et al., *Haptic Guidance for Laparoscopic Surgery Immersive Training and Mentoring*.
2. Nistor, V., et al. *Immersive training and mentoring for laparoscopic surgery*. in *The 14th International Symposium on: Smart Structures and Materials & Nondestructive Evaluation and Health Monitoring*. 2007. International Society for Optics and Photonics.
3. Son, J., et al., *Quantification of intraocular surgery motions with an electromagnetic tracking system*. *Studies in health technology and informatics*, 2008. **142**: p. 337-339.
4. Nistor, V., et al., *Construct Validity for the UCLA Laparoscopic Training System*.
5. Allen, B., et al., *Support vector machines improve the accuracy of evaluation for the performance of laparoscopic training tasks*. *Surgical endoscopy*, 2010. **24**(1): p. 170.
6. Burpee, S.E., et al., *The metabolic and immune response to laparoscopic versus open liver resection*. *Gastroenterology*, 2000. **118**(4): p. A1506.
7. Zitsman, J.L., *Current concepts in minimal access surgery for children*. *Pediatrics*, 2003. **111**(6): p. 1239-1252.
8. Senagore, A.J., *Laparoscopic techniques in intestinal surgery*. *Surgical Innovation*, 2001. **8**(3): p. 183-188.
9. Nagle, A., et al., *Laparoscopic adhesiolysis for small bowel obstruction*. *The American journal of surgery*, 2004. **187**(4): p. 464-470.
10. Vierra, M., Mark, *Minimally invasive surgery*. *Annual review of medicine*, 1995. **46**(1): p. 147-158.
11. Garry, R., *The benefits and problems associated with minimal access surgery*. *Australian and New Zealand journal of obstetrics and gynaecology*, 2002. **42**(3): p. 239-244.
12. Chiasson, P.M., et al., *Minimally invasive surgical practice: a survey of general surgeons in Ontario*. *Canadian journal of surgery*, 2004. **47**(1): p. 15.
13. Rosser, J.C., et al., *Telementoring and teleproctoring*. *World journal of surgery*, 2001. **25**(11): p. 1438-1448.
14. Rosser, J., et al., *Telementoring*. *Surgical endoscopy*, 1997. **11**(8): p. 852-855.

15. Moore, R., et al., *Telementoring of laparoscopic procedures*. *Surgical endoscopy*, 1996. **10**(2): p. 107-110.
16. FDA. *SOCRATES Robotic Telementoring System 510(k) Summary*. 2001 [cited 2004 03/24/2004].
17. Inc, C.M. *ZEUS Surgical System Approved in Canada for Full Cardiac and Telesurgical Clinical Applications; Health Canada Grants ZEUS Highest Regulatory Clearance Classification*. 10/29/2002 [cited 2004 03/24/2004]; [http://www.findarticles.com/cf\\_dls/m0EIN/2002\\_Oct\\_29/93538829/p1/article.jhtml](http://www.findarticles.com/cf_dls/m0EIN/2002_Oct_29/93538829/p1/article.jhtml)].
18. Canada, B. *CSTAR and Bell Canada collaborate to expand delivery of telemedicine services to Canadians*. 2003 [cited 2003 6/10/2003]; Available from: <http://www.bce.ca/en/news/releases/bc/2003/05/26/70286.html>.
19. Providers, T.A.o.T.S. *Live Telepresence Surgeries Performed Daily at ACS Congress*. 2002 [cited 2004 03/24/2004]; Available from: <http://www.atsp.org/news/spo.asp?contentID=1223&FullStory=>.
20. Systems, C. *Business Solutions Case Studies: Bell Canada and St. Joseph's Hospital Pioneer the Use of Telerobotics*. 2003 [cited 2004 03/24/2004]; Available from: [http://business.cisco.com/prod/tree.taf%3Fasset\\_id=100896&ID=44749&public\\_view=true&kbns=1.html](http://business.cisco.com/prod/tree.taf%3Fasset_id=100896&ID=44749&public_view=true&kbns=1.html).
21. Surgical, I. *Project Brief: A new concept for minimally invasive surgical training using robotics and tele-collaboration*. 2003 [cited 2004 03/24/2004]; Available from: <http://jazz.nist.gov/atpcf/prjbriefs/prjbrief.cfm?ProjectNumber=00-00-4595>.
22. Liu, A., et al., *A survey of surgical simulation: applications, technology, and education*. *Presence: Teleoperators and Virtual Environments*, 2003. **12**(6): p. 599-614.
23. Howe, R.D. and Y. Matsuoka, *Robotics for surgery*. *Annual Review of Biomedical Engineering*, 1999. **1**(1): p. 211-240.
24. Satava, R.M. *Telemanipulation, telepresence, and virtual reality for surgery in the year 2000*. in *Photonics for Industrial Applications*. 1995. International Society for Optics and Photonics.
25. Szekely, G., *Surgical simulators*. *Minimally Invasive Therapy & Allied Technologies*, 2003. **12**(1-2): p. 14-18.
26. Kuhn, C., et al., *Karlsruhe Endoscopic Surgery Trainer*. *Forschungszentrum Karlsruhe*, January, 1997.
27. Ayache, N., *Epidaure: a research project in medical image analysis, simulation, and robotics at INRIA*. *IEEE Transactions on medical imaging*, 2003. **22**(10): p. 1185-1201.

28. Cavusoglu, M.C., et al., *A laparoscopic telesurgical workstation*. IEEE Transactions on Robotics and automation, 1999. **15**(4): p. 728-739.
29. Cenk Çavuşoğlu, M., et al., *Robotics for telesurgery: Second generation Berkeley/UCSF laparoscopic telesurgical workstation and looking towards the future applications*. Industrial Robot: An International Journal, 2003. **30**(1): p. 22-29.
30. Munz, Y., et al., *Laparoscopic virtual reality and box trainers: is one superior to the other?* surgical endoscopy and other interventional techniques, 2004. **18**(3): p. 485-494.
31. Aggarwal, R., K. Moorthy, and A. Darzi, *Laparoscopic skills training and assessment*. British Journal of Surgery, 2004. **91**(12): p. 1549-1558.
32. Schijven, M. and J. Jakimowicz, *Virtual reality surgical laparoscopic simulators*. Surgical endoscopy, 2003. **17**(12): p. 1943-1950.
33. Speich, J.E. and J. Rosen, *Medical robotics*. Encyclopedia of biomaterials and biomedical engineering, 2004. **983**: p. 993.
34. Basdogan, C., et al., *Haptics in minimally invasive surgical simulation and training*. IEEE computer graphics and applications, 2004. **24**(2): p. 56-64.
35. Funda, J., et al. *Comparison of two manipulator designs for laparoscopic surgery*. in *Photonics for Industrial Applications*. 1995. International Society for Optics and Photonics.
36. Meyer, K., H.L. Applewhite, and F.A. Biocca, *A survey of position trackers*. Presence: Teleoperators & Virtual Environments, 1992. **1**(2): p. 173-200.
37. Mcinerney, J. and D.W. Roberts, *Frameless stereotaxy of the brain*. Mount Sinai Journal of Medicine, 2000. **67**(4): p. 300-310.
38. Foxlin, E., *Motion tracking requirements and technologies*. Handbook of virtual environment technology, 2002. **8**: p. 163-210.
39. Sung, G.T. and I.S. Gill, *Robotic laparoscopic surgery: a comparison of the da Vinci and Zeus systems*. Urology, 2001. **58**(6): p. 893-898.
40. Kosugi, Y., et al., *An articulated neurosurgical navigation system using MRI and CT images*. IEEE Transactions on Biomedical Engineering, 1988. **35**(2): p. 147-152.
41. Kwoh, Y.S., et al., *A robot with improved absolute positioning accuracy for CT guided stereotactic brain surgery*. IEEE Transactions on Biomedical Engineering, 1988. **35**(2): p. 153-160.

42. Gumprecht, H.K., D.C. Widenka, and C.B. Lumenta, *BrainLab VectorVision Neuronavigation System: technology and clinical experiences in 131 cases*. Neurosurgery, 1999. **44**(1): p. 97-104.
43. Schlaier, J., J. Warnat, and A. Brawanski, *Registration accuracy and practicability of laser-directed surface matching*. Computer Aided Surgery, 2002. **7**(5): p. 284-290.
44. Inc, N.D. *Optotrak*. 2004 [cited 2004 03/24/2004]; Available from: <https://www.ndigital.com/msci/products/optotrak-certus/>.
45. Bucholz, R.D. and K.R. Smith, *A comparison of sonic digitizers versus light emitting diode-based localization*. Interactive image-guided neurosurgery, 1993: p. 179-200.
46. Technologies, A. *Laer BIRD*. 2002 [cited 05/01/2004]; Available from: <https://www.ascension-tech.com/products/laserbird-2/>.
47. Depsey, M., *Indoor positioning systems in healthcare*. Radianse Inc., White Paper, 2003. **123**.
48. Reynolds, M.S., *A phase measurement radio positioning system for indoor use*. 1998, Massachusetts Institute of Technology.
49. Adelstein, B.D., E.R. Johnston, and S.R. Ellis, *Dynamic response of electromagnetic spatial displacement trackers*. Presence: Teleoperators & Virtual Environments, 1996. **5**(3): p. 302-318.
50. Yu, W. and J.R. Pretlove. *Development of a Polhemus-based telemanipulation system*. in *Intelligent Systems & Advanced Manufacturing*. 1997. International Society for Optics and Photonics.
51. Nixon, M.A., et al., *The effects of metals and interfering fields on electromagnetic trackers*. Presence: Teleoperators and Virtual Environments, 1998. **7**(2): p. 204-218.
52. Stoll, J., P. Dupont, and R.D. Howe. *Ultrasound-based servoing of manipulators for telesurgery*. in *Intelligent Systems and Advanced Manufacturing*. 2002. International Society for Optics and Photonics.
53. Tatar, F., J. Mollinger, and A. Bossche. *Ultrasound system for measuring position and orientation of laparoscopic surgery tools*. in *Sensors, 2003. Proceedings of IEEE*. 2003. IEEE.
54. Reinhardt, H. and H.-J. Zweifel, *Interactive sonar-operated device for stereotactic and open surgery*. Stereotactic and functional neurosurgery, 1990. **54**(1-8): p. 393-397.
55. Gronningsaeter, A., et al., *SonoWand, an ultrasound-based neuronavigation system*. Neurosurgery, 2000. **47**(6): p. 1373-1380.



56. Filip, M., P. Linzer, and D. Skoloudik, *Virtual Navigation—A New Modality in Perioperative Brain Tumor Imaging*. 2012.
57. Zijlmans, M., et al., *Navigated laparoscopy—liver shift and deformation due to pneumoperitoneum in an animal model*. *Minimally Invasive Therapy & Allied Technologies*, 2012. **21**(3): p. 241-248.
58. Jaffe, R., S. Bonomi, and A.M. Madni. *Miniature MEMS quartz INS/GPS description and performance attributes*. in *Proceedings of the 17th International Technical Meeting of the Satellite Division of The Institute of Navigation (ION GNSS 2004)*. 2001.
59. Nagle, B.J., *System analysis and design of a low-cost micromechanical seeker system*. 2008, Draper Laboratory.
60. Lee, J., et al., *The use of micro-electro-mechanical-systems technology to assess gait characteristics*. *The impact of technology on sport II*, 2007: p. 181-186.
61. Nasu-gun, T., *A Wearable Attitude-Measurement System Using a Fiberoptic Gyroscope*. 2002.
62. Barshan, B. and H.F. Durrant-Whyte, *Inertial navigation systems for mobile robots*. *IEEE Transactions on Robotics and Automation*, 1995. **11**(3): p. 328-342.
63. Foxlin, E. and L. Naimark. *Miniaturization, calibration & accuracy evaluation of a hybrid self-tracker*. in *Proceedings of the 2nd IEEE/ACM International Symposium on Mixed and Augmented Reality*. 2003. IEEE Computer Society.
64. Kindratenko, V., *A comparison of the accuracy of an electromagnetic and a hybrid ultrasound-inertia position tracking system*. *Presence: Teleoperators and Virtual Environments*, 2001. **10**(6): p. 657-663.
65. Chai, L., W.A. Hoff, and T. Vincent, *Three-dimensional motion and structure estimation using inertial sensors and computer vision for augmented reality*. *Presence: Teleoperators and Virtual Environments*, 2002. **11**(5): p. 474-492.
66. Grange, S., et al. *Delta Haptic Device as a nanomanipulator*. in *Intelligent Systems and Advanced Manufacturing*. 2001. International Society for Optics and Photonics.
67. Wall, S., *An investigation of temporal and spatial limitations of haptic interfaces*. Department of Cybernetics, vol. Ph. D. Reading: University of Reading, 2004.
68. Lawrence, D.A., et al. *Low cost actuator and sensor for high-fidelity haptic interfaces*. in *Haptic Interfaces for Virtual Environment and Teleoperator Systems, 2004. HAPTICS'04. Proceedings. 12th International Symposium on*. 2004. IEEE.
69. Grange, S., et al., *Overview of the delta haptic device*. 2001.

70. Birglen, L., *Haptic devices based on parallel mechanisms. state of the art.* 2003.
71. Henriques, D.Y. and J.F. Soechting, *Bias and sensitivity in the haptic perception of geometry.* Experimental Brain Research, 2003. **150**(1): p. 95-108.
72. Steele, M. and R.B. Gillespie. *Shared control between human and machine: Using a haptic steering wheel to aid in land vehicle guidance.* in *Proceedings of the human factors and ergonomics society annual meeting.* 2001. SAGE Publications Sage CA: Los Angeles, CA.
73. Griffiths, P. and R.B. Gillespie. *Shared control between human and machine: Haptic display of automation during manual control of vehicle heading.* in *Haptic Interfaces for Virtual Environment and Teleoperator Systems, 2004. HAPTICS'04. Proceedings. 12th International Symposium on.* 2004. IEEE.
74. Patton, J.L. and F.A. Mussa-Ivaldi, *Robot-assisted adaptive training: custom force fields for teaching movement patterns.* IEEE Transactions on Biomedical Engineering, 2004. **51**(4): p. 636-646.
75. Wickens, C.D., et al., *Engineering psychology & human performance.* 2015: Psychology Press.
76. Microsoft. *Visual C++.* [cited 2004 03/24/2004]; Available from: <https://www.microsoft.com/en-us/download/details.aspx?id=53840>.
77. GL, O. *Open GL.* 2004 [cited 2004 03/24/2004]; Available from: <https://www.opengl.org/>.
78. FLTK. *FLTK.* [cited 2004 03/24/2004]; Available from: <http://www.fltk.org/index.php>.
79. GTK. *GTK.* [cited 2004 03/24/2004]; Available from: <https://www.gtk.org/>.
80. Çavuşoğlu, M.C., D. Feygin, and F. Tendick, *A critical study of the mechanical and electrical properties of the phantom haptic interface and improvements for highperformance control.* Presence: Teleoperators and Virtual Environments, 2002. **11**(6): p. 555-568.
81. Biggs, S.J. and M.A. Srinivasan, *Haptic interfaces.* Handbook of virtual Environments, 2002: p. 93-116.
82. Lawrence, D.A., et al., *Rate-hardness: A new performance metric for haptic interfaces.* IEEE Transactions on Robotics and Automation, 2000. **16**(4): p. 357-371.
83. Salkauskas, K. and P. Lancaster, *Curve and Surface Fitting, An Introduction.* 1981, Academic Press.

84. Cosman, P.H., et al., *Virtual reality simulators: current status in acquisition and assessment of surgical skills*. ANZ journal of surgery, 2002. **72**(1): p. 30-34.
85. Eubanks, T.R., et al., *An objective scoring system for laparoscopic cholecystectomy*. Journal of the American College of Surgeons, 1999. **189**(6): p. 566-574.
86. Meijer, D., J.J. Bannenberg, and J. Jakimowicz, *Hand-assisted laparoscopic surgery*. Surgical endoscopy, 2000. **14**(10): p. 891-895.
87. Kitano, S. and N. Shiraishi, *Laparoscopic surgery for gastrointestinal malignancies*. Nihon Geka Gakkai zasshi, 2000. **101**(8): p. 525-530.
88. Rosser, J.C., L.E. Rosser, and R.S. Savalgi, *Skill acquisition and assessment for laparoscopic surgery*. Archives of Surgery, 1997. **132**(2): p. 200-204.
89. Rosser Jr, J.C., L.E. Rosser, and R.S. Savalgi, *Objective evaluation of a laparoscopic surgical skill program for residents and senior surgeons*. Archives of surgery, 1998. **133**(6): p. 657-661.
90. Martin, J., et al., *Objective structured assessment of technical skill (OSATS) for surgical residents*. British journal of surgery, 1997. **84**(2): p. 273-278.
91. Aggarwal, R., J. Hance, and A. Darzi, *Surgical education and training in the new millennium*. Surgical endoscopy, 2004. **18**(10): p. 1409-1410.
92. Chen, W., et al., *Operative time is a poor surrogate for the learning curve in laparoscopic colorectal surgery*. Surgical endoscopy, 2007. **21**(2): p. 238-243.
93. Aucar, J.A., et al., *A review of surgical simulation with attention to validation methodology*. Surgical Laparoscopy Endoscopy & Percutaneous Techniques, 2005. **15**(2): p. 82-89.
94. Kothari, S., et al., *Training in laparoscopic suturing skills using a new computer-based virtual reality simulator (MIST-VR) provides results comparable to those with an established pelvic trainer system*. Journal of laparoendoscopic & advanced surgical techniques. Part A, 2002. **12**(3): p. 167.
95. Duffy, A., et al., *Construct validity for the LAPSIM laparoscopic surgical simulator*. Surgical Endoscopy and Other Interventional Techniques, 2005. **19**(3): p. 401-405.
96. Langelotz, C., et al., *LapSim virtual reality laparoscopic simulator reflects clinical experience in German surgeons*. Langenbeck's Archives of Surgery, 2005. **390**(6): p. 534-537.
97. Larsen, C., et al., *Objective assessment of gynaecologic laparoscopic skills using the LapSimGyn virtual reality simulator*. Surg Endosc. 2006 Sep; **20** (9): 1460-6. Virtual Reality Simulation in Laparoscopic Gynaecology, 2006. **20**(9): p. 57.

98. Schijven, M. and J. Jakimowicz, *Construct validity*. Surgical Endoscopy and Other Interventional Techniques, 2003. **17**(5): p. 803-810.
99. Schijven, M. and J. Jakimowicz, *Face-, expert, and referent validity of the Xitact LS500 laparoscopy simulator*. Surgical endoscopy, 2002. **16**(12): p. 1764-1770.
100. Schijven, M. and J. Jakimowicz, *The learning curve on the Xitact LS 500 laparoscopy simulator: profiles of performance*. Surgical Endoscopy And Other Interventional Techniques, 2004. **18**(1): p. 121-127.
101. Downes, M., T. Goktekin, and M.C. Cavusoglu, *A Virtual Environment Testbed for Training Laparoscopic Surgical Skills*.
102. Stylopoulos, N., et al., *Computer-enhanced laparoscopic training system (CELTS): bridging the gap*. Surgical Endoscopy and Other Interventional Techniques, 2004. **18**(5): p. 782-789.
103. Maithel, S., et al., *Construct and face validity of MIST-VR, Endotower, and CELTS*. Surgical Endoscopy and Other Interventional Techniques, 2006. **20**(1): p. 104-112.
104. Gallagher, A., et al., *Discriminative validity of the Minimally Invasive Surgical Trainer in Virtual Reality (MIST-VR) using criteria levels based on expert performance*. Surgical Endoscopy And Other Interventional Techniques, 2004. **18**(4): p. 660-665.
105. Adamsen, S., et al., *A comparative study of skills in virtual laparoscopy and endoscopy*. Surgical Endoscopy And Other Interventional Techniques, 2005. **19**(2): p. 229-234.
106. Avgerinos, D., et al., *Comparison of the sensitivity of physical and virtual laparoscopic surgical training simulators to the user's level of experience*. Surgical Endoscopy and Other Interventional Techniques, 2005. **19**(9): p. 1211-1215.
107. Hackethal, A., M. Immenroth, and T. Bürger, *Evaluation of target scores and benchmarks for the traversal task scenario of the minimally invasive surgical trainer-virtual reality (MIST-VR) laparoscopy simulator*. Surgical Endoscopy And Other Interventional Techniques, 2006. **20**(4): p. 645-650.
108. Madan, A.K., C.T. Frantzides, and L.M. Sasso, *Laparoscopic baseline ability assessment by virtual reality*. Journal of Laparoendoscopic & Advanced Surgical Techniques, 2005. **15**(1): p. 13-17.
109. Windsor, J. and F. Zoha, *The laparoscopic performance of novice surgical trainees*. Surgical Endoscopy And Other Interventional Techniques, 2005. **19**(8): p. 1058-1063.
110. McNatt, S. and C. Smith, *A computer-based laparoscopic skills assessment device differentiates experienced from novice laparoscopic surgeons*. Surgical Endoscopy, 2001. **15**(10): p. 1085-1089.

111. Torkington, J., et al., *Skill transfer from virtual reality to a real laparoscopic task*. Surgical endoscopy, 2001. **15**(10): p. 1076-1079.
112. Kimura, T., et al., *Usefulness of a virtual reality simulator or training box for endoscopic surgery training*. Surgical Endoscopy And Other Interventional Techniques, 2006. **20**(4): p. 656-659.
113. Ahlberg, G., et al., *Does training in a virtual reality simulator improve surgical performance?* Surgical endoscopy, 2002. **16**(1): p. 126-129.
114. Hummel, J.B., et al., *Design and application of an assessment protocol for electromagnetic tracking systems*. Medical physics, 2005. **32**(7): p. 2371-2379.
115. Wentink, M., et al., *Rasmussen's model of human behavior in laparoscopy training*. Surgical endoscopy and other interventional techniques, 2003. **17**(8): p. 1241-1246.
116. Cotin, S., et al., *Metrics for laparoscopic skills trainers: The weakest link!* Medical image computing and computer-assisted intervention—MICCAI 2002, 2002: p. 35-43.
117. Tendick, F., et al., *A virtual environment testbed for training laparoscopic surgical skills*. Presence: Teleoperators and Virtual Environments, 2000. **9**(3): p. 236-255.
118. Flash, T. and N. Hogan, *The coordination of arm movements: an experimentally confirmed mathematical model*. Journal of neuroscience, 1985. **5**(7): p. 1688-1703.
119. Vassiliou, M., et al., *The MISTELS program to measure technical skill in laparoscopic surgery*. Surgical Endoscopy And Other Interventional Techniques, 2006. **20**(5): p. 744-747.
120. Datta, V., et al., *The use of electromagnetic motion tracking analysis to objectively measure open surgical skill in the laboratory-based model*. Journal of the American College of Surgeons, 2001. **193**(5): p. 479-485.
121. Aggarwal, R., et al., *Motion tracking systems for assessment of surgical skill*. Surgical endoscopy, 2007. **21**(2): p. 339-339.
122. Stilma, J., et al., *Points of action in the campaign against blindness in developing countries*. Documenta Ophthalmologica, 1991. **78**(3): p. 285-305.
123. Tsirbas, A., C. Mango, and E. Dutson, *Robotic ocular surgery*. British journal of ophthalmology, 2007. **91**(1): p. 18-21.
124. Cremers, S.L., et al., *Objective assessment of skills in intraocular surgery (OASIS)*. Ophthalmology, 2005. **112**(7): p. 1236-1241.
125. Everhart, J.E., et al., *Prevalence and ethnic differences in gallbladder disease in the United States*. Gastroenterology, 1999. **117**(3): p. 632-639.

126. Lazcano-Ponce, E.C., et al., *Epidemiology and molecular pathology of gallbladder cancer*. CA: a cancer journal for clinicians, 2001. **51**(6): p. 349-364.
127. Lopez-Gonzalez L, P.G., Washington R, Weiss AJ, *Characteristics of Medicaid and Uninsured Hospitalizations, 2012. HCUP Statistical Brief #182. October 2014. Agency for Healthcare Research and Quality, Rockville, MD, R. Agency for Healthcare Research and Quality, MD, Editor. 2014, Agency for Healthcare Research and Quality: Rockville, MD.*
128. Soper, N.J., et al., *Laparoscopic cholecystectomy the new “gold standard“?* Archives of Surgery, 1992. **127**(8): p. 917-923.
129. Gurusamy, K., et al., *Meta-analysis of randomized controlled trials on the safety and effectiveness of day-case laparoscopic cholecystectomy*. British Journal of Surgery, 2008. **95**(2): p. 161-168.
130. NIH, *Gallstones and Laparoscopic Cholecystectomy, NIH Consensus Statement*. 1992. **10**(3): p. 1-20.
131. Issenberg, S.B., et al., *Simulation technology for health care professional skills training and assessment*. Jama, 1999. **282**(9): p. 861-866.
132. Garcia-Ruiz, A., et al., *Manual vs robotically assisted laparoscopic surgery in the performance of basic manipulation and suturing tasks*. Archives of surgery, 1998. **133**(9): p. 957-961.
133. Jourdan, I., et al., *Stereoscopic vision provides a significant advantage for precision robotic laparoscopy*. British journal of surgery, 2004. **91**(7): p. 879-885.
134. Grantcharov, T.P., *Virtual reality simulation in training and assessment of laparoscopic skills*. European Clinics in Obstetrics and Gynaecology, 2006. **2**(4): p. 197-200.
135. Gallagher, A.G., et al., *Virtual reality simulation for the operating room: proficiency-based training as a paradigm shift in surgical skills training*. Annals of surgery, 2005. **241**(2): p. 364-372.
136. Kothari, S.N., et al., *Training in laparoscopic suturing skills using a new computer-based virtual reality simulator (MIST-VR) provides results comparable to those with an established pelvic trainer system*. Journal of laparoendoscopic & advanced surgical techniques, 2002. **12**(3): p. 167-173.
137. Stefanidis, D., et al., *Skill retention following proficiency-based laparoscopic simulator training*. Surgery, 2005. **138**(2): p. 165-170.
138. Grantcharov, T.P., et al., *Learning curves and impact of previous operative experience on performance on a virtual reality simulator to test laparoscopic surgical skills*. The American journal of surgery, 2003. **185**(2): p. 146-149.

139. Rosser Jr, J.C. and L.E. Giammaria, *Essential Characteristics of the Successful Bariatric Surgeon: Skills, Knowledge, Advocacy*, in *Minimally Invasive Bariatric Surgery*. 2007, Springer. p. 25-30.
140. Spencer, F., *Teaching and measuring surgical techniques: the technical evaluation of competence*. Bull Am Coll Surg, 1978. **63**(3): p. 9-12.
141. Schauer, P., et al., *The learning curve for laparoscopic Roux-en-Y gastric bypass is 100 cases*. Surgical Endoscopy and Other Interventional Techniques, 2003. **17**(2): p. 212-215.
142. Kopta, J.A., *An approach to the evaluation of operative skills*. Surgery, 1971. **70**(2): p. 297-303.
143. Bridges, M. and D.L. Diamond, *The financial impact of teaching surgical residents in the operating room*. The American Journal of Surgery, 1999. **177**(1): p. 28-32.
144. Rosen, J. and M. Solazzo, *Objective Laparoscopic Skills Assessments of Surgical Residents Using*. Medicine Meets Virtual Reality 2001: Outer Space, Inner Space, Virtual Space, 2001. **81**: p. 417.
145. Taffinder, N., et al., *An Objective assessment of surgeons' psychomotor skills: validation of the MISTVR laparoscopic simulator*. British Journal of Surgery, 1998. **85**(1): p. 75-75.
146. Darzi, A., S. Smith, and N. Taffinder, *Assessing operative skill: needs to become more objective*. BMJ: British Medical Journal, 1999. **318**(7188): p. 887.
147. Hance, J., et al., *Assessment of psychomotor skills acquisition during laparoscopic cholecystectomy courses*. The American Journal of Surgery, 2005. **190**(3): p. 507-511.
148. Satava, R.M., A. Cuschieri, and J. Hamdorf, *Metrics for objective assessment*. Surgical endoscopy, 2003. **17**(2): p. 220-226.
149. Chmarra, M.K., et al., *Retracting and seeking movements during laparoscopic goal-oriented movements. Is the shortest path length optimal?* Surgical endoscopy, 2008. **22**(4): p. 943-949.
150. Seymour, N.E., et al., *Virtual reality training improves operating room performance: results of a randomized, double-blinded study*. Annals of surgery, 2002. **236**(4): p. 458-464.
151. Nistor, V., et al. *Haptic guided telementoring and videoconferencing system for laparoscopic surgery*. in *Proceedings of the SPIE 14th international symposium on smart structures and materials and nondestructive evaluation and health monitoring, San Diego, CA*. 2007.
152. Fraser, S., et al., *Evaluating laparoscopic skills*. Surgical endoscopy, 2003. **17**(6): p. 964-967.

153. Vapnik, V.N. and V. Vapnik, *Statistical learning theory*. Vol. 1. 1998: Wiley New York.
154. Donias, H.W., et al., *Survey of resident training in robotic surgery*. The American Surgeon, 2002. **68**(2): p. 177.
155. Nio, D., et al., *Efficiency of manual versus robotical (Zeus) assisted laparoscopic surgery in the performance of standardized tasks*. Surgical Endoscopy and Other Interventional Techniques, 2002. **16**(3): p. 412-415.
156. Aggarwal, R., et al., *An evidence-based virtual reality training program for novice laparoscopic surgeons*. Annals of surgery, 2006. **244**(2): p. 310-314.
157. Adrales, G.L., et al., *A valid method of laparoscopic simulation training and competence assessment 1, 2*. Journal of Surgical Research, 2003. **114**(2): p. 156-162.
158. Chang, C.-C. and C.-J. Lin, *LIBSVM: a library for support vector machines*. ACM Transactions on Intelligent Systems and Technology (TIST), 2011. **2**(3): p. 27.
159. Hanley, J.A. and B.J. McNeil, *The meaning and use of the area under a receiver operating characteristic (ROC) curve*. Radiology, 1982. **143**(1): p. 29-36.
160. Welch, B.L., *The generalization of student's' problem when several different population variances are involved*. Biometrika, 1947. **34**(1/2): p. 28-35.
161. Silva, V.d., et al., *Telementoring and Telesurgery: Future or Fiction?*, in *Robot Surgery*, S.H. Baik, Editor. 2010, InTech: Rijeka. p. Ch. 03.
162. Taniguchi, K., et al., *Classification, Design and Evaluation of Endoscope Robots*, in *Robot Surgery*, S.H. Baik, Editor. 2010, InTech: Rijeka. p. Ch. 01.
163. Stamper, R.E., *A three degree of freedom parallel manipulator with only translational degrees of freedom*. 1997.
164. Hannaford, B., *A design framework for teleoperators with kinesthetic feedback*. IEEE transactions on Robotics and Automation, 1989. **5**(4): p. 426-434.